

**TREATMENT OF PHENOL IN WATER USING
MICROWAVE-ASSISTED ADVANCED OXIDATION PROCESSES**

A Thesis

Submitted to the College of Graduate Studies and Research

in partial fulfillment of the requirements

for the degree of

Master of Science

in the

Department of Chemical and Biological Engineering

University of Saskatchewan

Saskatoon, Saskatchewan

by

Abha Verma

© Copyright Abha Verma, April, 2014. All rights reserved.

PERMISSION TO USE

In presenting this thesis in partial fulfillment of the requirements for a Masters from the University of Saskatchewan, I agree that the Libraries of this University may make it freely available for inspection. I further agree that permission for copying of this thesis in any manner, in whole or in part, for scholarly purposes may be granted by the professor or professors who supervised my thesis work or, in their absence, by the Head of the Department or the Dean of the College in which my thesis work was done. It is understood that any copying or publication or use of this thesis or parts thereof for financial gain shall not be allowed without my written permission. It is also understood that due recognition shall be given to me and to the University of Saskatchewan in any scholarly use which may be made of any material in my thesis. Requests for permission to copy or to make other use of material in this thesis in whole or part should be addressed to:

Head of the Department of Chemical Engineering

University of Saskatchewan

Saskatoon, Saskatchewan S7N 5A9

Canada

or

Dean of the College of Graduate Studies and Research

University of Saskatchewan

107 Administration Place

Saskatoon, Saskatchewan S7N 5A2

Canada

ABSTRACT

Phenol and its compounds are highly toxic even in low concentration, and have become the subject of intense research during the last two decades. Effluents from industries such as oil refining, paper milling, olive oil extraction, wood processing, coal gasification and textiles and resin manufacturing and agro-industrial wastes discharge phenols at levels much higher than the toxic levels set for this compound. Advanced Oxidation Processes (AOPs) such as UV, UV-TiO₂, UV-H₂O₂, O₃ and UV-O₃ have become popular in recent years as efficient treatment methods for recalcitrant compounds like phenol.

The effect of microwave (MW) and combined MW-UV treatment on degradation of phenol was studied in aqueous solution in the presence and absence of TiO₂ under controlled temperature conditions. It was found that the efficiency of MW and MW-UV processes for the degradation of phenol was less than 10% after 120 minutes of treatment. However, the efficiencies of MW-TiO₂ (hydrothermal) and MW-TiO₂ (sol-gel) were slightly more than those of the above processes at 12 to 15% after 120 minutes, which might be due to adsorption of the phenol on the surface of TiO₂ particles. It also was observed that MW-UV-TiO₂ was superior to any other process studied for the degradation of phenol. At natural pH, the degradation efficiency of MW-UV-TiO₂ (HT) on 1500 ppm of phenol in water was 23%, and for MW-UV-TiO₂ (SG) it was 20%. Hence, it can be concluded that the catalyst (TiO₂) prepared by the hydrothermal (HT) method had better catalytic activity than TiO₂ prepared by the sol-gel (SG) method, which might be due to its structural and optical characteristics. Of the two developed reactors which are MW and a combined MW-UV reactor, MW-UV combined with TiO₂ could be used for most successful degradation of phenol.

ACKNOWLEDGEMENTS

I would like to thank my supervisors Dr. Venkatesh Meda and Dr. Ajay Dalai for their guidance throughout this project as well as providing me with many opportunities throughout my graduate studies. I also would like to thank other members of my advisory committee, Dr. Lope Tabil, Dr. Jafar Soltan, and Dr. Oon - Doo Baik for assisting throughout the completion of this thesis and for providing various aspects of scientific expertise. I sincerely thank Dr. Robert Tyler for his extensive editorial help.

Additionally, I would like to thank the following people for providing technical assistance integral to the completion of this project: Mr. Richard Blondin, Ms. Heli and, Mr. Louis Roth. My sincere thanks go to my friends, especially Sandeep Badoga, Priyanka Gupta, Anup Rana, Poonam Rana and Dr. Pardeep Kumar, for being a constant source of support throughout my graduate schooling. Finally, I would like to thank my colleagues in the Department of Chemical and Biological Engineering at the University of Saskatchewan for their support and friendship. Thank you for making the past few years such a memorable experience. My sincere thanks to all of my family members in India, especially my father, Dr. Sushil Kumar Verma, and my sisters, Smita Verma and Vibha Verma, for their unlimited love, support and encouragement and also for loving me for who I am. I also want to thank my parents-in-law, brother-in-law and sister-in-law for being such nice people and for their continuous encouragement.

Finally, my hearty thanks to Sandeep Kumar, my husband and my best friend forever; for all his support, help and understanding, and I also want to thank my baby, Sarthak Kumar for letting me complete my degree.

DEDICATION

This thesis is dedicated in loving memory of my Mother

TABLE OF CONTENTS

Permission to Use.....	i
Abstract.....	ii
Acknowledgement.....	iii
Dedication.....	iv
Table of Contents.....	v
List of Tables.....	viii
List of Figures.....	ix
List of Symbols and Acronyms.....	xi

CHAPTER 1. INTRODUCTION

1.1 Water pollution problem.....	1
1.2 Phenol.....	3
1.3 Objective.....	5
1.4 Organization of thesis.....	6

CHAPTER 2. LITERATURE REVIEW

2.1 Phenol.....	7
2.2 Structure of phenol.....	7
2.3 Chemical and physical properties of phenol.....	8
2.4 Sources of phenol contaminants.....	8
2.5 Environmental problems.....	10
2.6 Toxicity of phenol.....	11
2.7 Reported techniques for phenol analysis.....	11
2.8 An overview of available treatment methods for removal/destruction of phenol.....	12
2.8.1 Incineration.....	12
2.8.2 Adsorption onto activated carbon.....	12
2.8.3 Biodegradation of phenolic wastes	13

2.8.4 Chemical oxidation.....	14
2.8.4.1 Advanced oxidation processes (AOPs).....	14
2.8.4.2 Photocatalysis.....	15
2.8.4.3 H ₂ O ₂ photolysis.....	16
2.8.5 Ultrasonic technology.....	16
2.8.6 Microwave treatment.....	17
2.8.7 Microwave theory and the role of dielectric properties.....	18
2.9 Titanium dioxide (TiO ₂).....	19
2.9.1 Occurrence of TiO ₂	20
2.9.2 Structure of TiO ₂	21
2.9.3 Requirement of TiO ₂ Nanoparticles.....	22
2.9.4 Characterization techniques for TiO ₂ nanoparticles.....	22
2.9.4.1 Fourier transform infra red spectroscopy.....	22
2.9.4.2 X- ray diffraction	24
2.9.4.4 Scanning electron microscopy.....	26
2.9.4.5 Brunauer-Emmett-Teller.....	27
2.9.4.6 Thermogravimetric analysis.....	28

CHAPTER 3. DIELECTRIC PROPERTIES OF PHENOL–WATER MIXTURE AT MICROWAVE FREQUENCIES FROM 1 TO 5 GHz

3.1 Abstract.....	30
3.2 Introduction.....	31
3.3 Experimental Methods.....	32
3.3.1 Sample preparation	32
3.3.2 Measurement setup	33
3.3.3 Dielectric measurements.....	34
3.4 Results.....	36
3.5 Discussion.....	47
3.6 Sample holder design.....	48
3.7 Conclusion.....	49

CHAPTER 4. DEGRADATION OF PHENOL WITH MICROWAVE AND MICROWAVE UV IRRADIATION TREATMENT SYSTEM USING NANO-TiO₂

4.1 Abstract.....	50
4.2 Introduction.....	50
4.3 Materials and Methods.....	54
4.3.1 Chemicals.....	54
4.3.2 Sol-gel route.....	54
4.3.3 Hydrothermal method.....	55
4.3.4 Characterization method.....	56
4.3.5 Experimental Setup for microwave treatment system	57
4.3.6 Analytical methods.....	61
4.3.7 Experimental methodology	61
4.4 Results and Discussion.....	63
4.5 Summary.....	75
CHAPTER 5. SUMMARY, CONCLUSIONS AND RECOMMENDATIONS.....	76
List of References.....	81
Appendix.....	95

LIST OF TABLES

<u>Table</u>	<u>Page</u>
Table 2.1: Chemical and physical properties of phenol.....	8
Table 2.2: Phenol concentrations in industrial effluents.....	9
Table 3.1: Crystal Structure of TiO ₂	21
Table 4.1: Summary of the properties of TiO ₂ nanoparticles calcinite at 500°C	65

LIST OF FIGURES

<u>Figure</u>	<u>Page</u>
Figure 2.1: Structure of Phenol.....	7
Figure 2.2: Schematic of Formation of electron-hole pairs in TiO_2	15
Figure 2.3: Crystal structure of (a) Rutile and (b) Anatase.....	21
Figure 2.4: Schematic representation of stretching and bending vibrational modes.....	23
Figure 2.5: Schematic diagram of Fourier Transform Infra Red spectroscopy.....	24
Figure 2.6: Bragg's Law reflection.....	25
Figure 2.7: Schematic view of the operation of SEM.....	26
Figure 2.8: Schematic of a Thermobalance.....	28
Figure 3.1: Permittivity measurement setup showing HP 8510 system with coaxial probe.....	34
Figure 3.2: Schematic of a HP 8510 Vector Network Analyzer and measurement system.....	34
Figure 3.3: Variation of relative dielectric constant with frequency an concentration.....	37
Figure 3.4: variation of relative dielectric constant with frequency and temperatur.....	38
Figure 3.5: Variation of relative loss factor with frequency and concentration.....	39
Figure 3.6: Variation of loss factor with frequency and temperature.....	40
Figure 3.7: Variation of loss tangent with different frequency and concentration.....	41
Figure 3.8: Variation of loss tangent with different frequency and temperature.....	42
Figure 3.9: Variation of power factor with frequency and concentration.....	43
Figure 3.10: Variation of power factor with frequency and temperature.....	44
Figure 3.11: Variation of depth of penetration with frequency and concentration.....	45
Figure 3.12: Variation of depth of penetration with frequency and temperature.....	46
Figure 3.13: Photographic view of sample holder.....	48

Figure 3.14: Schematic of sample holder used in microwave treatment system.....	49
Figure 4.1 Schematic diagram for the synthesis of TiO ₂ powder by a sol-gel method.....	55
Figure 4.2 Schematic diagram for the synthesis of TiO ₂ powder by hydrothermal method.....	56
Figure 4.3: Schematic of Microwave combined UV Treatment System.....	58
Figure 4.4: Photographic View of Experimental Setup.....	58
Figure 4.5: Photographic View of Microwave Electrodeless Lamp inside the reactor.....	59
Figure 4.6: Methodology Flow Chart.....	62
Figure 4.7: X-ray diffraction (XRD) patterns of TiO ₂ prepared by sol-gel (SG) and hydrothermal (HT) Methods.....	64
Figure 4.8: TGA curves of TiO ₂ prepared by sol-gel (SG) and hydrothermal (HT) Methods.....	65
Figure 4.9: Fourier Transform Spectra of TiO ₂ prepared by sol-gel (SG) and hydrothermal (HT) Methods.....	66
Figure 4.10: SEM image of TiO ₂ nanoparticles prepared by Sol-Gel method.....	67
Figure 4.11: SEM image of TiO ₂ nanoparticles prepared by Hydrothermal method.....	68
Figure 4.12: Change in water temperature during microwave irradiation.....	69
Figure 4.13: Decrease in phenol concentration as a function of microwave irradiation exposure time obtained for sol-gel and hydrothermal derived TiO ₂ nanoparticle.....	71
Figure 4.14: Decrease in phenol concentration as a function of microwave combined UV irradiation exposure time obtained for sol-gel and hydrothermal derived TiO ₂ nanoparticles.....	72
Figure 4.15: Effect of MW-UV-TiO ₂ on Initial Concentration for Phenol degradation.....	74

LIST OF SYMBOLS AND ACRONYMS

AOPs	Advanced oxidation processes
AOS	Athabasca oil sands
BET	Brunauer-Emmett-Teller
ecb ⁻	Electron in the conduction band
EPA	Environmental Protection Agency
FTIR	Fourier transform infrared spectroscopy
HPLC	High performance liquid chromatography
hvb ⁺	Hole in the Valance band
Milli-Q	deionized and ultra-filtered water
MW	Microwave
SEM	Scanning Electron Microscopy
T	Reaction temperature, °C
TGA	Thermogravimetric Analysis
TiO ₂	Titanium dioxide
TTIP	Titanium tetra isopropoxide
UV	Ultraviolet
XRD	X-ray diffraction
HT	Hydrothermal method
SG	Sol-Gel method
MWL	Microwave electrodeless lamp
MAP	Microwave assisted photocatalytic

CHAPTER 1

INTRODUCTION AND OBJECTIVES

Water covers 70% of the earth's surface, most of it is saline. However, it is a problem these days to obtain fresh, clean and uncontaminated water due to increasing population and fast industrialization. Water pollution occurs when harmful materials are added beyond the capacity of a water body to break it down, degrading the quality of water for other uses.

1.1 Water pollution problem

Nature as well as anthropogenic sources are responsible for causing pollution. Toxic wastes, released into the environment causing environmental contamination are a point of concern. Strict guidelines for maximum contamination levels in waste from several industries and a desire to protect the environment have increased the level of interest in developing and improving existing technologies for the removal of toxic compounds from wastewater. Petroleum may pollute water bodies due to oil spills resulting from the rupture of oil carrying pipes, sudden releases from oil wells and leakage from storage tanks.

Sources of Water Pollution

There are two main sources of water pollution. Point sources includes industries, wastewater treatment facilities and other sources, directly discharging waste into water sources. Non-point these sources are more difficult to identify, because they are not a particular location and include runoff containing fertilizer, chemicals and animal wastes, construction sites and mines. Substances

leaching from landfills into water supplies also can be non-point sources of pollution (Agarwal et al. 2009).

Contaminants

Contaminants, present in water sources may include the microbial contaminants, such as bacteria and viruses, may come from sewage treatment plants and agricultural livestock operations. Inorganic contaminants includes metals and salts, which can occur naturally or can result from urban storm water runoff, domestic or industrial wastewater, oil and gas production. Organic chemical pollutants, consists synthetic and volatile organic chemicals, resulting byproducts of industrial processes and petroleum production. Radioactive contaminants, that can be found naturally or by the result of oil and gas production. (Ellen et al. 1997).

From an environmental point of view, persistent materials are most worrisome among the various waste products as various sectors of the environment can be affected if they are not receiving a specific treatment necessary for their destruction. These types of pollutants are more problematic as their small volume can contaminate a large volume of water and they cannot be stored for a long period of time. A large number of compounds can be transformed into potentially dangerous substances during their treatment, for example chlorination of compounds can result in the formation of chlorocarbons (Mishra et al.2009).

These types of compounds in wastewater are non-biodegradable in nature rendering the most commonly used biological treatments ineffective unless there is an additional specific treatment. Toxic and biologically recalcitrant compounds demand additional non-biological technologies for their destruction such as advanced oxidation processes (Kumar et al. 2010).

1.2 Phenol

The use of phenol and its compounds in industrial processes and their presence in the resulting wastewaters is an issue of environmental concern. Their high toxicity, even at low concentrations, has motivated the search for and improvement of many treatment techniques (Arana et al. 2007). During the last two decades, phenolic compounds have become the subject of accelerated research in the preservation of our environment.

Phenol and phenolic substances are toxic aromatic compounds present in wastewaters generated from various industries, including petroleum refining, resin, plastic, leather and textile manufacturing, chemical and petrochemical plants, rubber reclamation plants, pharmaceutical manufacturing and agro-industrial operations (Moussavi et al. 2009). Water sources near the Athabasca oil sands region and the Fort Murray oil sands production facility in Alberta, Canada are highly contaminated with various toxic organic compounds released as industrial effluent from the oil extraction processes, and include oil and grease, naphthenic acids, cyanide and phenols (Erik et al. 2008). Organic compounds detected in tailings-pond water include bitumen, naphthenic acids, asphaltenes, benzene, creosols, humic and fulvic acids, phenols, phthalates, polycyclic aromatic hydrocarbons, and toluene (Stroscher and Peake 1978; MacKinnon and Retallack 1981; Gulley 1992; MacKinnon and Sethi 1993; Madill et al. 2001; Rogers et al. 2002b).

Phenol is one of the most important intermediates product in the oxidation of higher-molecular weight aromatic hydrocarbons in the chemical industry. Thus, it is usually taken as a model compound for advanced wastewater treatment studies. It is listed as a priority pollutant in the list of Environmental Protection Agency (EPA-2002). Due to its toxic nature, the EPA has set a discharge limit of less than 1 part per billion (ppb) of phenol in surface water (Busca et al. 2008). Therefore, the disposal of phenols has become a major global concern and industries are forced to

apply advanced and efficient technologies for treating phenolic effluents before discharging into the environment. Although phenol is toxic, it is frequently used in producing some of industrially important chemicals (Schmidt 1999, Busca 2007). Kumar et al. (2010) listed some of the main uses of phenol:

- Bisphenol A is a product of the reaction of two moles of phenol and one mole of acetone and is used to produce polycarbonates and automotive components.
- Phenolic resins are produced by condensation of phenol and formaldehyde. It is used as adhesives in the plywood industry and as a disinfectants.

Many of the treatment methods including chemical and biological methods, are already in use for treatment of waste water contaminated with phenol. Low rates of degradation, low mineralization, high costs of operation or operating conditions, and the time involved in these methods and formation of hazardous by-products, limit their effective use (Agustina et al. 2005). Processes combining microwave treatment combined with advanced oxidation are still in the developmental stages, but and have high potential for use in the treatment of contaminated water (Mishra et al. 2009).

The scope of the present study is to develop an integrated Microwave-Ultraviolet (MW-UV) reactor using an the electrode-less UV lamp inside a microwave reactor (so that the lamp is not affected by the microwave field) and to use this reactor to study the degradation of phenolic pollutants at controlled temperature.

Furthermore a knowledge gap exists with respect to understanding the effect of MW-UV irradiation combined with a catalyst (TiO_2) synthesized by two different methods, hydrothermal and

sol-gel. There is a valid need to develop, and evaluate microwave-assisted advanced oxidation process treatment systems for treatment of high concentrations of phenol. It was hypothesized that a MW assisted advanced oxidation treatment system would have high potential for rapid degradation of phenol in a phenol water mixture.

1.3 Objectives

Based on the above knowledge gap, the overall objective of the proposed research was to investigate the efficiency of degradation of high concentrations of phenol in two developed treatment systems, along with the effect of two different methods of catalyst (TiO_2) preparation on the rate and extent of phenol degradation. The specific objectives were:

- to determine the dielectric properties of phenol-water mixtures over the microwave frequency range of 1 to 5 GHz;
- to synthesize (hydrothermal and sol-gel methods) and characterize TiO_2 catalysts, and compare the photocatalytic activity of the prepared catalysts using two developed treatment systems, microwave only and microwave-assisted UV irradiation combined with AOPs for the degradation of phenol; and
- to investigate the microwave assisted UV treatment system at 2.45 GHz for the catalytic (TiO_2) degradation of phenol.

1.4 Organization of the Thesis

The thesis is organized according to the University of Saskatchewan guidelines for manuscript-based theses. Chapter 1 introduces the subject matter and the overall and specific objectives of the research. The review of literature on phenol properties, sources, toxicity and

different treatment methods is presented in Chapter 2. Chapter 3 presents the study on dielectric properties of phenol- water mixtures, i.e. the effect of phenol concentration, temperatures and microwave frequency, and results and discussion. Chapter 4 presents the synthesis of TiO_2 catalyst by two methods, development of combined microwave-UV reactor and investigations on the degradation of phenol, including methods, materials, results, and discussion. Chapter 5 provides a general summary of all results obtained, conclusions, and recommendations for future studies.

CHAPTER 2

LITERATURE REVIEW

The literature on phenol structure, physical and chemical properties, dielectric properties, sources of contamination, environmental problems, toxicity and different methods available for its treatment, is reviewed and presented in this chapter as an understanding of the topics is required prior to developing a thermo-chemical reactor.

2.1 Phenol

Phenol is the common name of hydroxybenzene, C_6H_5OH , the simplest member of a family of compounds in which an -OH group is attached directly to a benzene ring. At room temperature it is a white, crystalline solid. It consists of an hydroxyl group (-OH) attached to a phenyl ($-C_6H_5$) ring. It is only mildly acidic in nature but requires careful handling because of its toxic nature and can cause severe burns.

2.2 Structure of Phenol

Phenol is an aromatic molecule consisting of an hydroxyl group attached to a benzene ring (Figure 2.1).

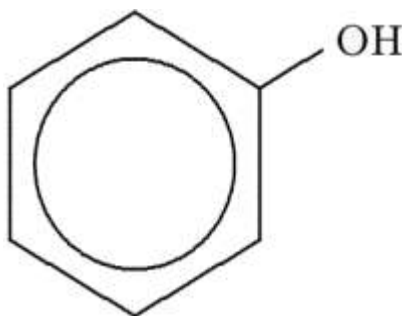


Fig. 2.1: Chemical structure of phenol (<http://en.wikipedia.org/wiki/Phenol>)

2.3 Chemical and Physical Properties of Phenol

Phenol at room temperature is a colorless, hygroscopic crystalline solid. It is highly soluble in water and in many organic solvents (such as alcohols, ethers, chloroform and several other polar solvents). Table 2.1 explains the chemical and physical properties of phenol.

Table 2.1: Chemical and physical properties of phenol (Kirk-Othmer et al. 1999)

PROPERTIES	PHENOL
Formula	C ₆ H ₅ OH
Molecular weight (g/mol)	94.11
Water solubility (g/L at 25°C)	87
Melting point (°C, 100 kPa)	43
Boiling point (°C, 100 kPa)	181.8
Acidity pK_a	9.89 X 10 ⁻¹⁰
Density (solid) (g/cm ³) (at 25 °C)	1.071
Dielectric constant (50°F)	4.3
Vapor pressure at 25°C (Pa)	47

2.4 Sources of Phenol Contaminants

Phenols are the most common pollutant found in wastewater streams from the agri-food, pharmaceutical, chemical and petrochemical industries (Gimeno et al. 2007). All industries that either produce or use phenol are responsible for the release of this compound into the environment. Phenol concentrations ranging from a few hundred up to 10,000 mg/ L have been reported in wastewater (Fedorak and Hrudey et al. 1988). Hunter et al. (1971) stated that in domestic

wastewater the concentration of phenol is between 0.1 and 1 mg/L. Table 2.2 shows the concentration of phenol in the effluents generated in several industrial operations.

Table 2.2: Phenol concentrations in industrial effluents (Busca et al. 2008).

Industry	Phenol concentration, mg/L
Coking operations	28 – 3900
Coal processing	9 – 6800
Petrochemicals	2.8 – 1220
Pulp and paper	0.1 – 1600
Gas production	4000
Refineries	6 – 500
Pharmaceuticals	1000
Benzene manufacturing	50

Phenol and related phenolic compounds enter our environment from industrial and from natural sources, and in very low concentrations from anthropogenic activity. For example, in a high altitude spruce forest phenol compounds present in the capillary water of the soil showed a total monomer concentration of 2 μ M. These monomers includes vanillic acid, 4-hydroxybenzoic acid and cinnamic acid, and represented only 1% of the total phenolic compounds (Gallet and Pellisier et al. 1997). Any type of bioresource (plant) material, such as fresh or decaying leaves, roots, shoots and flowers can leach phenolic compounds into the environment. Some of these compounds, for example 4-hydroxybenzoate, p-coumaric, vanillic and cinnamic acids act as chemoattractants for microbes in the soil, like *Pseudomonas* and *Rhizobium* species (Harwood et al. 1986; Kape et al.

1992). In marine systems, natural phenols are, produced by marine algae, plants, and invertebrates, and degraded by microbial populations (Boyd and Carlucci et al. 1993). Phenols are produced during the anaerobic degradation of ligninaceous plant materials in ruminant animals and are excreted in urine and feces (Martin et al. 1982).

2.5 Environmental Problems

Phenolic compounds in water are a cause of various environmental problems. At a low concentration of approximately 5 ppb, they result in unpleasant tastes and odours and are highly toxic at concentrations greater than 2 mg L^{-1} , which creates several problems for aquatic life (Luis et al. 2011). Chlorination of drinking water containing phenols produces chlorophenols, which are more toxic than phenol and are very difficult to remove. Deichmann and Klepinger (1981) reported that ingestion of substances containing as little as 1 mg L^{-1} of phenol can have fatal consequences in humans. Phenol concentrations higher than 2 mg L^{-1} are toxic to fish, and concentrations between 10 and 100 mg L^{-1} result in the death of most aquatic life (Huang et al. 2007). Drinking water contaminated with phenol causes diarrhea, mouth sores, damage to kidneys and even paralysis of the central nervous system (Senturk et al. 2009). Due to its harmful effects on living organism, phenol is listed as a priority pollutant by the US Environmental Protection agency (EPA) (Kumar et al. 2010), which requires decreasing the phenol concentration below 1 mg/L before a contaminated water stream can be released into the environment (Ayranci and Duman 2005).

2.6 Toxicity of Phenol

Exposure to phenol can disturb central nervous system, resulting coma and reduction in body temperature (hypothermia) and can also results in myocardial depression. Phenol causes a burning effect, and whitening and peeling of the skin. Phenol contact can cause irritation in the eye,

conjunctival swelling, corneal whitening and, finally, blindness. Chronic exposure may result in anorexia, dermal rash, gastrointestinal disturbance, vomiting, weightlessness, hepatic tenderness and nervous disorders. It is also suspected that exposure to phenol may cause paralysis, cancer and genotofibre striation (Nair et al. 2008).

2.7 Reported Techniques for Phenol Analysis

There are various analytical techniques reported in the literature for the determination of phenol concentration after degradation and for identification of the intermediates formed in the reactions. Analysis of the samples has been done using a Chemito 2500 UV–VIS recording spectrophotometer at 270 nm (wang et al. 2005). HPLC was used for the analysis of phenol and its degradation products as presented by Mahamuni et al. (2006). The phenol concentration in advanced oxidation processes can be determined by HPLC with a UV detector (Esplugas et al. 2002). A UV/VIS spectrophotometer was adapted to analyze the degradation of phenol with ultrasonic radiation by Ismail et al. (2010). Kumar et al. (2010) identified the intermediates of phenol oxidation in solution using high resolution liquid chromatography (Waters 2695, Milford MA, USA) coupled to an inline diode array detector (Waters 996 PDA) connected in series to a Quattro Ultima triple quadrupole mass spectrometer equipped with an electrospray interface (ESI) (Micromass, Manchester UK) operating in the negative ion mode.

2.8 An Overview of Available Treatment Methods for Removal/Degradation of Phenol

“Most conventional treatment processes are effective in water treatment but they only transfer the contaminants from one medium to another or generate waste that requires further treatment and disposal” (Crittenden et al. 1997, Topodurti et al. 1993). Removal of contaminants to

allowable discharge limits is important, whether by single method or a combination of methods. Several methods are reported in the literature for the treatment of phenol and its compounds in water.

2.8.1 Incineration

This method is used for treating small quantities of wastes having high pollutant concentrations, but there are some disadvantages to this method: 1) high investment costs for instruments and high operating costs for energy because it requires additional fuels; and 2) production of carbon oxides and nitrogen oxides resulting from the oxidation of organic compounds at high temperatures (Kumar et al. 2010).

2.8.2 Adsorption onto Activated Carbon

This is a method whereby the organic pollutants are removed from wastewater by adsorption onto the surface of solid particles, where it is stored for future extraction. Adsorption of phenol onto activated carbon is a frequently studied treatment method because of the affinity of phenols for the active surface of carbon (Garcia-Araya et al. 2003). Several other adsorbents were discussed for removal of phenols, including bentonite and perlite, hydrotalcite and its calcined product, bituminous shale, water-insoluble cationic starch, and porous clay heterostructure (Chen et al. 2007). The disadvantage of this method is the high costs associated with recovering activated carbon particles from the treated wastewater (Banat et al. 2000). This process also suffers from a lack of continuity, and the adsorbent gets saturated with pollutants which lowers its removal efficiency. The disposal of solid adsorbent after use is also a serious concern.

2.8.3 Biodegradation of phenolic wastes

Biological treatment in comparison to other treatment options is the most economical alternative. The cost of biodegradation of pollutants is stated to be 5 to 20 times lower than chemical treatments such as ozonation (Mantzavinos et al. 1999). Several microorganisms, such as *Pseudomonas resinovorans* strain P-1, *Brevibacillus* sp. strain P-6, *Pseudomonas aeruginosa* and *Pseudomonas pseudomallei*, are reported to use phenol as a carbon and energy source but at low concentrations only (Yang and Lee et al. 2007). Biodegradation is a very useful and suitable treatment method for degradation of phenol concentrations within the range of 5-500 mg/L. Concentrations higher than 1450 mg/L are toxic and can kill the whole population of microorganisms present in the wastewater (Sevillano et al. 2008). Biological treatment alone is not a suitable treatment method for phenol at a concentration higher than 1450 mg L⁻¹ and concentrations up to 50 mg/ L are effective for biological removal of phenol in water, so that other methods or combinations of methods are required for degrading higher concentrations of phenol (Yavuz et al. 2010). Biological treatments need to be combined with other treatments such as chemical oxidation for effectively removing higher concentrations of phenol from wastewater in an economical manner.

2.8.4 Chemical oxidation

Chemical oxidation methods for treating organic pollutants is a promising alternative when wastewater cannot be treated by biodegradation. Chemical oxidation can be divided into two types of processes, classical chemical treatments and advanced oxidation processes (AOPs). Classical chemical oxidation is the process in which there is a direct addition of the oxidant to the

wastewater. The following are the most common chemical oxidants discussed by Kumar et al. (2010):

- **Chlorine** The main disadvantages of adding chlorine are its low selectivity and formation of more harmful chlorinated compounds after the reaction with pollutants.
- **Potassium permanganate** The disadvantage of potassium permanganate is the formation of manganese dioxide after oxidation, which precipitates and needs to be removed by clarification or filtration.
- **Hydrogen peroxide** Hydrogen peroxide is a very strong oxidant and can be used alone or with a addition of a catalyst. There are numerous advantages of using this oxidants such as low cost, high oxidizing power and ease of handling compared to other oxidizing agents.

2.8.4.1 Advanced oxidation processes (AOPs)

AOPs can be used for the treatment of high concentrations of organic compounds and are popular for treating phenolic wastes (Villota et al. 2007). Advanced oxidation processes are processes in which there is a generation of reactive species, such as hydroxyl radicals (HO^\bullet), which are strong and non-specific oxidation agents (Zazo et al. 2007). AOPs based on the production of hydroxyl radicals (HO^\bullet), are strong and non-selective oxidizing agents, and have oxidation potential higher than those of ozone and hydrogen peroxide (Neyens and Baeyens et al. 2003). AOPs have the high oxidation potential of hydroxyl radicals, responsible for complete oxidation of organic contaminants. AOPs are divided into two main categories on the basis of the generation of hydroxyl radicals,

- UV- based processes (UV/O_3 , $\text{UV}/\text{O}_3/\text{H}_2\text{O}_2$, UV/TiO_2)
- Hydrogen peroxide - based processes ($\text{O}_3/\text{H}_2\text{O}_2$, $\text{H}_2\text{O}_2/\text{Fe}^{2+}$, $\text{UV}/\text{H}_2\text{O}_2$)

2.8.4.2 Photocatalysis

Photocatalytic processes use a semiconductor metal oxide as catalyst and oxygen as an oxidizing agent (Luo et al. 1996). Many catalysts have been studied so far, but TiO_2 in the anatase form seems to have the most promising nature such as high stability, good performance and low cost (Rajeshwar et al. 1995). When comparing other conventional chemical oxidation methods, photocatalysis is more effective because semiconductors are inexpensive and capable of degrading various recalcitrant compounds (Ku et al. 1996). The initiating step in a photocatalytic process is the absorption of radiation which results in the formation of electron-hole pairs in conduction and valence bands as shown in Figure 2.3 (Agustina et al. 2005).

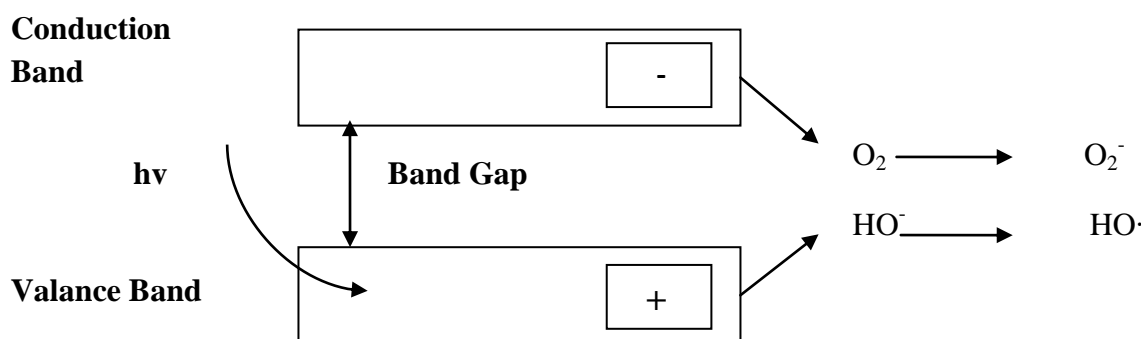
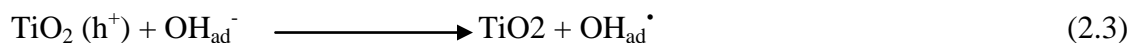
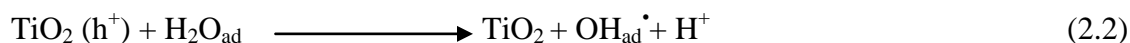


Fig. 2.2: Schematic of formation of electron-hole pairs in TiO_2 .

The electrons are able to reduce dissolved oxygen with the formation of the superoxide radical ion $\text{O}_2^{\bullet-}$, whereas remaining holes are capable of oxidizing H_2O or HO^- to reactive HO^\bullet radicals;



These reactions are of great importance in oxidative degradation processes due to the high concentration of H_2O and HO^\bullet adsorbed on the particle surface.

2.8.4.3 H_2O_2 photolysis

This process is effected by irradiating the pollutant solution containing H_2O_2 with UV light having wavelengths less than 280 nm. This causes the chemolytic cleavage of H_2O_2 .



2.8.5 Ultrasonic technology

Ultrasonic technology may be used for treatment of pollutants in wastewater due to its uniqueness. Application of this technology results in the decomposition of complex organic compounds to much simpler compounds due to a cavitation process (Mahvi et al. 2009). Destruction of microorganisms by ultrasonic energy has been a subject of interest since the 1920s when studies of Harvey and Loomis (1930) were published. Its mechanism is the cavitation phenomenon and associated shear disruption which results in localized heating and free radical formation. These radicals penetrate into water and oxidize dissolved organic compounds. Hydrogen peroxide (H_2O_2) is formed as a result of OH^\bullet and OOH^\bullet radical recombination on the outside of the cavitation bubble. There are two main mechanisms in the sonolysis system for pollutant decomposition:

- Pyrolysis reactions in cavitation bubbles.
- Radical reactions by radical species (H^\bullet , OH^\bullet) from water sonolysis.

These two mechanisms are as below (Crittenden et al. 2004):



2.8.6 Microwave treatment

Microwave (MW) radiation is a part of the electromagnetic spectrum in the frequency range of 300 MHz to 300 GHz. The first commercial microwave oven operating at 2.45 GHz was used in 1947. A great deal of interest is received by microwave irradiation in domestic, industrial, scientific and medical applications. Environmental applications of microwave are pyrolysis of sewage sludge (Menendez et al. 2002), hazardous and radioactive waste remediation (Wicks et al. 2001), desulphurization of coal (Ferrando et al. 1995), and microwave and microwave-assisted photocatalytic treatment of naphthenic acid in water (Mishra et al. 2009). Removal of ammonia nitrogen in wastewater by microwave radiation was studied by Lin et al. (2009). The combination of MW with oxidants, catalysts on AOPs (UV, TiO₂, Fenton process, H₂O₂) can enhance pollutant degradation. Microwave-enhanced photocatalytic degradation is an emerging field of research (Mishra et al. 2009). The use of an electrodeless microwave UV-VIS lamp to photodegrade pollutants in aqueous media was reported by Horikoshi et al. (2004). Klan et al. (2002) reported various advantages of using a microwave electrodeless lamp for water treatment, including the use of a commercially available microwave oven and the simplicity of the experimental setup using an electrodeless MW lamp.

The main advantage of energy produced by microwave irradiation over conventional heating methods is the way by which energy is used via radiation rather than from conductive heat transfer and convection. The conversion of energy into heat takes place evenly across the whole volume of the microwave absorbing heat exchanger, heating load or catalyst. Thermal and non-thermal effects govern microwave- assisted reactions. A typical thermal microwave effect was reported by Strosher et al. (1978) using the sulfonation of naphthalene as an example. Another thermal effect of microwave radiation is the formation of “hot spots”. Hot spots are areas which have higher temperatures than their surroundings because of greater interaction with the microwave field and their poor heat transfer properties. The increased number of OH[•] radicals and changes in hydrophilic/hydrophobic characteristics were attributed to the non-thermal effects of the microwave radiation (Mishra et al. 2009).

2.8.7 Microwave (MW) theory and the role of dielectric properties

The application of MW radiation is based on the properties of a fast and selective heating mechanism in environmental process engineering. Rapid heating of materials is a result of the dissipation factor of the material (loss tangent), which is the ratio of the relative loss factor (ϵ'') to the dielectric constant (ϵ') of the material. The relative measure of the MW energy density in the material is the dielectric constant, whereas, the relative loss factor accounts for the internal mechanism and shows the amount of MW energy that is lost in the material as heat energy. Materials having a high ϵ'' can easily absorb and convert energy into heat (Mishra et al. 2009).

Tian et al. (2005) concluded that the effect of MW irradiation on reaction kinetics was due to dielectric heating and non-thermal action. Microwave irradiation does not result in changes in the structure of a molecule. It is a non-ionizing radiation causing molecular motion by migration of ions

and rotation of dipoles in the molecule. The heating mechanisms of MW radiation are dipolar polarization which results from intermolecular inertia and is responsible for majority of MW heating, conduction mechanism and interfacial polarization (Remya et al. 2011). The principle of MW-induced separation of molecules was reported by Kong et al. (2006), whereas the dipole is subjected to a high frequency and varying electromagnetic field. Rotation of the dipole cannot keep up with the electromagnetic field of the MW, leading to a time delay and causing a conversion of a substantial quantity of the microwave energy to heat energy. The effect of concentration, temperature and MW frequency on the microwave permittivity of a naphthenic acid-water mixture was reported by (Mishra et al. 2007).

2.9 Titanium Dioxide (TiO₂) – A Catalyst

Titanium dioxide is a well known product with several important applications that are proven as safe in its use over decades. Titanium dioxide is defined as a white, solid, inorganic substance that is thermally stable, nonflammable and not classified as hazardous material (Hsien et al. 2000). It is an important material with a vast range of applications in industrial and consumer goods including paints, adhesives, photocatalysis, ceramic materials, fillers, paper and paperboard, coating, pigments, crayons, UV protection in sunscreens, cosmetics and pharmaceuticals, floor coverings, roofing materials, catalyst systems, food colorants, automotive products and water treatment agents, and has attracted attention in both fundamental research and practical development work (Porkodi et al. 2007). Among the various semiconductor materials, TiO₂ is the most widely used photocatalyst due to its non-toxicity, high activity, high stability, and relatively low cost (Hsien et al. 2000). The photocatalytic activity of TiO₂ varies depending on its crystallinity, particle size, crystal phase, surface area and method of preparation (Chen et al. 2007).

It is known that the anatase form of TiO_2 within small particle size and high crystallinity is required to obtain highly active photocatalysts (Thompson et al. 2006). Different preparation methods such as hydrothermal, sol-gel, and micro-emulsion to synthesize nanoparticles of TiO_2 have been reported. “The increase in surface area with a reduction in particle size means an increase in the number of active sites on which the electron acceptor and donor are adsorbed and participate in the redox reaction” (Kavitha et al. 2013). To obtain a photocatalyst with high performance, many structural parameters such as crystallite size, crystalline quality and specific surface area are important.

2.9.1 Occurrence of TiO_2

Pure TiO_2 is not found naturally and is derived from ilmenite or leucocene ores. TiO_2 is present in three crystalline structures: *rutile*, *anatase*, and *brookite*. Anatase shows better photocatalytic activity because of the lower recombination probability of electron-hole pairs (Doll et al. 2005, Hsien et al. 2000). This structure needs 3.2 eV for activation energy and requires UV light for activation (Mishra et al. 2009). Rutile is the most stable form, has a band gap of 3 eV and can be activated by solar radiation. Anatase and brookite both have a tendency to change into the rutile form upon heating.

2.9.2 Structure of TiO_2

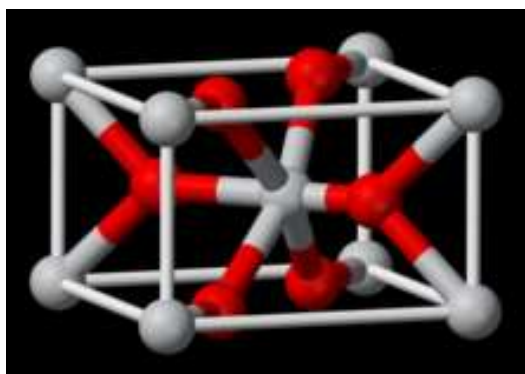
Structure of anatase and rutile is a chain of TiO_6 octahedrals in which Ti^{4+} ions are surrounded by six O^{2-} ions.

Chen et al. (2007) reported that in the “rutile phase each octahedron shares a corner with eight neighbors and shares edges with two other neighbors and forms a linear chain. In the anatase

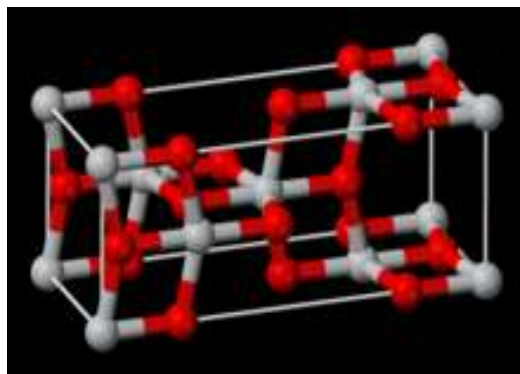
structure, each octahedron shares a corner with four neighbors and shares edges with other neighbors and forms a zig-zig chain with a screw axis”. Table 2.3 presents the crystal structure of TiO_2 . Figure 2.4 shows the crystal structure of the anatase and rutile phases.

Table 2.3: Crystal Structure of TiO_2 (Doll et al. 2005)

Phase	Crystal structure
Anatase	Tetragonal
Rutile	Tetragonal
Brookite	Orthorhombic



(a)



(b)

Fig. 2.3: Crystal structure of (a) Rutile and (b) Anatase (http://en.wikipedia.org/wiki/Titanium_dioxide).

2.9.3 Requirement of TiO_2 Nanoparticles

When the particle size decreases, part of atoms on the surface increases providing higher surface area to volume ratio, responsible for better catalytic activity (Hoffmann et al. 1995).

With the decrease in nanoparticles size there is a increase in the band gap energy and resulting potentially enhance redox potential of the holes in valence band and conduction band

electrons, allows photo-redox reaction which might not take place in the bulk materials to occur readily (Hoffmann et al. 1995).

2.9.4 Characterization techniques for TiO₂ nanoparticles

Characterization of prepared catalysts has been done on the basis of their crystallinity, crystallite size and structural properties. X-ray diffraction (XRD) is used to calculate crystallite size. Scanning electron micrography (SEM) is used to determine the grain size. Efficiency for degradation of phenol using two prepared catalysts with the two developed systems (microwave and microwave-assisted UV treatment systems) has been investigated in this study.

2.9.4.1 Fourier Transform Infrared spectroscopy (FTIR)

In infrared spectroscopy IR radiation passes through a material; some of the infrared radiation is absorbed and some is transmitted. The resulting spectrum shows the molecular absorption and transmission, and creating a molecular fingerprint of the material. The IR region shows vibrations of bound atoms. When the bound atoms vibrate, they have a tendency to absorb infrared energy meaning they exhibit IR absorption bands (Silverstein et al. 2005). There are two types of molecular vibrations:

Stretching: It is a vibration which shows rhythmical movement along the bond axis resulting in either increases or decreases in intermolecular distance, and may be symmetrical stretching or asymmetrical stretching (Silverstein et al. 2005).

Bending: It is a vibration which creates a change in angle between bonds with a common atom. There can be four types of bending- twisting, rocking, scissoring and wagging (Silverstein et al. 2005).

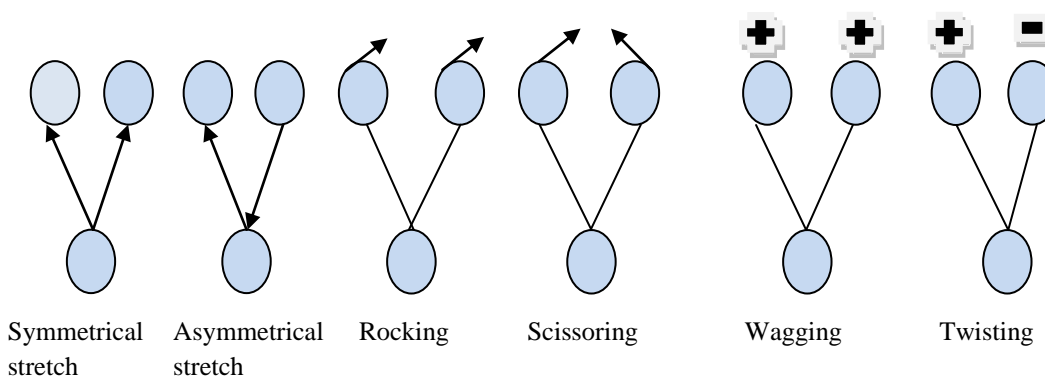


Fig. 2.4: Schematic representation of stretching and bending vibrational modes.

Instrumentation

“The components of an IR machine are the IR source, beam splitter, monochromator, transducer, analog to digital converter and a digital machine to quantify the readout” (Skoog et al. 2007). Figure 2.6 shows a schematic of a FTIR spectrophotometer. IR radiation with wavelengths between $(4000 \text{ and } 400\text{cm}^{-1})$ is split into two beams. One beam has a fixed length and other one varies. “The difference between the two path lengths results in a sequence of constructive and destructive interference and hence variation of intensities which is called an interferogram. Fourier transformation converts this interferogram from the time domain to the frequency domain. Sample and reference interferograms are separately transformed. Then, the ratio of both is automatically calculated and displayed as an IR transmission spectrum” (Silverstein et al. 2005).

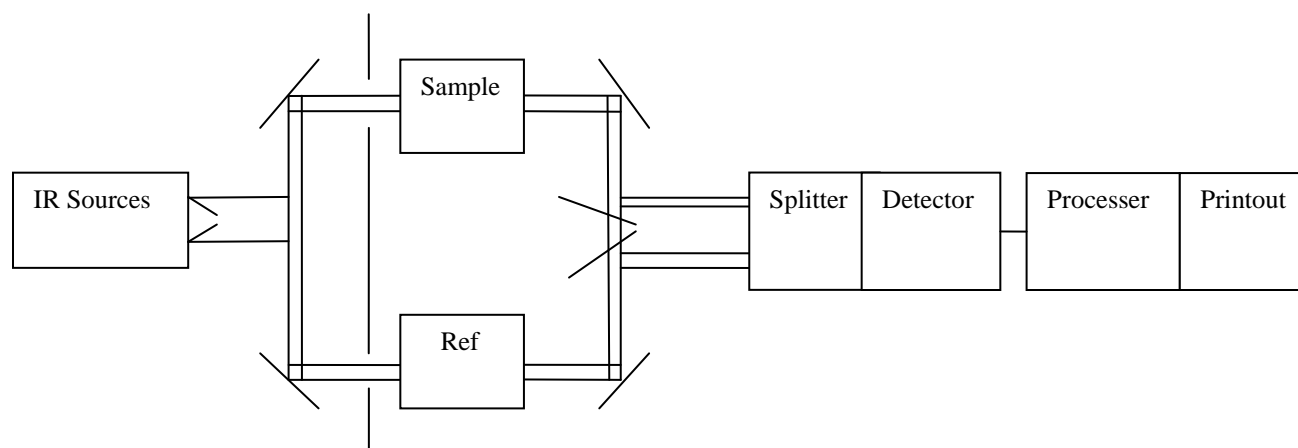


Fig. 2.5: Schematic of Fourier Transform Infra Red spectroscopy (Pavia et al. 2009).

2.9.4.2 X-ray diffraction (XRD)

X-ray diffraction is an analytical technique which is used for phase identification of a crystalline material. It can provide information about the unit cell dimensions of natural and synthesized compounds (Satterfield et al. 1996).

X-ray diffraction is based on the constructive interference of monochromatic X-rays with a crystalline material. These X-rays are generated by a cathode tube and then filtered to produce monochromatic radiation, collimated to concentrate, and directed toward the test material. “The interaction of these incident rays with the sample produces constructive interference along with a diffracted ray when conditions satisfy Bragg's Law. “This law relates the wavelength of electromagnetic radiation to the diffraction angle and the lattice spacing in a crystalline sample. These diffracted X-rays are then detected, processed and counted. By scanning the sample through a range of 2θ angles, all possible diffraction directions of the lattice should be attained due to the random orientation of the powdered material. Conversion of the diffraction peaks to d-spacings

allows identification of the material because each material has a set of unique d-spacings. Typically, this is achieved by comparison of d-spacings with standard reference patterns” (Harold et al. 2009). The relationship between the wavelength of the incident X-rays, angle of incidence and spacing between the crystal lattice planes of atoms is known as Bragg's Law (Figure 2.7), which is expressed as

$$n \lambda = 2d \sin\theta \quad (2.9)$$

where, n (an integer) is the "order" of reflection, λ is the wavelength of the incident X-rays, d is the interplanar spacing of the crystal and θ is the angle of incidence.

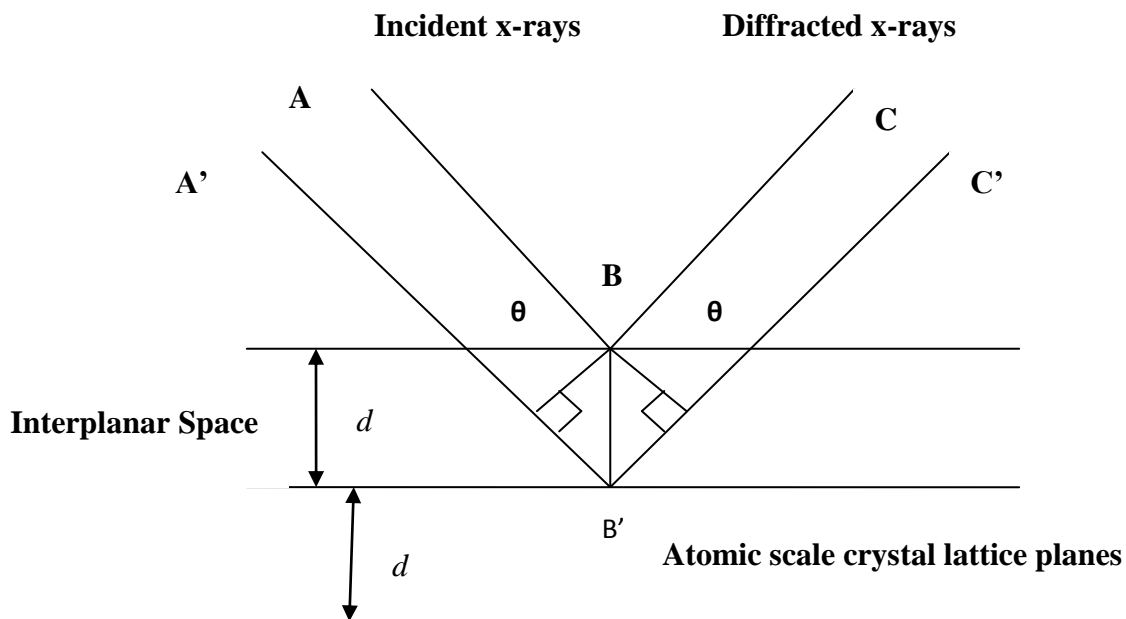


Fig. 2.6: Bragg's Law reflection. The diffracted X-rays exhibit constructive interference when the distance between paths ABC and A'B'C' differs by an integral number of wavelengths.

2.9.4.3 Scanning Electron Microscopy (SEM)

Scanning electron microscopy (SEM) is used as a tool to obtain the image of a surface, with a magnification that is sufficiently large for both macro- and micro-structures (Castle et al. 1997). The SEM uses electrons rather than light for making the image. There are many advantages to using SEM over a light microscope. The SEM has a large depth of field which is why it can focus on a large amount of the sample at a time. The SEM also produces images with high resolution (Satterfield et al. 1996).

Preparation of the samples for SEM is very easy, and requires only that the sample be conductive. The combination of higher magnification, larger depth of field, higher resolution and ease of sample preparation makes the SEM one of the most important scientific tools used in research today (Drzazga et al. 2006). A schematic of an SEM is shown in Figure 2.9.

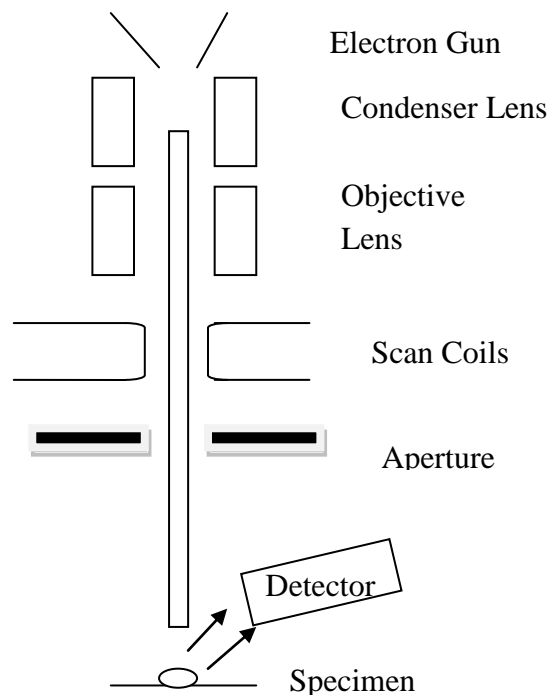


Fig. 2.7: Schematic view of the operation of SEM

“The specimen is placed inside the microscope's vacuum column through an air-tight door. Then, the air is pumped out of the column, and an electron gun, situated at the top, emits a beam of high energy electrons. This beam travels downward through a series of magnetic lenses which are designed to focus the electrons to a very fine spot. Near the bottom, a set of scanning coils has lens that focus the beam back and forth across the specimen. As the electron beam hits each spot on the specimen, secondary electrons are knocked loose from the specimen surface. An electron detector counts these electrons and reflects the signals back to an amplifier. The final image is built up from the number of electrons emitted from each spot on the test specimen (Castle et al. 1997).

2.9.4.4 Brunauer–Emmett–Teller (BET) Theory

Brunauer–Emmett–Teller (BET) theory explains the physical adsorption of gas molecules on a solid surface. It is an important analytical technique for the measurement of the specific surface area of a material. This theory is an extension of the Langmuir theory which basically describes monolayer molecular adsorption and multilayer adsorption with the following hypotheses (Satterfield et al. 1996):

- gas molecules physically adsorb on a solid in layers infinitely
- there is no interaction between each adsorption layer, and
- the Langmuir theory can be applied to each layer.

2.9.4.5 Thermogravimetric analysis (TGA)

Thermogravimetric analysis is used for material characterization. This is a technique which measures the change in mass of a material as a function of temperature. This analysis is carried out primarily to determine the following:

- the composition of materials (whether it is organic or inorganic)
- to predict their thermal stability at high temperatures.

A plot of mass change versus temperature, called a thermogravimetric (TG) curve, is plotted which helps in determining the extent of purity of analytical samples and the mode of their transformations within the specified temperature range (Satterfield et al. 1996).

Instrumentation

A Thermogravimetric analyzer uses a thermobalance, which consists of the following components: a) balance b) furnace c) programmer unit for temperature measurement and control and d) recording unit for mass and temperature changes.

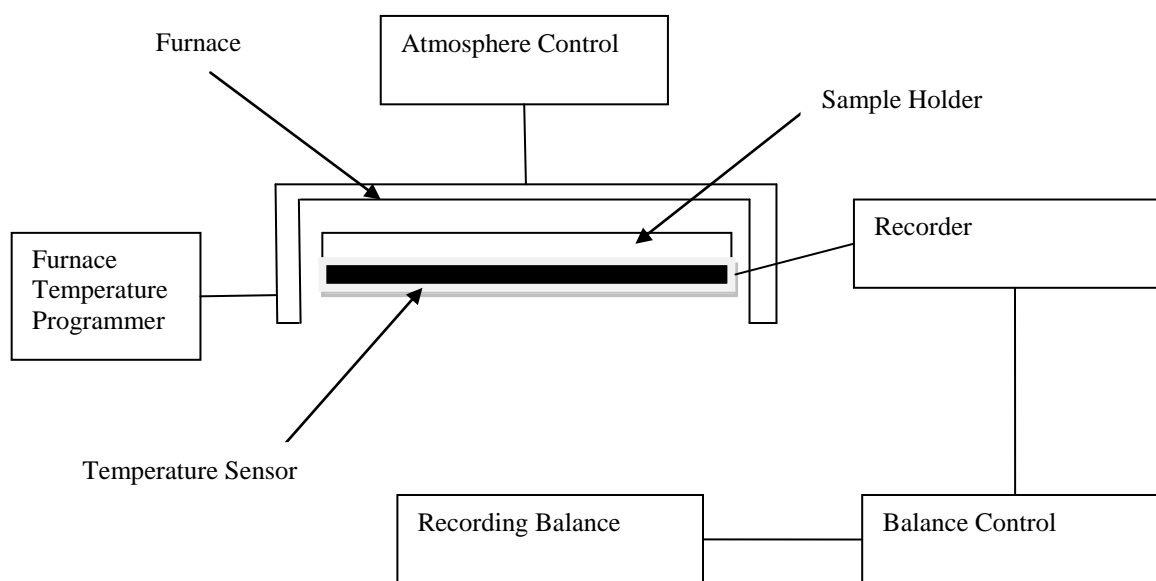


Fig. 2.8: Schematic of a thermobalance equipment (Satterfield et al. 1996).

Summary

It can be concluded from the literature review that the concept of microwave photochemistry already has become an important topic in wastewater treatment. However, microwave photochemistry has not reached a degree of maturity. Some obstacles have been overcome with time, but the effect of microwave radiation on photochemical reactions is still in the developmental stage. TiO_2 plays an important role in photocatalytic reactions and its catalytic activity depends on its properties such as surface area, particle size, pore size and pore volume. In this research two different methods will be used to synthesize TiO_2 catalysts and will be compared. The combined effect of MW-UV irradiation and TiO_2 on a high concentration of phenol will be investigated in this study. Previous studies have shown that the metal electrodes in conventional UV lamps were easily damaged under microwave irradiation. Hence, a microwave electrodeless lamp, which comprises an envelope or bulb containing a plasma-forming medium, was substituted for a conventional lamp as the light source for UV energy.

CHAPTER 3

DIELECTRIC PROPERTIES OF PHENOL-WATER MIXTURES AT MICROWAVE FREQUENCIES FROM 1 TO 5 GHz

This chapter addresses the first research objective, and covers the experimental set-up and the procedure adopted to determine the permittivity of phenol-water mixtures. Dielectric properties were measured using a HP 8510 Vector Network Analyzer and a coaxial probe reflection method. In this study, the effects of frequency of microwave radiation, temperature and concentration on dielectric properties were determined.

3.1 Abstract

Phenol and its compounds constitute an important family of priority pollutants in aquatic environments. Phenol is a typical contaminant easily found in wastewaters coming from agricultural manufacturing activities, petroleum industries and oil refining industries. The contaminated water results in unpleasant taste and odors; are very toxic and have high oxygen demands and needs to be treated before using as potable drinking water by the remote and rural communities. Microwave treatment can provide an effective technology for the removal and degradation of phenol from wastewater. In this case dielectric properties information can be useful in designing a microwave applicator, to be used for the treatment of water containing phenol. Dielectric properties of phenol in water were measured using a HP 8510 Vector Network Analyzer and a coaxial probe reflection method. In this study the effect of frequency, concentration and temperature on dielectric properties was determined.

3.2 Introduction

Phenol is one of the most common organic water pollutants and is of concern due to its toxicity at a low concentration. It can come to the environment from natural as well as anthropogenic sources. Disinfection and oxidation processes for phenol can lead further to form more harmful substituted compounds. Phenol is a compound of interest in environmental research because it is the most ubiquitous contaminant in wastewaters from several industrial activities. For example, the agri-food, pharmaceutical, chemical, and petrochemical industries (Gimeno et al. 2007), oil refineries, paper mills, olive oil mills, wood processing, coal gasification, and textile and, resin manufacturing discharge (Ahmaruzzaman et al. 2005) phenols in much higher concentrations than the toxic levels set for this compound. Use of microwave irradiation rather than conventional heating has improved product selectivity as well as accelerated reaction rates (Buffler et al. 1993; Zhang et al. 2001, 2003). Each material has a unique dielectric spectrum in the microwave frequency range because of its particular structure and dissimilar response to an external field.

The dielectric property, the ability to convert electromagnetic energy into thermal energy, can be described using complex permittivity, ϵ . The real part, ϵ' , shows the ability of a material to store charge, and ϵ'' , the imaginary part, characterizes the heat related to electromagnetic losses in the material (Polaert et al. 2005). Dielectric properties depend on the composition and, density of a material, temperature and frequency.

Accurate dielectric measurements play an important role in many engineering applications such as microwave and microwave-assisted systems for environmental applications including the treatment of wastewater pollutants. Knowledge of dielectric properties is important to understand the interaction between a phenol-water mixture and an electromagnetic field. The behaviour of phenol-water samples with frequency and temperature should be helpful in dielectric heating

applications and in developing a dielectric-property-based microwave applicator for treatment of phenol-water mixtures.

To design a combined microwave-photocatalytic treatment system for phenol in water, it was deemed necessary to understand the response of phenol-water mixtures to microwave radiation. Penetration depths calculated in this chapter were used in designing the reactor, e.g. height, thickness, described in the next chapter such; that it would allow proper penetration of microwaves through the wall of the sample holder and the phenol-water samples at a microwave frequency of 2.45 GHz. In this study, a HP 8510 Network Analyzer and the coaxial probe reflection method was used to measure the dielectric properties of phenol-water mixtures. Over three decades, the open ended coaxial probe technique with an automated vector network analyzer has been applied to liquids, colloids and suspensions because of reported advantages over the transmission line method (Bao et al. 1994).

3.3 Experimental Method

3.3.1 Sample preparation

The samples were prepared with commercially available phenol (analytical grade) and Milli-Q water. A stock solution of phenol (2500 ppm) was prepared. Milli-Q water was added for making the samples of desired concentration for experimental analysis. The actual concentration of phenol in wastewater from various industries varies from 0.1 to 6800 ppm; a concentration higher than 1450 ppm is lethal to microorganism. Keeping this in mind, the samples were prepared with concentrations of 1000, 1500 and 2000 ppm.

3.3.2 Measurement Setup

A high performance microwave vector network analyzer (VNA) system (Figure. 3.1) having a frequency range of 0.045 to 26.5 GHz was used for permittivity measurement with a coaxial probe. One side of the coaxial transmission line was connected to an HP 8515A S-Parameter Test Set and the other end was inserted into the sample solution. Figure 3.2 shows a block diagram of the network analyzer configuration which consisted of a HP 8510B network analyzer, a HP 8341B microwave signal source and a HP 8515A S-Parameter test set. All the units in the system were controlled by the commands issued through the HP 8510B network analyzer. The HP 8510B dielectric probe kit consisting of the probe, related software and calibration standard was used for the coaxial probe measurements. The control software (Agilent Tech V: 85070D) was modified in the attached computer for measuring the dielectric property values. Microwave signals are transmitted by the VNA to the coaxial probe and this conveys these signals to the sample from where a reflected part of the signal is returned back to the network analyzer from which the values for dielectric properties were obtained. The magnitude of the reflected signals depends upon the dielectric properties of the material under test. Based on the microwave signals transmitted to and received from the material under test, the vector network analyzer measures the reflection coefficients at the surface of the probe and test material. Then the reflection coefficients are sent to the work station where it is converted into the ϵ'' of the material under test. (Mishra et al. 2006 a,b, 2007; J.Z. Bao et al. 1994).

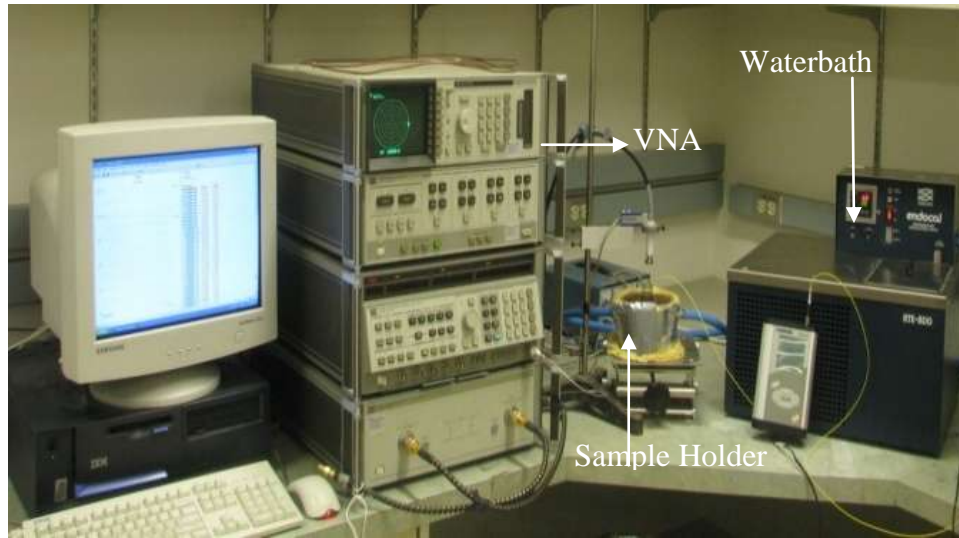


Fig. 3.1: Permittivity measurement setup showing the HP 8510 system with coaxial probe.

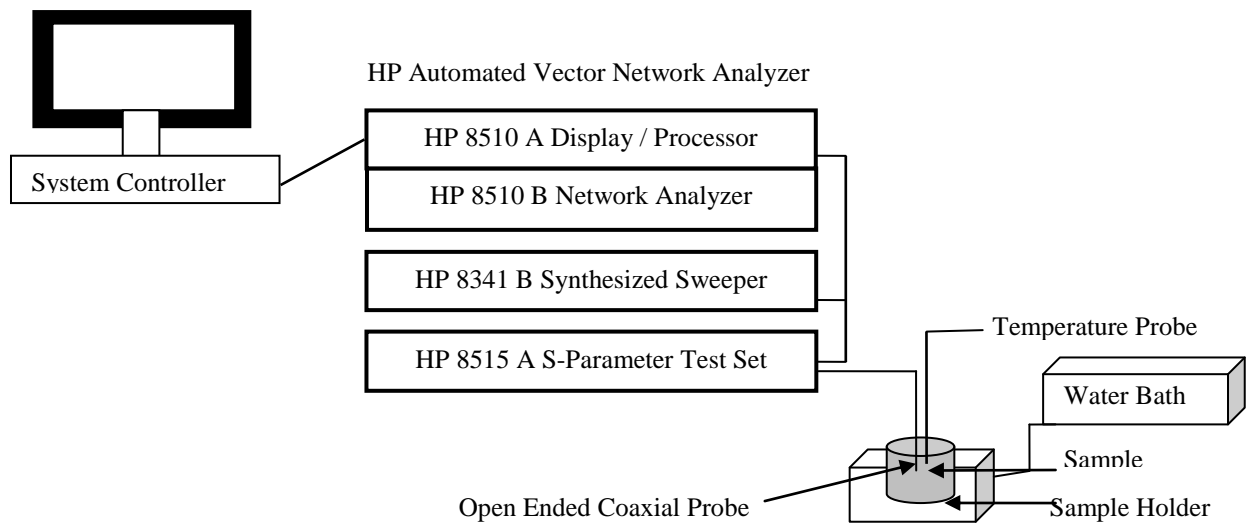


Fig. 3.2: Schematic of a HP 8510 Vector Network Analyzer and measurement system.

3.3.3 Dielectric measurement

The HP 8510 measurement system was used to measure the dielectric constant (ϵ') and loss factor (ϵ'') in the laboratory because of its availability and accuracy in measuring dielectric properties over a wide range of frequencies. To eliminate any systematic errors, calibration was

performed each time before taking readings by measuring the properties of three known standards, open by exposing the coaxial probe open end to the air, a short block and distilled water at room temperature. The solutions of known dielectric properties were measured following the user manual in the software; in this case the reference material used was “methanol”, (National Physical Laboratory Report MAT 23. Jan, 2012). All the dielectric constant values were within $\pm 5\%$ error and loss factor values were within $\pm 10\%$ error at 25°C and 40°C for methanol as shown in the appendix.

The frequency range was tuned in the system from 1-5 GHz and the work station was used for the measurement of the dielectric values. Samples of the phenol-water mixtures (each of 5 mL) prepared in triplicate with concentrations of 1000, 1500 and 2000 ppm were used for the dielectric measurements at two temperatures, 25°C and 40°C . The lower temperature of 25°C was chosen because of its proximity to room temperature. During treatment in the microwave, the temperature will rise, and therefore a temperature of 40°C also was used. A refrigerated circulating temperature bath was used to maintain the temperature at the desired level and measurement of sample temperature was done at regular intervals using an external thermocouple and sensors (FISO Tech Ltd.).

Dielectric constants and loss factor values were measured in triplicate for each sample and average values were calculated. The other parameters, including loss tangent or dissipation factor ($\tan\delta$), power factor (P_f) and the penetration depth (d_p) were calculated. In this experiment, the effect of concentration on dielectric properties at 25°C for all three concentrations, as well as the effect of temperature at 40°C for 1500 ppm were studied (Venkatesh et al. 2004, 2005; Mishra et al. 2006a, b).

3.4 Results

The dielectric properties of water-phenol mixtures including ϵ' and ϵ'' , were measured with the method described above and $\tan\delta$, P_f and d_p were calculated as described below. The effects of concentration, temperature and frequency on the dielectric properties of the mixtures are presented below. The mathematical expression for the complex permittivity (ϵ) of a material is, $\epsilon = \epsilon' - j \epsilon''$, where $j = \sqrt{-1}$. $\tan\delta$ is the ratio, ϵ''/ϵ' . Materials with higher ϵ'' values indicate faster microwave energy absorption rates. Power factor is a function of the loss tangent and is defined as $P_f = \tan\delta/\sqrt{1 + \tan^2\delta}$. Penetration depth is defined as the depth in the sample where the power density of microwave radiation is reduced to $1/e$ or 36.8% of its initial value at the surface. It is a function of the relative dielectric constant and the relative loss factor (Meda et al. 2005). Having the dielectric constant and the loss factor, the power penetration depth can be calculated by the following relationship (Buffler et al. 1993)

$$d_p = \frac{c}{2\sqrt{2}\pi f \left\{ \epsilon_r' \left[\sqrt{1 + \left(\frac{\epsilon_r''}{\epsilon_r'} \right)^2} - 1 \right] \right\}^{1/2}} \quad (3.1)$$

where d_p is the penetration depth (m) and c is the speed of light ($3 \times 10^8 \text{ ms}^{-1}$) in a vacuum.

3.4.1 DIELECTRIC CONSTANT (ϵ')

3.4.1.1 Effect of concentration

Three concentrations, 1000, 1500 and 2000 ppm, of the phenol-water mixture were used to measure the dielectric constant at a constant temperature of 25°C to see how the relative dielectric

constant changed with concentration. It was found that the value ranged from 77.6 ± 0.8 to 68.9 ± 0.6 at 1000 ppm, 75.9 ± 1.0 to 66.9 ± 1.1 at 1500 ppm, and 73.2 ± 1.0 to 66.5 ± 1.2 at 2000 ppm over the frequency range of 1-5 GHz (Figure 3.3).

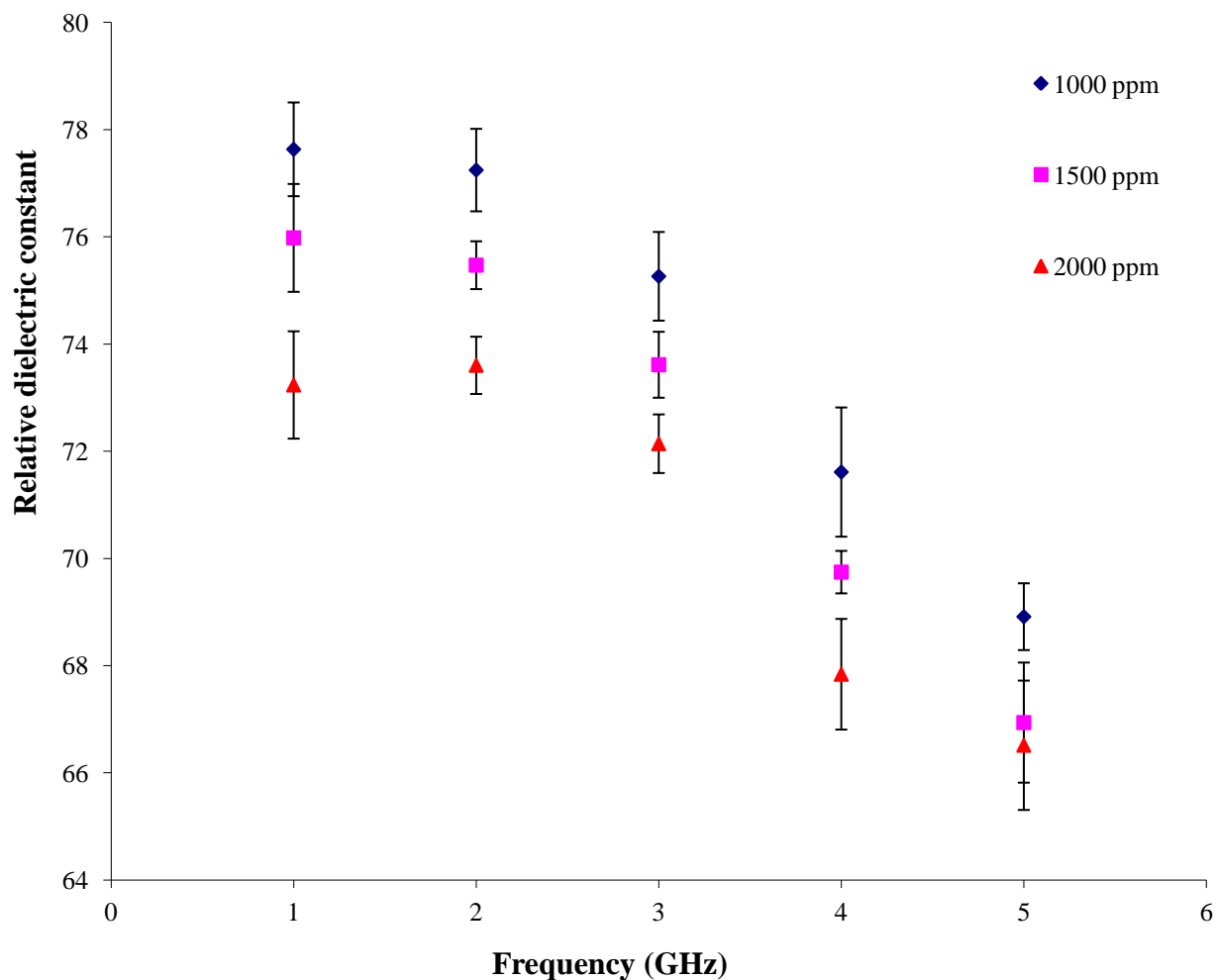


Fig. 3.3: Variation of the dielectric constant with frequency and concentration of phenol-water mixture. Error bars represent one standard deviation and may not be visible in some cases due to small values.

3.4.1.2 Effect of temperature

The relative dielectric constant of the phenol-water mixture at a concentration of 1500 ppm was measured at two temperatures, 25°C and 40°C, over the frequency range of 1-5 GHz. The values varied from 75.9 ± 1.0 to 66.9 ± 1.1 at 25°C and 70.8 ± 1.0 to 63.9 ± 0.7 at 40°C (Figure 3.4).

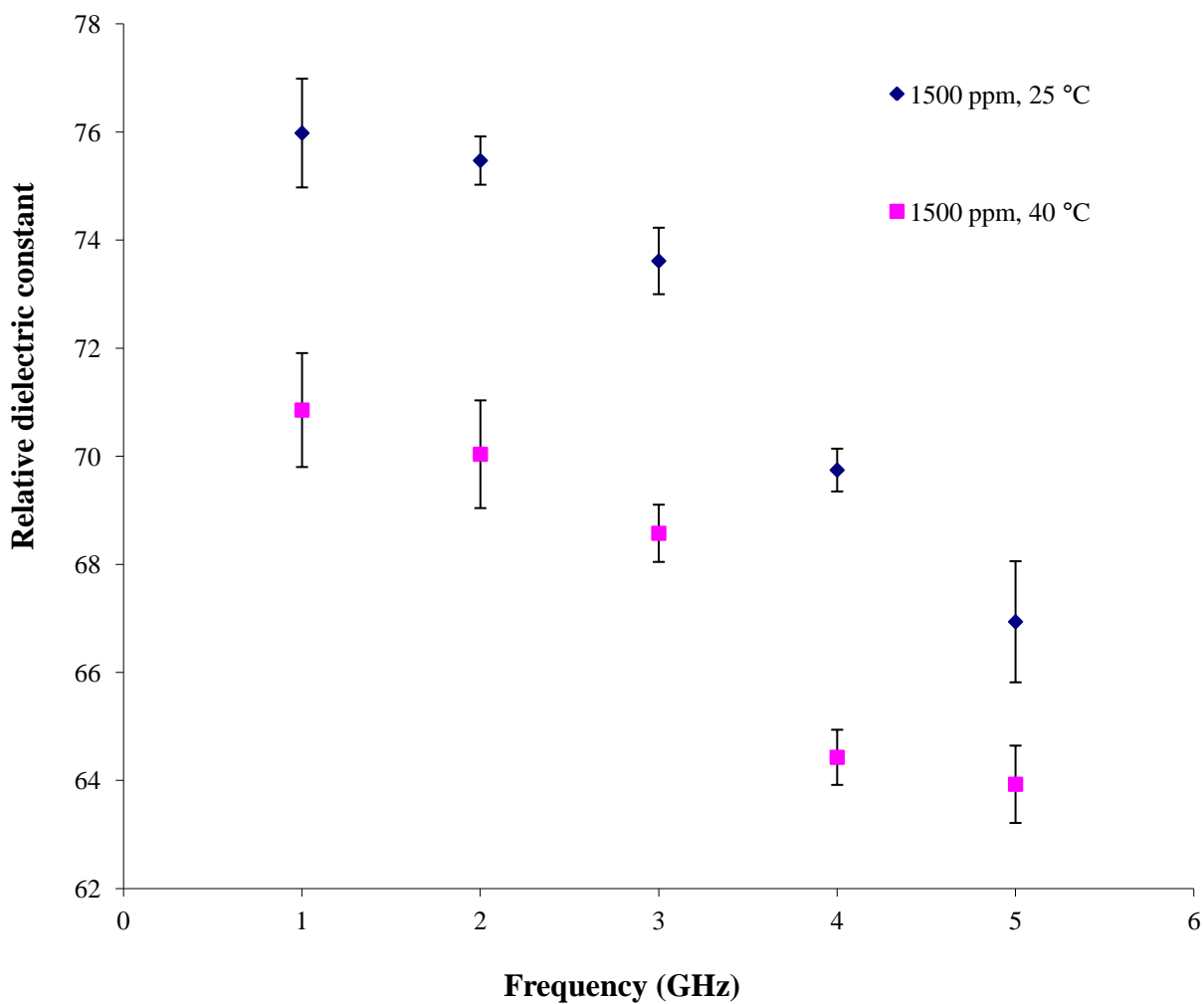


Fig. 3.4: Variation of the dielectric constant with frequency and temperature of phenol-water mixture. Error bars represent one standard deviation and may not be visible in some cases due to small values.

3.4.2 LOSS FACTOR (ϵ'')

3.4.2.1 Effect of concentration

Loss factor showed an increasing trend with frequency. Experimental results showed that the three concentrations had almost the same loss factor over the frequency range of 1-5 GHz, and that the relative loss factor increased as frequency increased for all three concentrations. For the 1000 ppm concentration, the value increased from 4.9 ± 1.0 to 17.1 ± 1.2 , for 1500 ppm from 4.8 ± 1.1 to 16.6 ± 2.7 , and for 2000 ppm the relative loss factor increased from 4.3 ± 0.4 to 16.1 ± 1.2 (Figure 3.5).

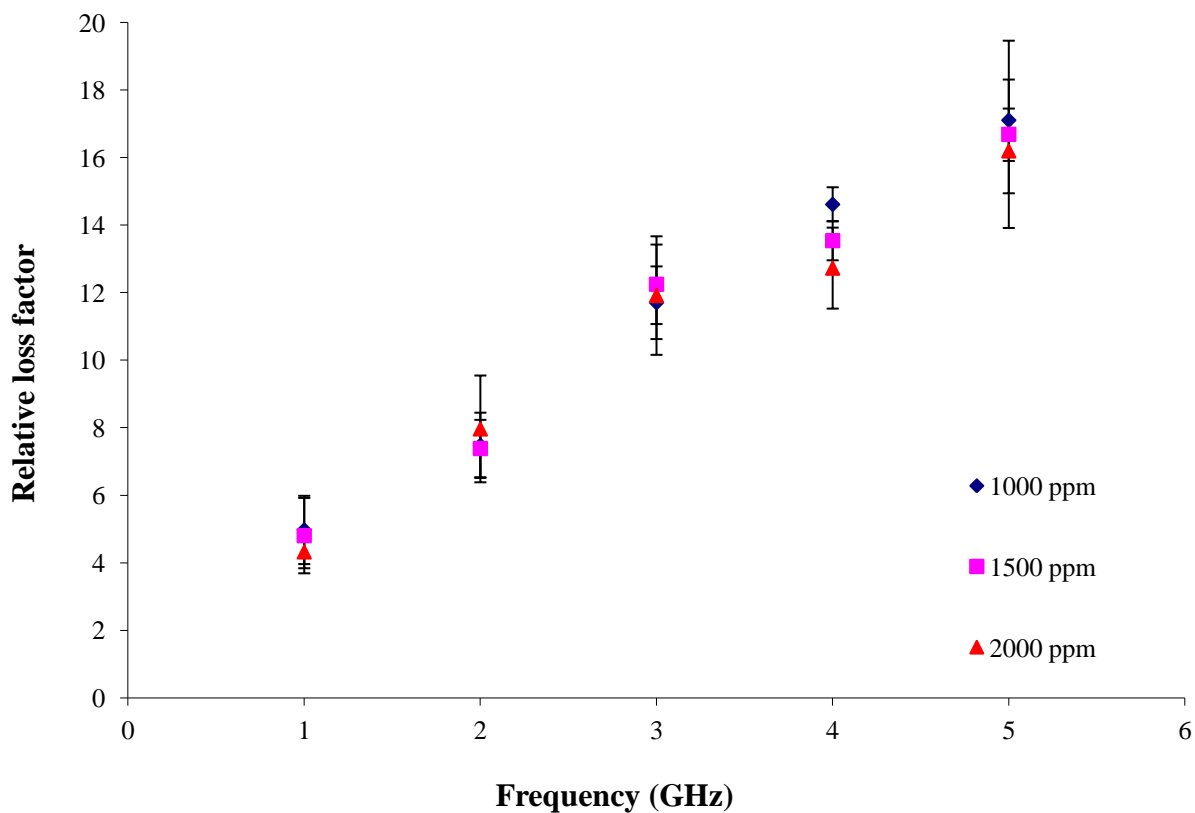


Fig. 3.5: Variation of the loss factor with frequency and concentration of phenol-water mixture.

bars represent one standard deviation and may not be visible in some cases due to small values.

3.4.2.2 Effect of temperature

The loss factor of the phenol-water mixture at 1500 ppm concentration was measured at 25°C and 40°C, and decreased with an increase in temperature at a particular frequency. It was found that the value ranged from 4.8 ± 1.1 to 16.6 ± 2.7 at 25 °C, and from 4.9 ± 1.6 to 11.0 ± 1.0 at 40°C over the frequency range of 1-5 GHz (Figure 3.6).

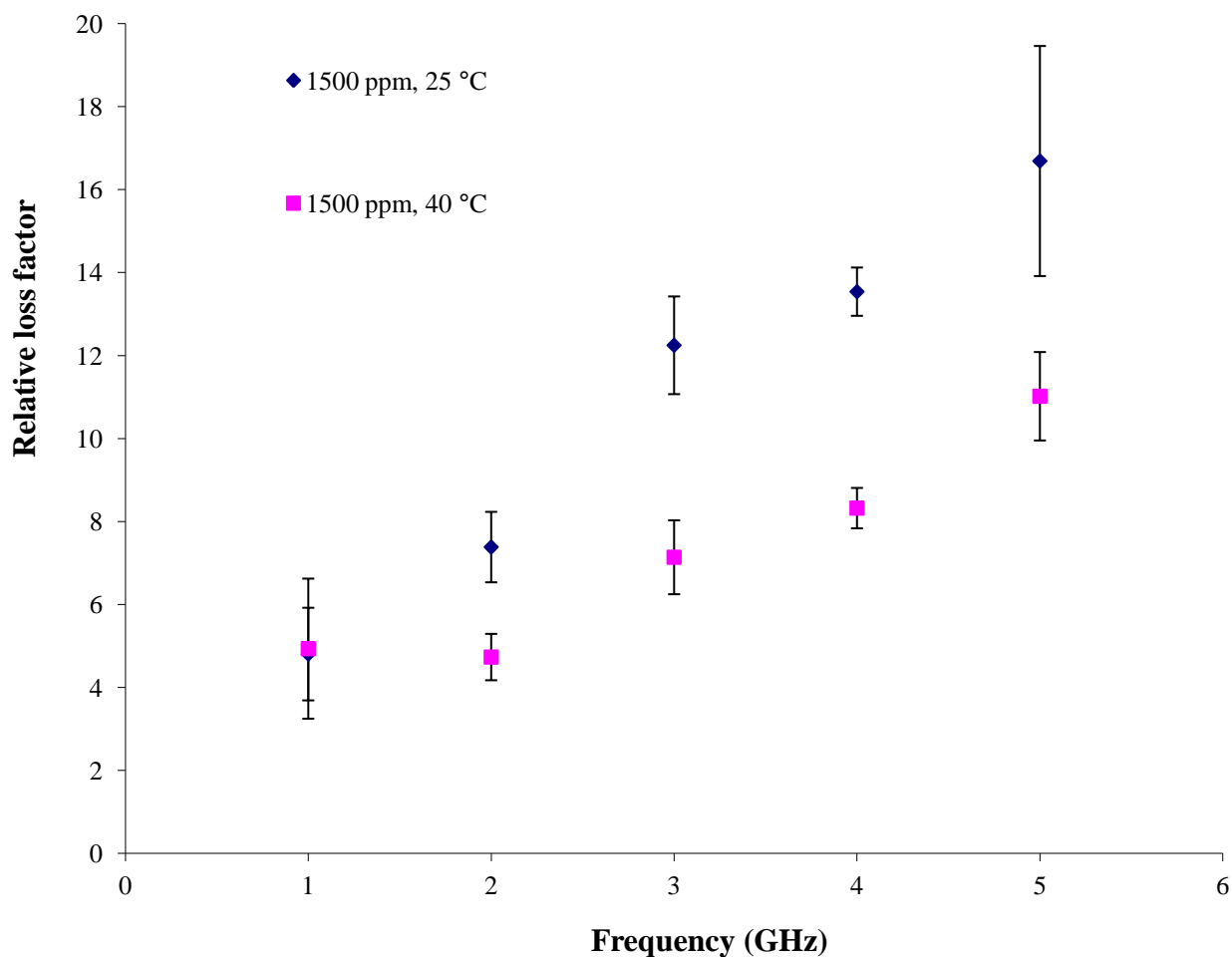


Fig. 3.6: Variation of the loss factor with frequency and temperature of phenol-water mixture.

Error bars represent one standard deviation and may not be visible in some cases due to small values.

3.4.3 LOSS TANGENT ($\tan \delta$)

3.4.3.1 Effect of concentration

The loss tangent values increased steadily with frequency over the range of 1-5 GHz. The trend showed that concentrations did not have much effect on the loss tangent over the frequency range tested and the values ranged from 0.06 to 0.2 for 1000 ppm, 1500 ppm and 2000 ppm over the frequency range of 1-5 GHz, with a maximum standard deviation of ± 0.04 (Figure 3.7).

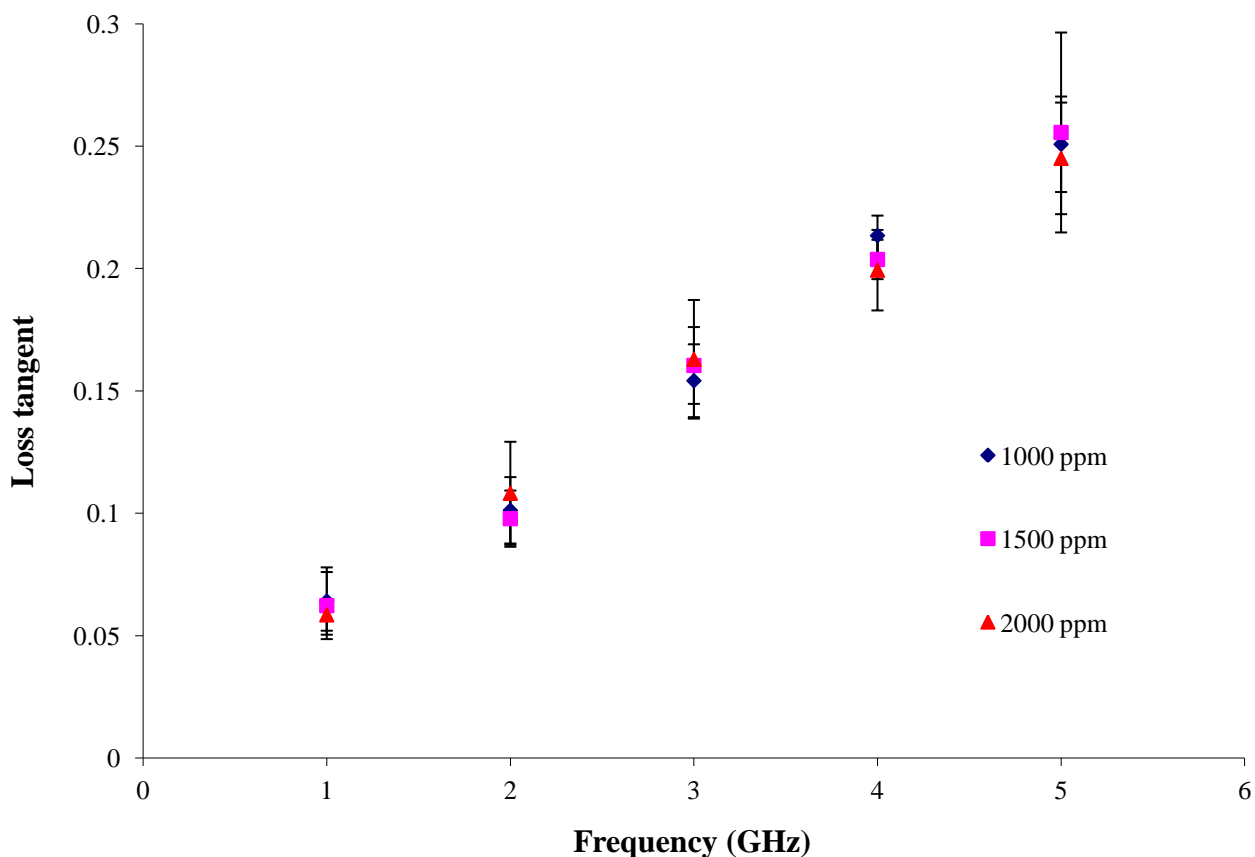


Fig. 3.7: Variation of the loss tangent with different frequency and concentration of phenol-water mixture. Error bars represent one standard deviation and may not be visible in some cases due to small values.

3.4.3.2 Effect of temperature

Loss tangent values for a phenol-water mixture of 1500 ppm concentrations were measured at 25°C and 40°C. The values were lower at higher temperatures at a particular frequency. Calculated values ranged from 0.06 to 0.2 at 25°C, and from 0.06 to 0.1 at 40°C, with a maximum standard deviation of ± 0.02 . At a frequency of 1 GHz, values were the same at 25°C and 40°C and values were lower at 40°C at 2 GHz or higher (Figure 3.8).

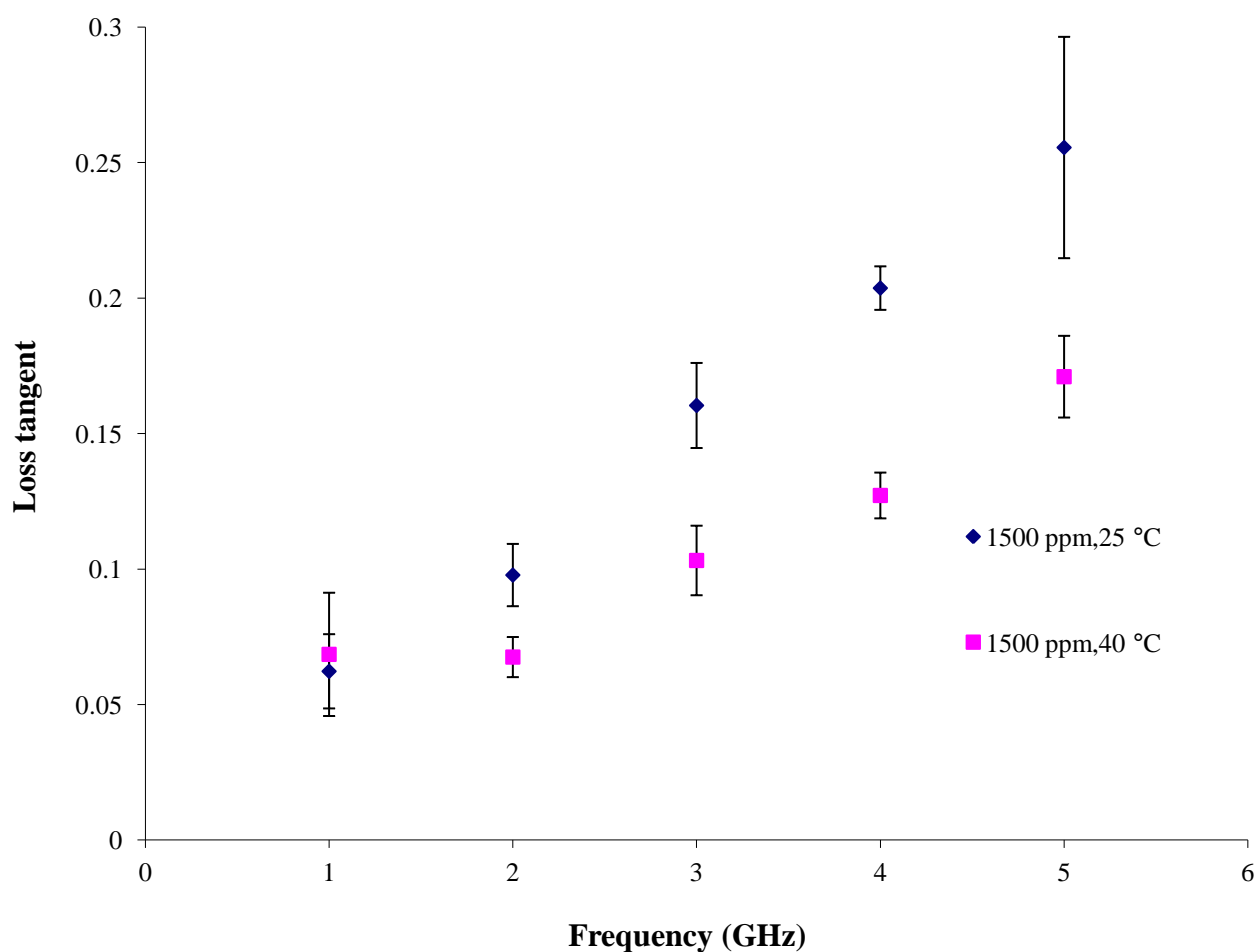


Fig. 3.8: Variation of the loss tangent with different frequency and temperature of phenol-water mixture. Error bars represent one standard deviation and may not be visible in some cases due to small values.

3.4.4 POWER FACTOR (P_f)

3.4.4.1 Effect of concentration

Power factor values exhibited a similar trend as did loss tangent, increasing steadily with frequency over the range of 1-5GHz, values ranged from 0.03 to 0.1 for the three concentrations (1000, 1500, and 2000 ppm) over the frequency range, with a small standard deviation (Figure 3.9).

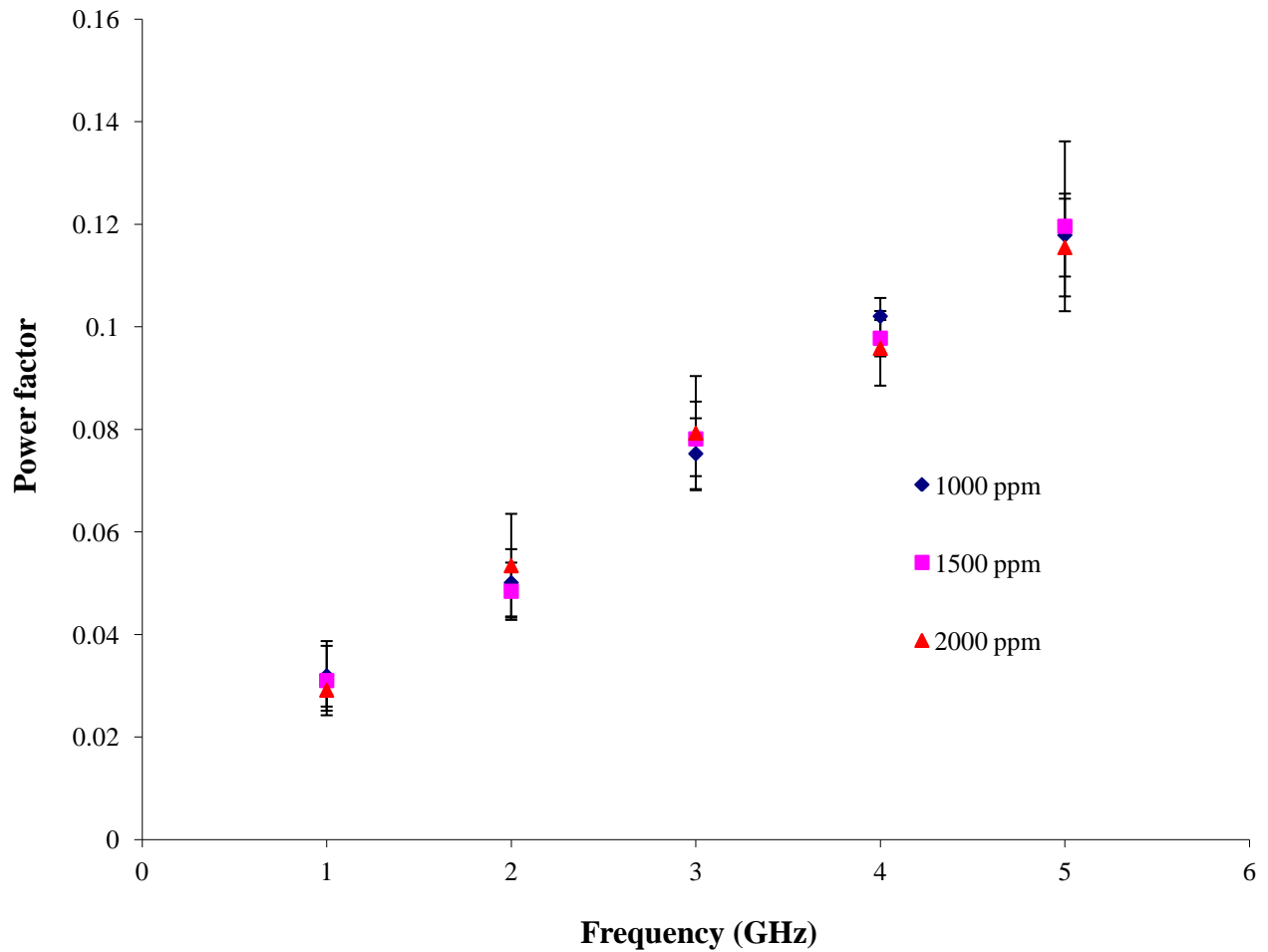


Fig. 3.9: Variation of the power factor with frequency and concentration of phenol-water mixture.

Error bars represent one standard deviation and may not be visible in some cases due to small values.

3.4.4.2 Effect of temperature

Power factor values for the phenol-water mixture were calculated for a concentration of 1500 ppm at 25°C and 40°C. Values ranged from 0.03 to 0.1 at 25°C, and from 0.03 to 0.08 at 40°C over the frequency range of 1-5 GHz. At 1 GHz the values were the same for 25°C and 40°C, but values were lower at 40°C at 2 GHz or higher (Figure 3.10).

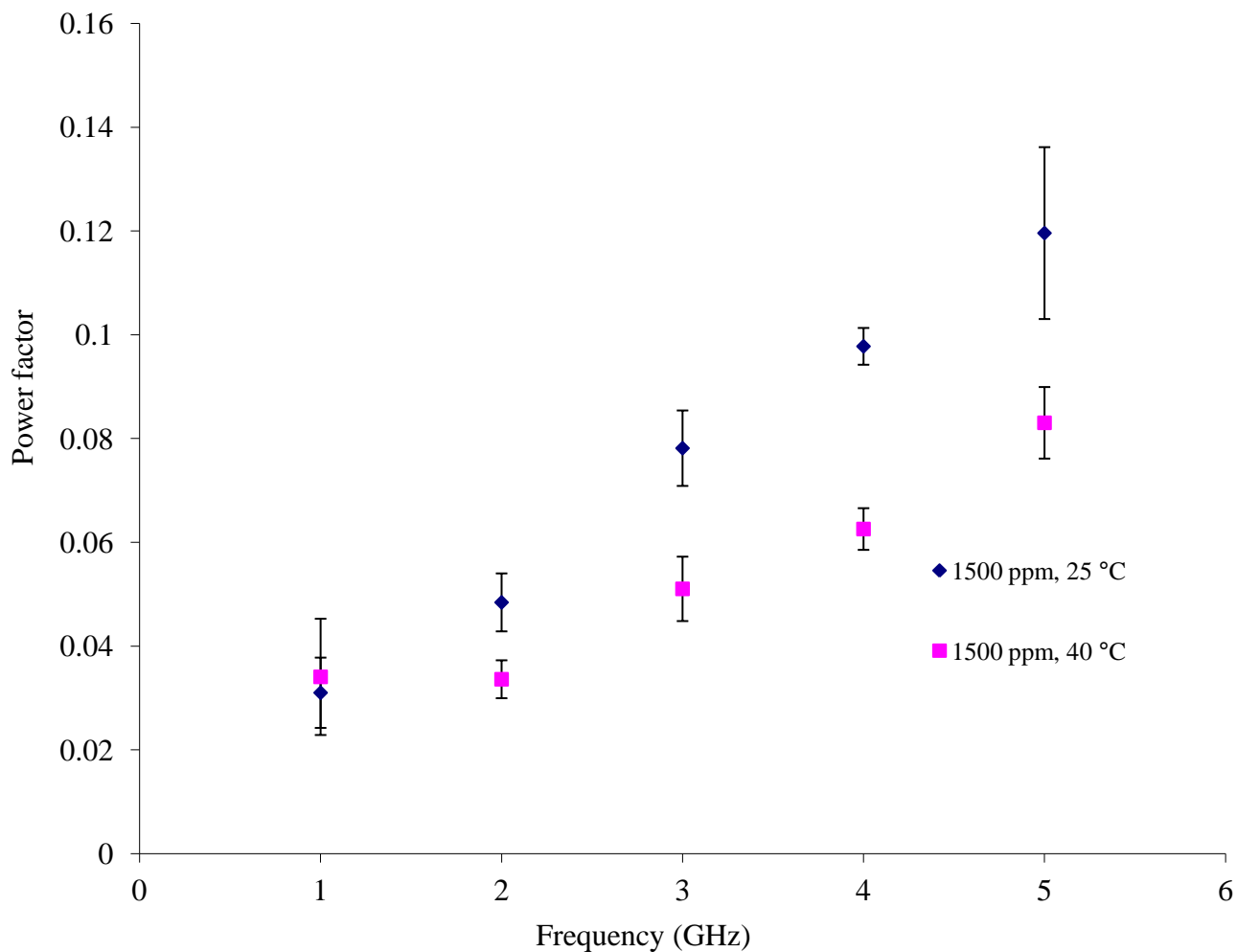


Fig. 3.10: Variation of the power factor with frequency and temperature of phenol-water mixture.

Error bars represent one standard deviation and may not be visible in some cases due to small values.

3.5.5 PENETRATION DEPTH (d_p)

3.5.5.1 Effect of concentration

Penetration depth for the three concentrations (1000, 1500 and 2000 ppm) were calculated using equation 3.1 and the results showed that it decreased sharply over the frequency range of 1-2 GHz, and then steadily decreased with an increase in frequency to 5 GHz. It was found that the value ranged from 8.7 ± 1.8 to 0.4 ± 0.03 for 1000 ppm, 8.1 ± 0.8 to 0.5 ± 0.01 for 1500 ppm, and 10.1 ± 0.07 to 0.4 ± 0.04 for 2000 ppm. For a concentration of 2000 ppm, the value for the penetration depth at 1 GHz was higher than for the other two concentrations (Figure 3.11).

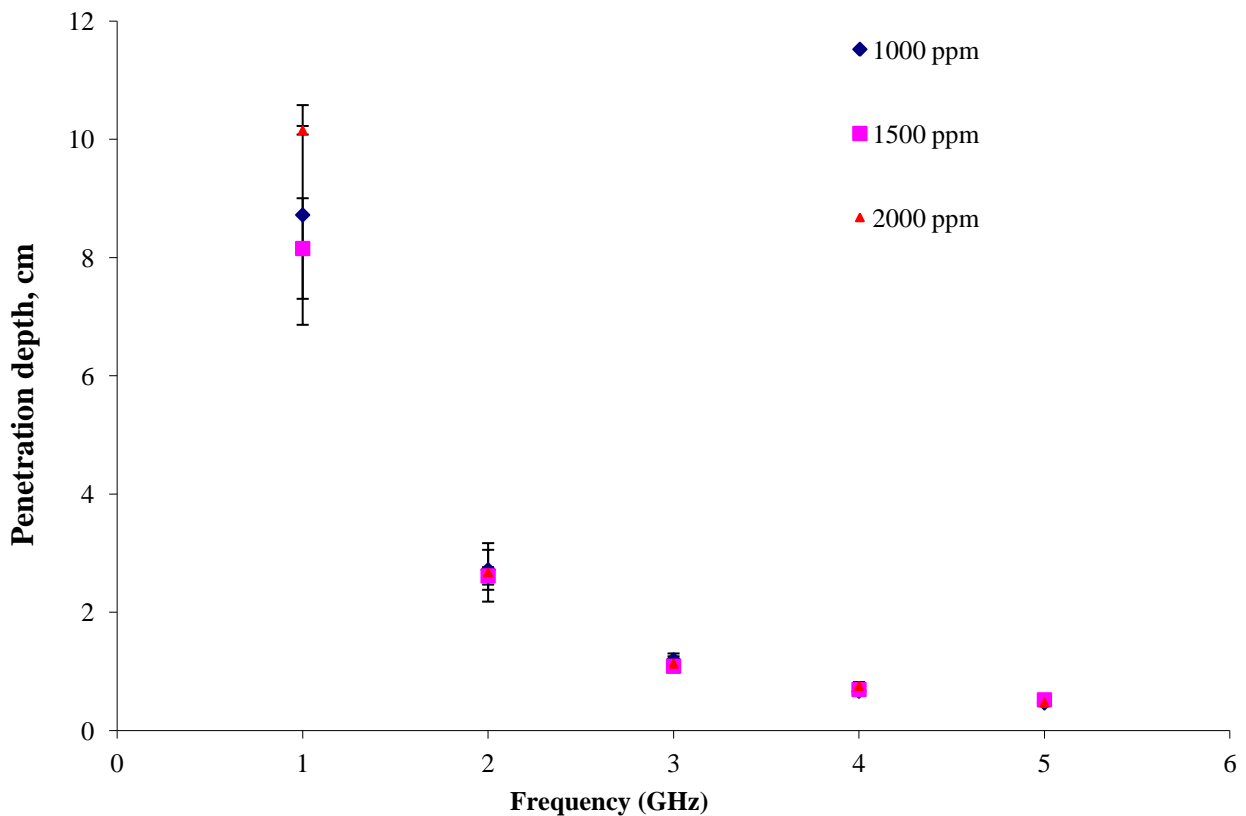


Fig. 3.11: Variation of the penetration depth with frequency and concentration of phenol-water mixture. Error bars represent one standard deviation and may not be visible in some cases due to small values.

3.5.5.2 Effect of temperature

To examine the effect of temperature (25°C and 40°C) on penetration depth, values were calculated for a concentration of 1500 ppm using equation 3.1. It was found that values ranged from 8.1 ± 0.8 to 0.45 ± 0.01 at 25°C, and from 8.9 ± 3.1 to 0.7 ± 0.06 at 40°C. It can be seen in (Figure 3.12) that penetration depth decreased sharply over the frequency range of 1-2 GHz, and then decreased steadily until 5 GHz. At the 40°C, penetration depth had a higher or similar value at 25°C.

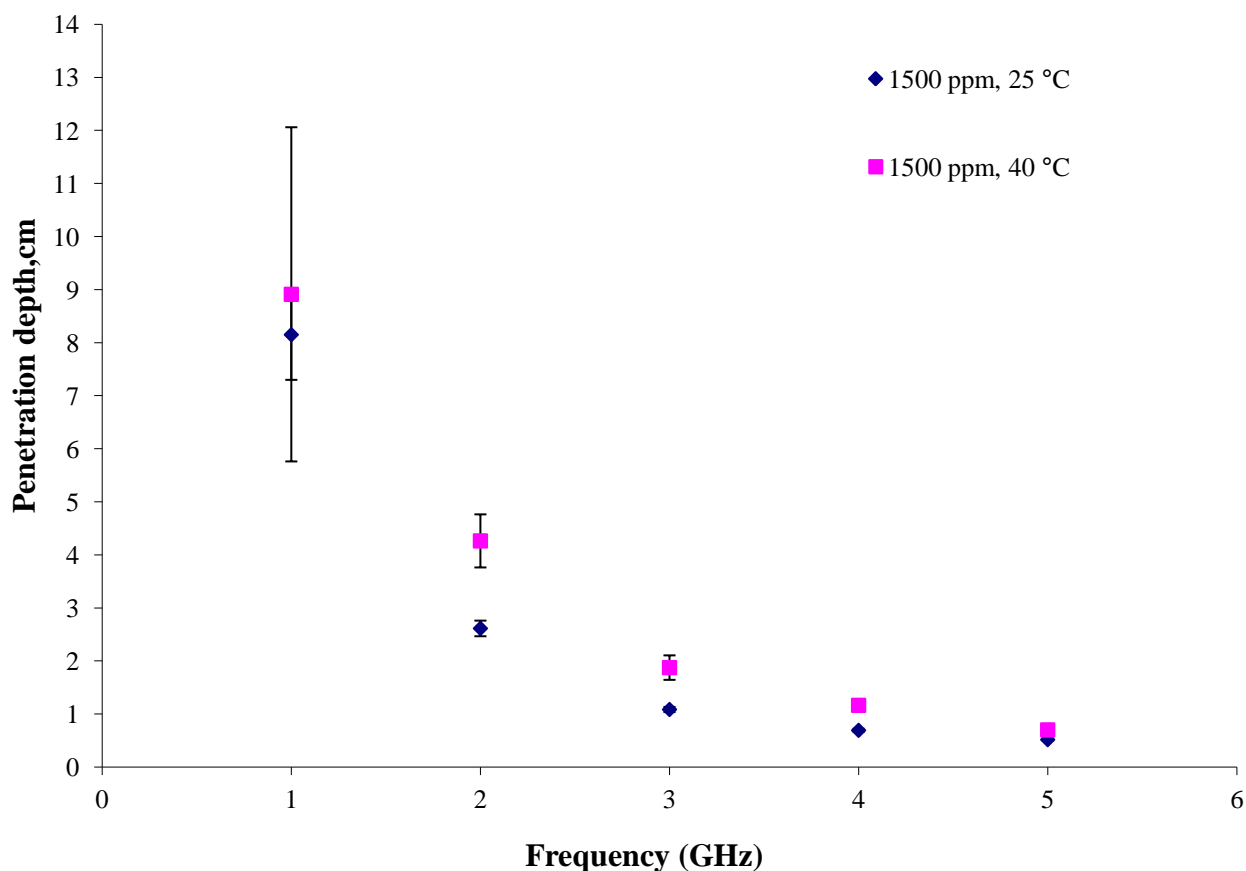


Fig. 3.12: Variation of the penetration depth with frequency and temperature of phenol-water mixture. Error bars represent one standard deviation and may not be visible in some cases due to small values.

3.5 Discussion

The experimental results show the variation in dielectric constant, loss factor, loss tangent, power factor and penetration depth as a function of frequency, concentration and temperature for phenol-water mixtures. It was observed that frequency and concentration had significant effects on the dielectric properties of phenol-water mixtures.

The dielectric constant decreased as the concentration of the sample increased for a particular frequency. With an increase in frequency, there was a decrease in the value of the dielectric constant as the temperature increased at a particular frequency, because a higher temperature results in randomized agitation and Brownian movement of the molecules in the sample (Bottcher et al. 1973). Concentration did not have a significant effect on the loss factor over the frequency range tested. At higher temperatures, the loss factor decreased at frequencies of 2 GHz or higher. Mishra et al. (2009) reported similar results for naphthenic acid in water, in that for a particular frequency the dielectric constant and the loss factor decreased as the concentration of the sample or the temperature increased. Nia et al. (2010) measured the dielectric constants of water, methanol, ethanol, butanol and acetone, and observed that the dielectric constant of these fluids increased with a decrease in temperature.

Concentration had little effect on the value of the loss tangent or the loss factor at a particular frequency. Concentration had no effect on the power factor over the frequency range tested. At lower frequencies, temperature had no significant effect on the power factor, but at a frequency of 2 GHz or higher there was a decrease in the value of the power factor with an increase in temperature. At a particular frequency, concentration did not affect penetration depth. Penetration depth was greater at 40°C than at 25°C. The temperature and concentration dependence of the

dielectric parameters of a phenol-water mixture is quite complex, perhaps because of the nature of the molecular structure of phenol and its hydrogen bonding with water molecules.

3.6 Sample Holder Design

In this research, two types of systems, microwave and microwave-UV, were designed. The details are provided in Chapter 4. The sample holder was designed according to the penetration depths calculated in this chapter. The penetration depth of microwaves at 2.45 GHz was determined to be 2.91 cm for a 1500 ppm phenol-water mixture at 40 °C, and accordingly the dimensions of the sample holder were set to allow proper penetration of microwaves through the wall (height = 5.24 cm, external diameter = 3.91 cm, thickness = 0.5 cm) of the sample holder and the phenol-water samples. A photographic view of the sample holder is shown in Figure 3.13 and schematic in Figure 3.14. Two holes were made in the side wall of the sample holder to allow passage of phenol-water mixture to the water bath to maintain the temperature.



Fig 3.13: Photographic view of sample holder.

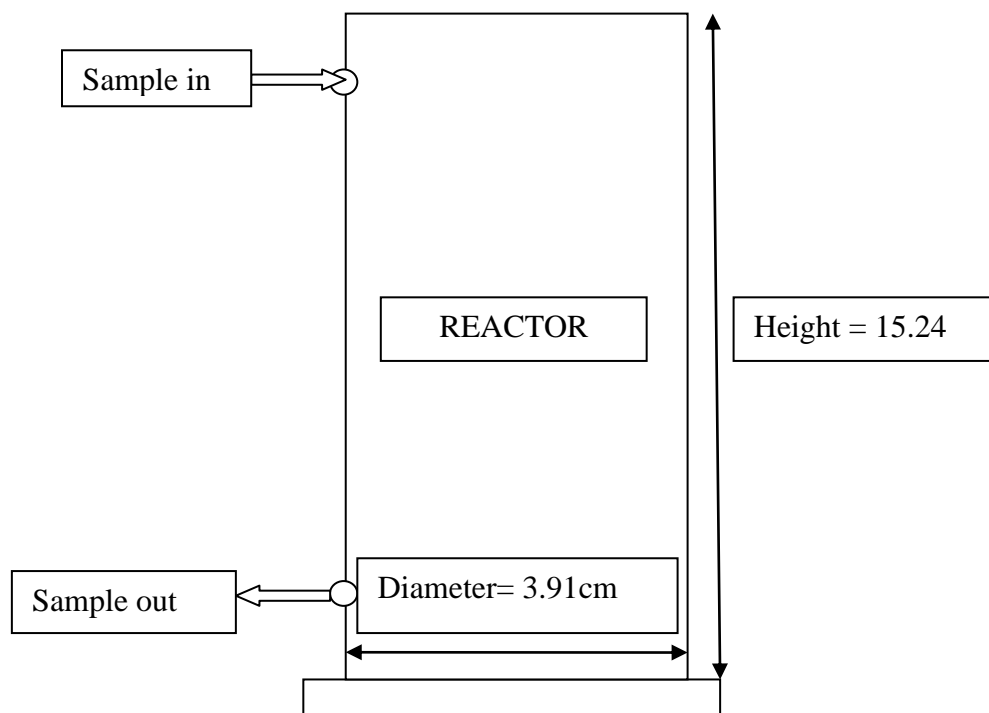


Fig. 3.14: Schematic of sample holder used in microwave treatment system.

3.7 Conclusions

Dielectric properties are fundamental and essential to the understanding, designing and modeling of microwave based applications. This has been the first reported study on measurement of the dielectric properties of phenol-water mixtures over a range of frequencies and at different temperatures. The frequency of most practical interest is 2.45 GHz and from the aforementioned results, it can be concluded that at this particular frequency, the dielectric properties (dielectric constant, dielectric loss factor) of phenol-water mixtures are appropriate for the design of a microwave-based treatment system. The data obtained in this study will inform the design of the microwave reactor employed in Chapter 4 and, potentially, commercial-scale systems.

CHAPTER 4

DEGRADATION OF PHENOL WITH A MICROWAVE-UV IRRADIATION TREATMENT SYSTEM USING NANO-TiO₂

In this chapter, the synthesis and characterization of titanium dioxide (TiO₂) nanoparticles by two different methods are discussed and their catalytic activity with microwave and combined microwave-UV irradiation systems was studied.

4.1 Abstract

TiO₂ nanoparticles with anatase structure were synthesized by hydrothermal and sol-gel methods using titanium tetra isopropoxide as a precursor. The particle size of hydrothermal synthesized catalyst was 16 nm and sol-gel synthesized catalyst was 20 nm after calcination at 500°C. Characterization of the synthesized catalysts was done on the basis of their crystallinity, crystallite size, and structural properties. X-ray diffraction (XRD) was used to calculate crystallite size. Scanning electron micrograph (SEM) technique was employed to determine the grain size. Two types of reactors, MW and MW-UV, were developed and catalytic activity of both the catalyst and efficiency of systems were studied. It was found that the MW-UV system with TiO₂ prepared with hydrothermal method was the most effective method to treat phenol-water solution.

4.2 Introduction

Oxide nanoparticles synthesized by several methods have gained importance because of their good electrical, optical and magnetic properties that are different from their bulk counterparts (Chen et al. 2007). Titanium dioxide (TiO₂) is a white, solid, inorganic substance that is thermally stable, non- flammable and not classified as hazardous material (Hsien et al. 2000). It is an

exceptionally important material with a vast range of applications in industrial and consumer goods including paints, adhesives, photocatalysis, ceramic materials, fillers, paper and paperboard, coatings, pigments, crayons, UV protection in sunscreens, cosmetics and pharmaceuticals, floor coverings, roofing materials, catalyst systems, food colorants, automotive products and water treatment agents. It has generated attraction in both fundamental research and practical development work (Porkodi et al. 2007). Among the various semiconductor materials, TiO_2 is the most widely used photocatalyst due to its non-toxicity, high activity, high stability, and low cost. It can generate highly reactive oxygen species such as O^{2-} and HO^\bullet , responsible for the oxidation of a wide variety of aliphatic and aromatic hydrocarbons (Granados & Paez-Mozo et al. 2005). TiO_2 exists in three forms and the band gap changes with a change in the phase from anatase (3.2 eV) to rutile (3.02 eV) to brookite (2.96 eV). Photocatalytic activity in the photodecomposition of organic pollutants of anatase is because of its large band gap (Patsoura et al. 2007; Bahnemann et al. 2007).

Nanosized TiO_2 has received much interest for applications such as optical devices and sensors, and photocatalysis has been used for environmental decontamination of a variety of organic compounds (Huang et al. 2007). The photocatalytic activity of titanium nanoparticles varies depending on its crystallinity, particle size, crystal phase, surface area, method of preparation, porosity, and shape and size distribution of pores (Chen et al. 2007; Thompson et al. 2006). It is known that the anatase form with small particle size and high crystallinity is required to obtain highly active titanium photocatalysts. Chhabra et al. (1995) has shown that only anatase TiO_2 particles act as a photocatalyst for the photodegradation of phenol, and that the rutile form is totally inactive for this reaction. The increase in surface area with a reduction in particle size means an increase in the number of active sites on which the electron acceptor and donor are adsorbed and participate in the redox reaction (Hoffmann et al. 1995). Photocatalytic oxidation reactions are

initiated when a photon of higher energy level or equal to the band gap energy is absorbed by a TiO_2 catalyst promoting an electron transfer (e^-) from the valence band to the conduction band with simultaneous generation of a positive hole (h^+) in the valence band (Mishra et al., 2009). The mechanism of radical generation ($\cdot\text{OH}$ and $\cdot\text{O}_2^-$) is presented as follows (Allen et al. 2008):



In the present work, TiO_2 nanoparticles were synthesized via hydrothermal and sol-gel methods because these methods are quite simple as compared to other methods such as dip-coating and refractive sputtering. Processing using these methods provides excellent chemical homogeneity and the possibility of deriving unique metastable structures. It involves the formation of a metal-oxo-polymer network from molecular precursors like metal alkoxides or metal salts. For example, the metal alkoxides may be hydrolyzed (eq. 4.4) and polycondensed (eq. 4.5 and 4.6) to form a metal oxide gel as follows:



where M is Si, Ti, Zr, Al, etc. and R is an alkyl group. The structure and properties of the resulting metal oxides are strongly influenced by relative rates of hydrolysis and polycondensation (Hafizah et al. 2009).

Characterization of the prepared catalyst has been done on the basis of their crystallinity, crystallite size, and structural properties. X-ray diffraction (XRD) was used to calculate crystallite size. Scanning electron micrograph (SEM) technique was used to determine the grain size. Efficiency for degradation of phenol using two prepared catalysts with the two developed systems (microwave and microwave assisted UV treatment) was studied.

Microwave energy has widely been applied in domestic, industrial and medical fields during the past two decades. It has been found that microwave irradiation not only can excite an electrodeless discharge lamp (MWL) to generate ultraviolet (UV) radiation which can excite TiO_2 for photocatalysis, but also could significantly improve the photocatalytic activity of TiO_2 for removing pollutants (Gao et al. 2007).

Using microwave irradiation rather than conventional heating has improved product selectivity and accelerated reaction rates (Zhang et al. 2001, 2003). It has been found that in the presence of microwave irradiation the photocatalytic efficiency of TiO_2 to remove pollutants was increased significantly (Horikoshi et al. 2004). The betterment of photocatalytic activity was because of the polarization effect of the highly defected catalysts in a microwave field, which increased transition probability of photon-generated electrons and decreased the electron-hole recombination on semiconductor surface (Zhihui et al. 2005). Horikoshi et al. (2004) illustrated that the synergistic effect of UV and microwave radiation in the presence of TiO_2 was superior for the degradation of rhodamine-B dye to TiO_2 photocatalytic degradation alone with UV radiation.

The objective in this chapter was to synthesize and characterise TiO_2 via two different methods (hydrothermal method and sol-gel method) and compare the photocatalytic activity of the prepared catalysts under two developed treatment systems, microwave only and microwave assisted UV irradiation combined with AOPs for the degradation of phenol.

4.3 Materials and Methods

4.3.1 Chemicals

Analytical grade reagents were used in the synthesis without further purification. Titanium (IV) isopropoxide ($\text{Ti} [\text{OC}_3\text{H}_7]_4$ TTIP) and anhydrous ethanol were purchased from Alfa Aesar. Phenol was obtained from Sigma Chemical Co. (St. Louis, MO, USA) and a stock solution of 2000 ppm phenol in water was prepared. All solutions were prepared using Milli-Q water from an EASY-pure ultrapure water system.

4.3.2 Synthesis of TiO_2 by the sol-gel route-

TiO_2 nanoparticles were synthesized by hydrolyzing titanium tetra isopropoxide in a mixture of anhydrous ethanol and water as shown in Figure 4.1. Two solutions were made: A, TTIP mixed with anhydrous ethanol and B, water mixed with ethanol. Solution A was added dropwise to solution B with constant and vigorous stirring for 2 h. Hydrolysis and condensation were conducted at room temperature and underwent aging for 12 h. The gel was dried in an oven at 80°C for 4h; it was then crushed into a fine powders with a mortar and pestle and then calcined at 500°C (Kavitha et al. 2013).

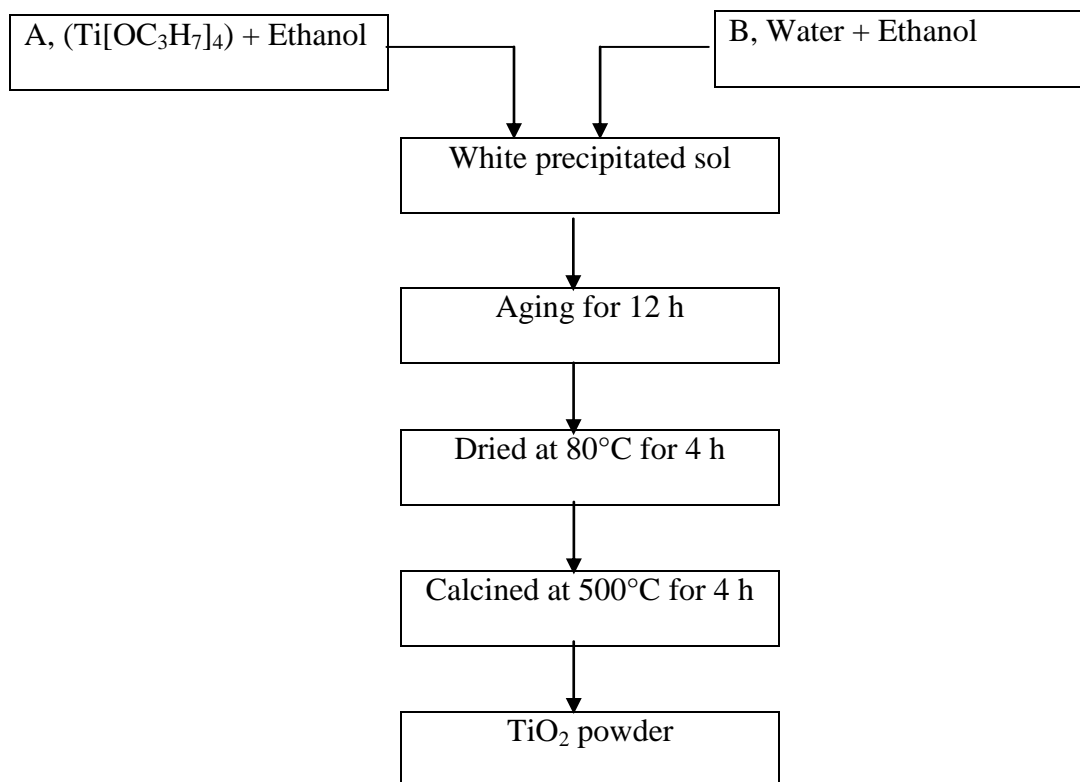


Fig. 4.1: Schematic diagram for the synthesis of TiO₂ powder by a sol-gel method.

4.3.3 Synthesis of TiO₂ by the hydrothermal method-

A schematic diagram for the synthesis of TiO₂ powder by the hydrothermal method is shown in Figure 4.2. After 2 h stirring, the solution was transferred in to a Teflon bottle and placed in an oven at 80°C for 24 h. The resulting solution was filtered and dried at 120°C for 24 h, then crushed into a fine powder with a mortar and pestle and calcined at 500°C for 4 h to produce TiO₂ powder (Kavitha et al. 2013).

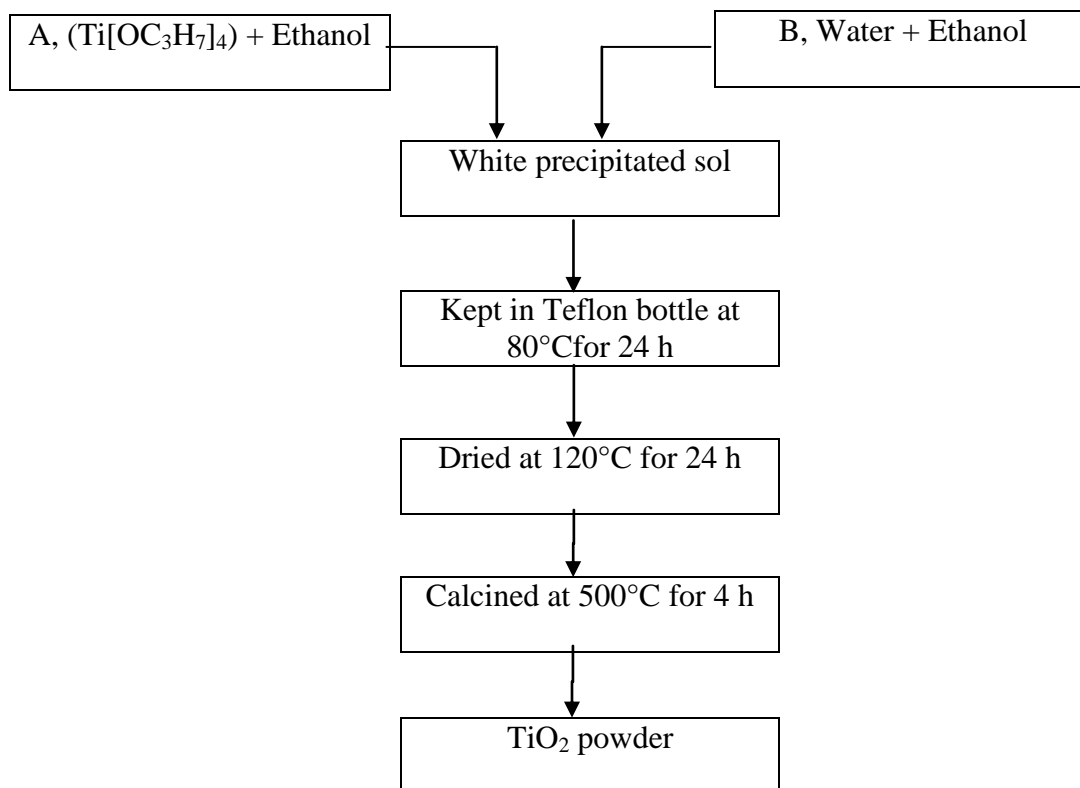


Fig. 4.2: Schematic diagram for the synthesis of TiO₂ powder by a hydrothermal method.

4.3.4 Catalyst Characterization Methods

4.3.4.1 X-ray diffraction (XRD) analysis

Phase analysis of calcined TiO₂ powder was carried out on a Bruker D8 Advance X-ray diffractometer using Cu K α radiation, which works on the Bragg-Bentano principle. The specimen was mounted in the center of the diffractometer and rotated by angle (θ) (Badoga et al. 2012).

4.3.4.2 Measurement of N₂ adsorption–desorption isotherms

The BET surface area and pore size distribution of the prepared catalyst via two different methods were measured with a Micromeritics ASAP 2000 instrument using low temperature N₂ adsorption-desorption isotherms. The sample was degassed in vacuum at 200°C before

measurement. The surface area was computed using the multi-point Brunauer-Emmett-Teller (BET) method from isotherms. The BJH method was used to determine pore diameter and pore volume (Badoga et al. 2012).

4.3.4.3 *Fourier transform infrared spectroscopy (FTIR)*

Fourier transform infrared (FTIR) spectra of the samples were obtained in the spectral range of 4000-400 cm^{-1} at a resolution of 4 cm^{-1} (Perkin-Elmer Spectrum GX). KBr pellet technique was used to obtain infrared spectra of the prepared catalysts via two different methods, hydrothermal and sol-gel at room temperature (Badoga et al. 2012).

4.3.4.4 *Scanning electron microscopy (SEM)*

Morphological analysis was carried out using a field-emission scanning electron microscope (JSM – 6010L V) operating at 20 keV.

4.3.4.5 *Thermogravimetric analysis (TGA)*

The thermal stability of the oxides was studied by thermogravimetric analysis (TA Instruments model STQ6000). TGA analysis was recorded on instrument in nitrogen with a heating rate of 10°C/min (Muneer et al. 2012).

4.3.5 Experimental setup for the MW-UV treatment system

Microwave experiments were performed using a household microwave (NNS615W, 1200 W, 2.45 GHz, Panasonic Canada Inc., Mississauga, ON) which was modified to accommodate the reaction chamber/ sample holder and tubing made of Teflon (Figure 3.14). The sample holder was

designed and fabricated in the Engineering Shops of the University of Saskatchewan, (Saskatoon, SK). A schematic of the experimental set up is shown in Figure 4.4 and a photographic view is presented in Figure 4.5.

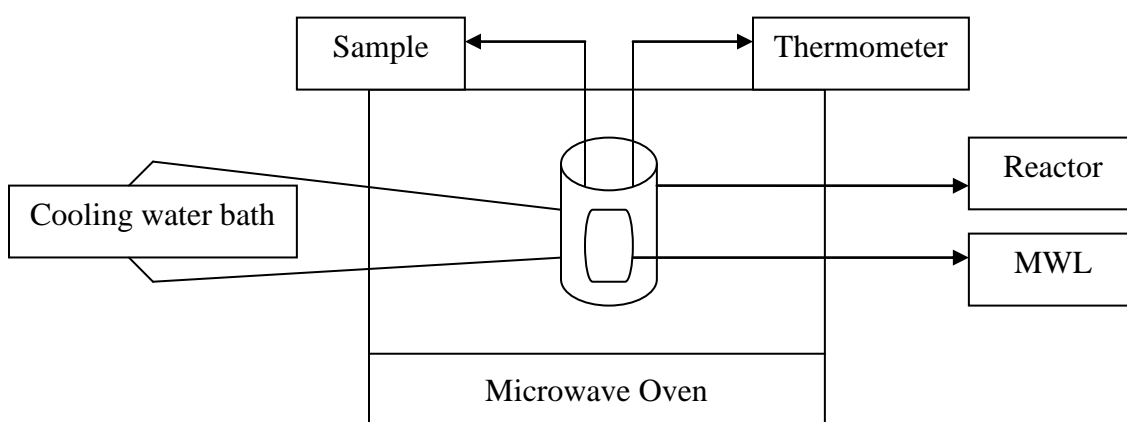


Fig. 4.3: Schematic of combined microwave-UV treatment system



Fig. 4.4: Photograph of the experimental setup

To make a combined microwave-UV treatment system, a microwave electrode-less lamp ($\lambda_{\text{max}} = 254 \text{ nm}$, power intensity 8W) placed centrally inside the reaction chamber was used as the source of ultraviolet rays (Figure 4.6).

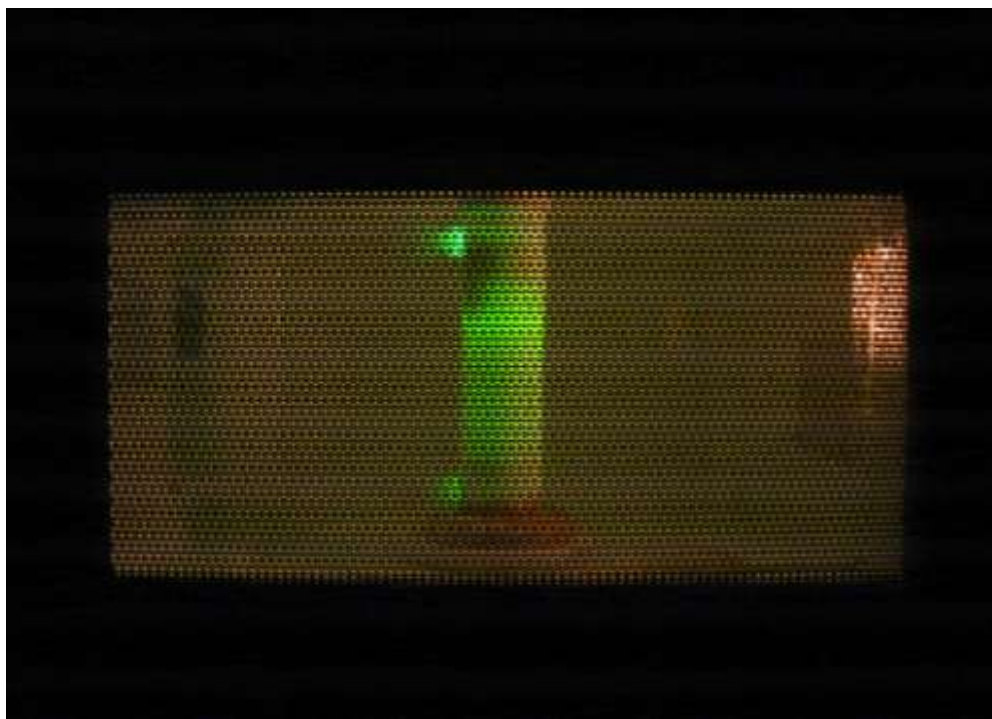


Fig. 4.5: Photograph of the microwave electrodeless lamp inside the reactor

This lamp was custom built and produced by Primarc UV Tech. (Easton, PA). Details on the working principle of this lamp are available in the literature (Klan et al. 2002). Microwave is absorbed by the electrodeless lamp which in turn emits the necessary UV rays for photocatalysis. An electrodeless lamp was used in this system because an electrode UV lamp in a microwave oven is not only difficult, but also unsafe because the lamp can be damaged by the electric discharge between the microwave oven and the metallic part of the lamp (Horikoshi et al. 2004). The turntable glass plate in the microwave oven was removed to stop rotation of the reactor and to avoid

damage to the reactor and mercury lamp. A round teflon plate was designed with the same circumference for the mercury lamp to stand vertically. Two holes were made at the top of the microwave, one was to take samples and the other was to insert the temperature sensor. Two holes were made in the side wall of microwave as well, the lower one was to get the sample out to the water bath and the upper one was for sample to come in again to the reactor after cooling. In this system, a 300 mL sample of 1500 ppm was mixed with 1 g of TiO_2 at 40°C with a flow rate of 400 mL/min for 120 min. no attempt was made to maintain the pH of the phenol-water solution of its initial value. The degradation of phenol in the presence of catalyst was studied.

A peristaltic pump was used to circulate the phenol-water mixture from the reaction chamber through a cooling coil. In this way the temperature of the sample could be maintained at 40°C . This also allowed the mixture to have sufficient residence time to stay inside the reaction chamber for maximum possible exposure to microwave radiation. The dosage of TiO_2 was as explained in the methodology flow chart. Samples were collected at 20 min or 120 min. Experiments were replicated three times at each level.

4.3.5.1 Estimation of Microwave Power

Microwave power was estimated using the following equation (4.7) and proposed by Cha et al (1999),

$$P = C_m \Delta T / t \quad (4.7)$$

where P = absorbed power of the microwave (W), m = mass of water (g), c = heat capacity of water ($4.184 \text{ J/g } ^\circ\text{C}$), ΔT = temperature rise ($^\circ\text{C}$) and t = irradiation time (s).

In this method, 20 mL of water was taken in a microwave safe container, stirred for about 10 seconds and then the temperature was measured and recorded. The container was placed on

center inside the microwave and heated from 10-60 s with an interval of 10 s at full power. After this, the container was immediately removed and the water was stirred for 10 s and the temperature was measured and recorded. The temperature of the water during experiments was measured with a temperature a sensor immediately after stopping microwave irradiation.

4.3.6 Analytical methods

Samples were taken with a 10 mL syringe from the reactor at different pre-determined reaction times. The collected photocatalysis samples were first filtered through a 20 μ m nylon filter to remove the TiO₂ particles prior to chemical analysis. All the samples were analyzed immediately to avoid any further reaction. The concentration of phenol was quantified by HPLC. A 20 μ L sample was injected into the D-7000 HPLC system (Hitachi, Japan) equipped with a C18 column (Hypersil, China. 250 \times 4.6 mm), which consisted of a L-7100 pump and a L-7420 UV-VIS detector. A 60% (v/v) aqueous acetonitrile solution and 40% water was used as the mobile phase; its flow rate was fixed at 1 mL/min. The wavelength employed for detecting phenol was 254 nm.

4.3.7 Experimental methodology

The phenol-water solution was (1500 ppm) prepared by dissolving pure phenol in Milli - Q water and stored in amber-coloured bottles. A total of 300 mL of the phenol-water solution was added to a batch reactor with the catalyst concentration as explained in the experimental methodology flow chart (Figure 4.7).

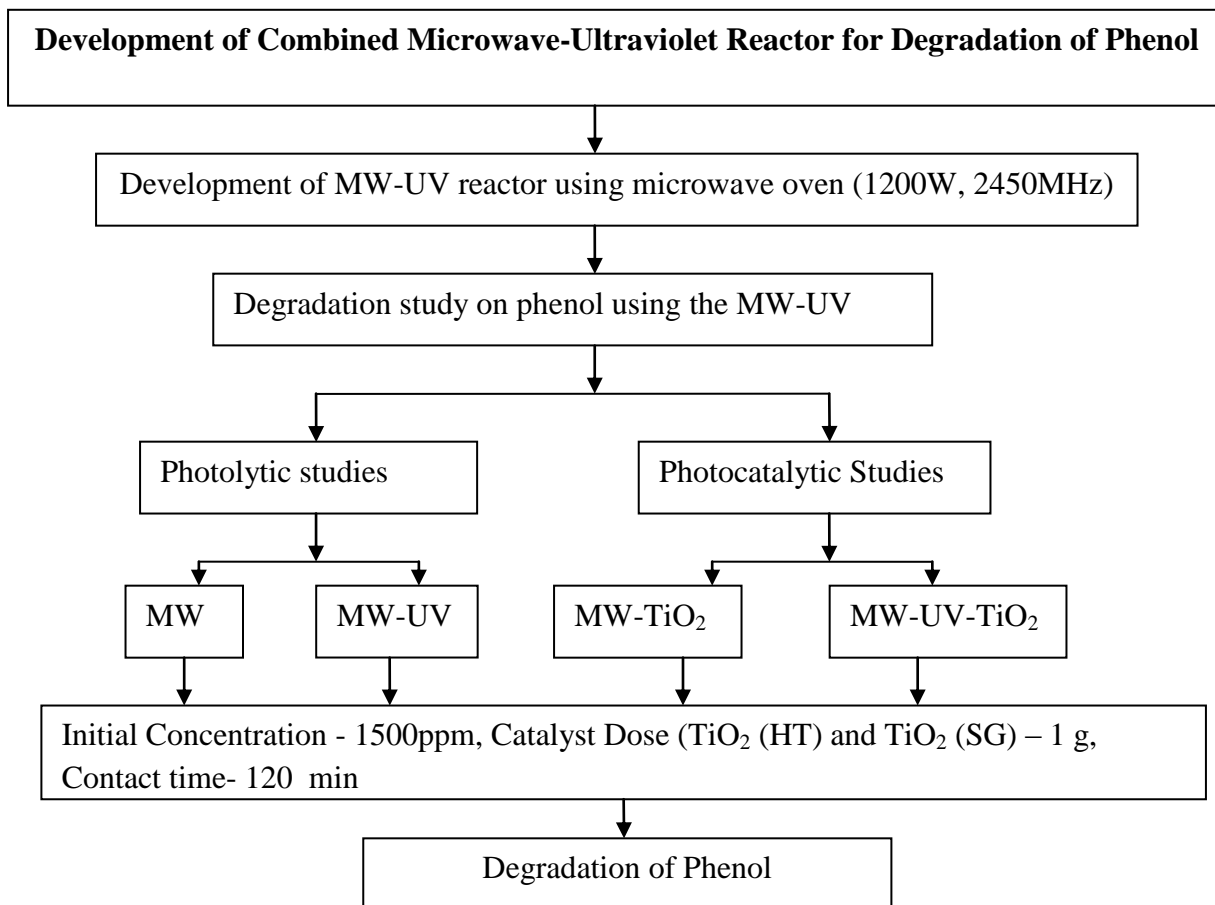


Fig. 4.6: Flow chart of the methods followed in experiments using the initial concentration 1500 ppm of phenol for 120 min with 1 g of catalyst prepared with hydrothermal and sol-gel methods.

The mixture of phenol-water and catalyst was homogenized with a magnetic stirrer before placing in the sample holder inside the microwave. The solution was circulated at 400 mL/min with a pump, and the temperature of phenol-water solution in the reactor vessel was kept constant at 40°C.

4.3 Results and Discussion

4.4.1 Characterization of the TiO₂ nanoparticles

- **X-ray diffraction (XRD)**

The structure and the crystallite size of the prepared samples were examined by high angle X-ray diffraction analysis. Figure 4.8 presents the XRD patterns of calcined TiO₂ nanopowder prepared by two different methods and calcined at 500°C. This technique can also be used to obtain crystalline phases of the calcined catalysts (Badoga et al. 2012). The peaks obtained at various 2θ were identified by comparison with ICDD (International Centre for Diffraction Data) which confirmed that the particles were crystalline with an anatase structure ($2\theta = 25.4^\circ$). The absence of peaks at Bragg angles (2θ) of 27.5° , 39.3° , and 54.2° confirmed the absence of the rutile phase in the samples. The average crystallite size of TiO₂ was estimated according to Scherrer's equation (4.8),

$$D = K\lambda / \beta \cos\theta \quad (4.8)$$

where K is the Scherer constant, λ the X-ray wavelength, β the peak width at half maximum, and θ is the Bragg diffraction angle.

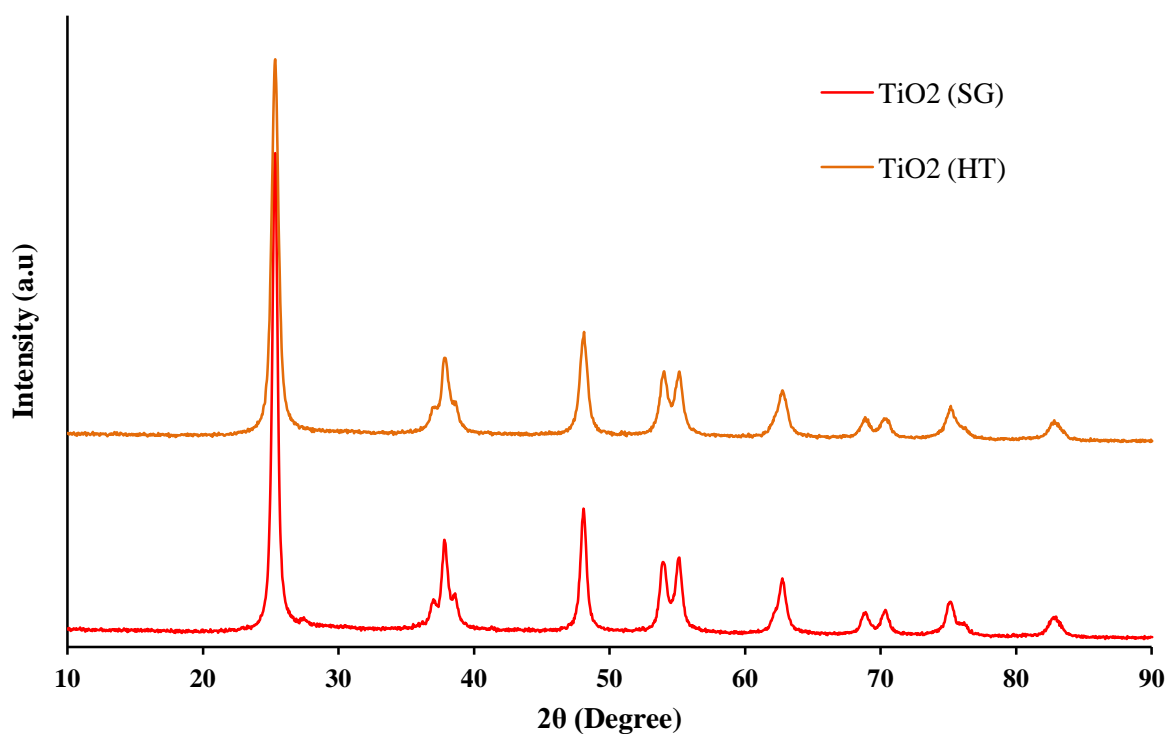


Fig. 4.7: X-ray diffraction (XRD) patterns of TiO₂ prepared by sol-gel (SG) and hydrothermal (HT) methods

- **N₂ adsorption – desorption isotherm**

Nitrogen sorption at 77 K using a Micromeritics ASAP 2020 instrument was used to measure the textural properties of the catalysts. The BET method was used for the determination of the surface area and pore volume of the samples using adsorption-desorption isotherms (Badoga et al. (2012)). The pore diameter and pore size distribution of the catalysts were determined using the BJH method. The numerical data obtained are summarized in Table 4.1 which shows a lower surface area of catalyst prepared by the hydrothermal process than by the sol-gel method, 85 m²/g to 36 m²/g. The average pore diameter of the catalyst prepared by the hydrothermal method was smaller than that of the sol-gel prepared catalyst 10.4 nm and 15.7 nm respectively. The pore volumes were similar 0.2 (cm³/g) for both catalysts.

Table 4.1: Summary of the properties of TiO₂ nanoparticles calcinite at 500°C

Properties	TiO ₂ (HT)	TiO ₂ (SG)
Surface area (m ² /g)	85	36
Avg. pore dia. (nm)	10	15
Pore Volume (cm ³ /g)	0.2	0.1

- **Thermogravimetric analysis (TGA)**

Figure 4.9 presents TGA curves for TiO₂ prepared by sol-gel and hydrothermal methods. Data was recorded on a TGA instrument under nitrogen with a heating rate of 10°C/min. There was no weight loss after 400°C for TiO₂ synthesized by the hydrothermal method or by the sol-gel method indicating that decomposition of the precursor was complete and could start as first calcinations temperature. Weight loss before 400°C was attributed to removal of residual ethanol and water. TiO₂ anatase can be transferred to the rutile phase between 550 and 600°C (Porkodi et al. 2007).

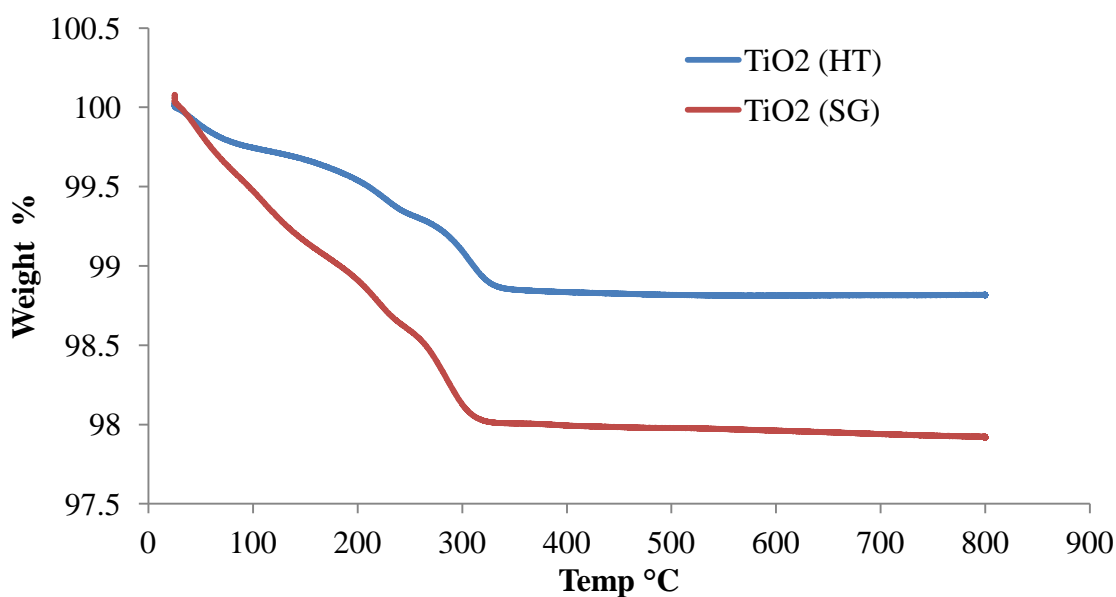


Fig. 4.8: TGA curves of TiO₂ prepared by sol-gel (SG) and hydrothermal (HT) Methods

- **Fourier transform infra red spectroscopy (FTIR)**

The FT-IR spectra of TiO₂ nanoparticles prepared with two different methods were analyzed and are presented in Figure 4.10. The spectra of the oxides TiO₂ (SG) and TiO₂ (HT), were collected in the frequency range of 4000-400 cm⁻¹. In TiO₂ prepared sample, between 3800 to 3300 cm⁻¹ a broad band was observed which shows stretching of hydroxyl (O-H), representing moisture (Muneer et al. 2012). The other peaks at 1628 cm⁻¹ were indicated to stretching of titanium carboxylate, which formed from TTIP and ethanol (Garcia-Serrano et al. 2009). A strong absorption peak was observed between 800 and 450 cm⁻¹ which was assigned to the Ti-O stretching bands and attributed to form of TiO₂ nanoparticles.

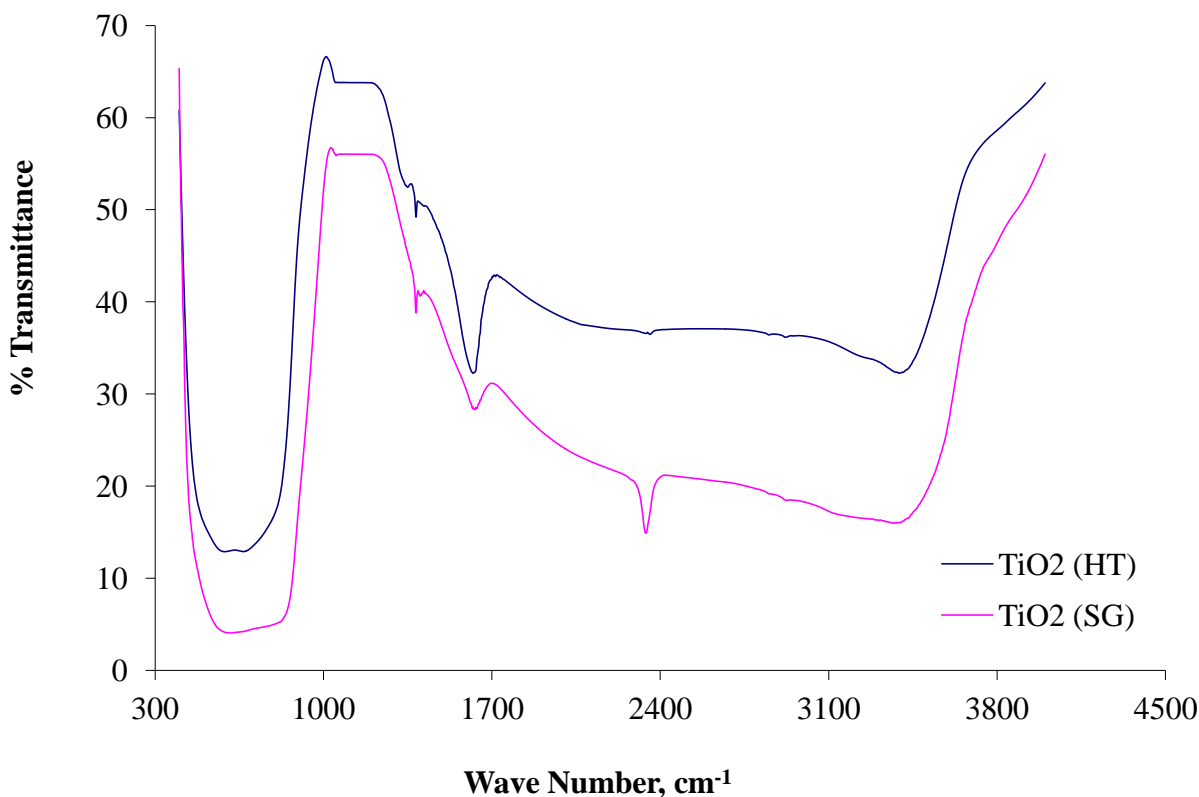


Fig. 4.9: Fourier Transform Spectra of TiO₂ prepared by sol-gel (SG) and hydrothermal (HT) Methods

- **Scanning electron microscopy (SEM)**

SEM is one method for the characterization of particle morphology and determination of the particle diameter. Micrographs of the calcined TiO_2 nanoparticles prepared by the sol-gel and hydrothermal methods are shown in Figure 4.11 and 4.12 respectively. It can be seen from the morphologies of the TiO_2 nanoparticles that the sol-gel sample showed more aggregation than the hydrothermal sample. The shape of the particles prepared by both methods was observed to be sphere like morphology with different sizes of spheres. Particles from the hydrothermal method were more uniform and smaller in size as compared to the sol-gel method.

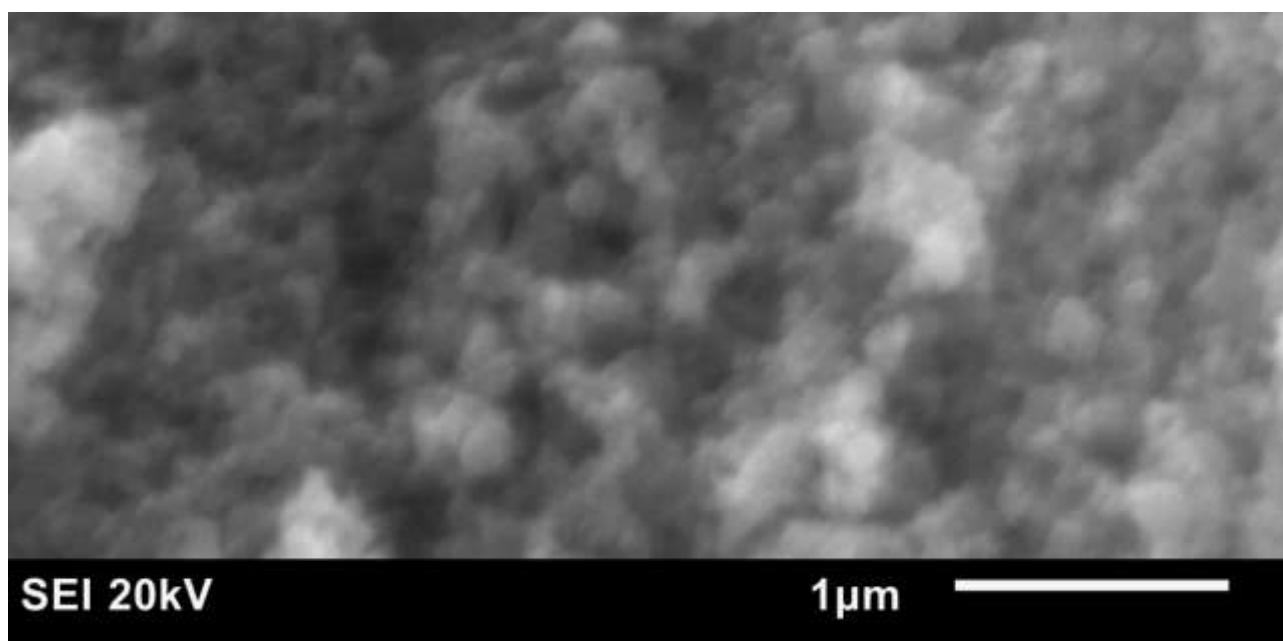


Fig. 4.10: SEM image of TiO_2 nanoparticles prepared by Sol-Gel method.

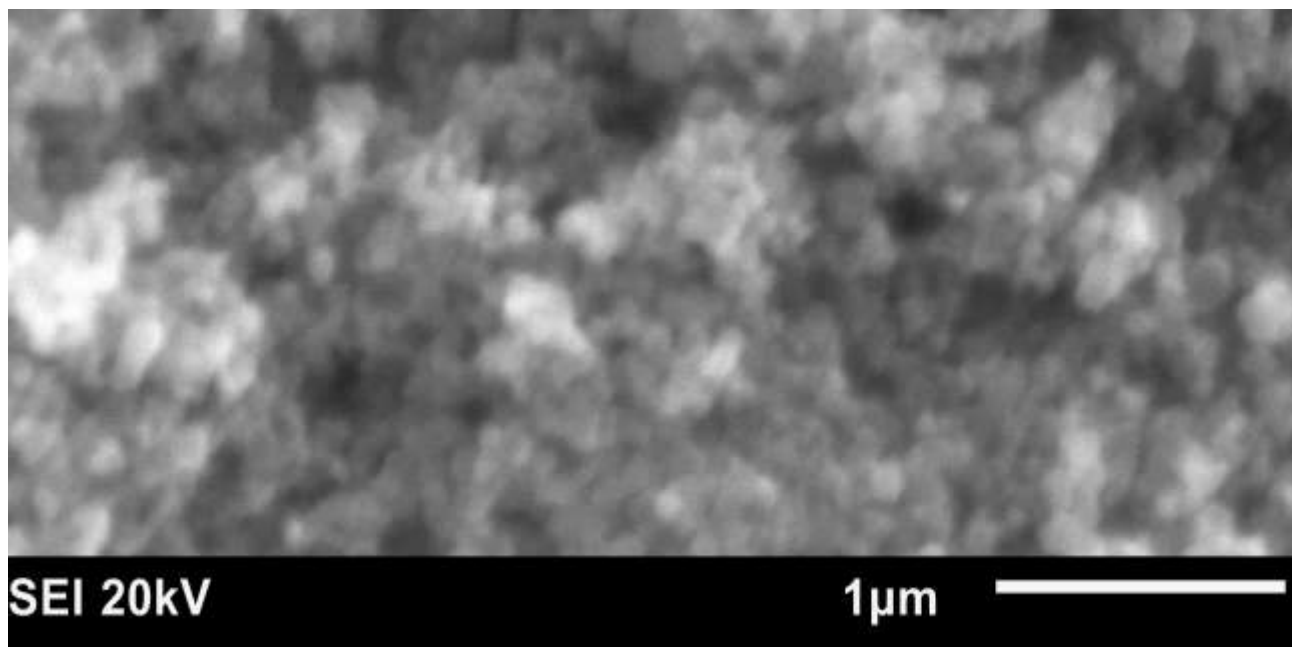


Fig. 4.11: SEM image of TiO₂ nanoparticles prepared by hydrothermal method.

4.4.2 Microwave output power calculation

Microwave power was tested as described in section 4.2.5.1 and equation (4.7) was used to calculate the actual microwave power used. Propagation of microwave energy easily raises the water temperature. The change in water temperature during microwave irradiation is presented in Figure 4.13. The average power was calculated using equation (4.7) to be 836 Watts.

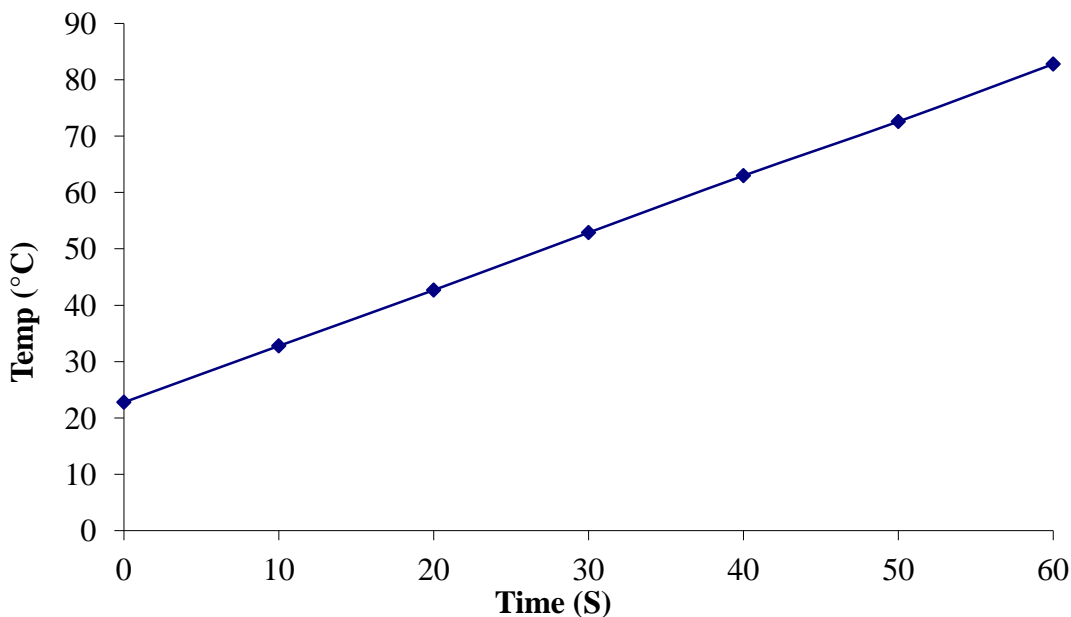


Fig. 4.12: Change in water temperature during microwave irradiation.

4.4.3 Catalytic activity of synthesized TiO₂ nanoparticles

The catalytic activity TiO₂ synthesized via two different methods was assessed by degrading a 1500 ppm phenol in water solution with two developed treatment systems; microwave and microwave-assisted UV, and compared with conventional heating. All experiments were conducted in triplicate.

4.4.3.1 Dark adsorption

In a typical dark adsorption experiment, a 300 mL sample containing 1500 ppm phenol in water was mixed with 1.0 g TiO₂ (hydrothermal or sol-gel) in a flask and covered with aluminum foil, and kept for 2 hours in a dark place. The initial pH of the phenol-water solution was not modified and adsorption phenol on TiO₂ was assessed. It was observed that initially phenol degradation not occurred in the dark process was none, which may be because of the stability of the

phenol molecule and the iso-electric point of TiO_2 . The iso-electric point of TiO_2 is about 6.0; at $\text{pH} > 6.0$, the TiO_2 surface is negatively charged and it is difficult for phenol to adsorb due to an electrostatic repulsive force (Chiou et al. 2008).

4.4.3.2 Effect of microwave radiation on degradation of phenol

The effect of microwave irradiation and catalyst prepared by two different methods on degradation of phenol in water was investigated with three processes: (1) MW without addition of catalyst (2) MW- TiO_2 (HT) and (3) MW- TiO_2 (SG).

The initial phenol concentration was 1500 ppm; 300 mL the volume treated was with 1 g of catalyst. The reaction time was 120 min. Figure 4.14 shows the decreases in phenol concentration with microwave irradiation with and without sol-gel and hydrothermal derived TiO_2 nanoparticles. It was observed that microwave irradiation did not have much effect without an oxidant, as the decrease in phenol concentration was only 4.47%. Addition of TiO_2 increased the degradation to some extent, which might be due to adsorption of the phenolic pollutants on the surface of TiO_2 particles. Of the catalysts prepared via the two methods, the hydrothermal catalyst showed better catalytic activity than did the sol-gel method catalyst by decreasing the phenol concentration 15.53% vs 12.33%. This can be attributed to the large catalyst surface area and smaller particle size of the catalyst prepared by the hydrothermal method. The decrease in phenol concentration indicated that a small quantity of phenol was adsorbed on the surfaces of the TiO_2 particles. Wei and Wan (1991) reported the kinetics is negative first order for photocatalytic decomposition of phenol, and there is a remarkable effect of the initial concentration of phenol on the rate constant.

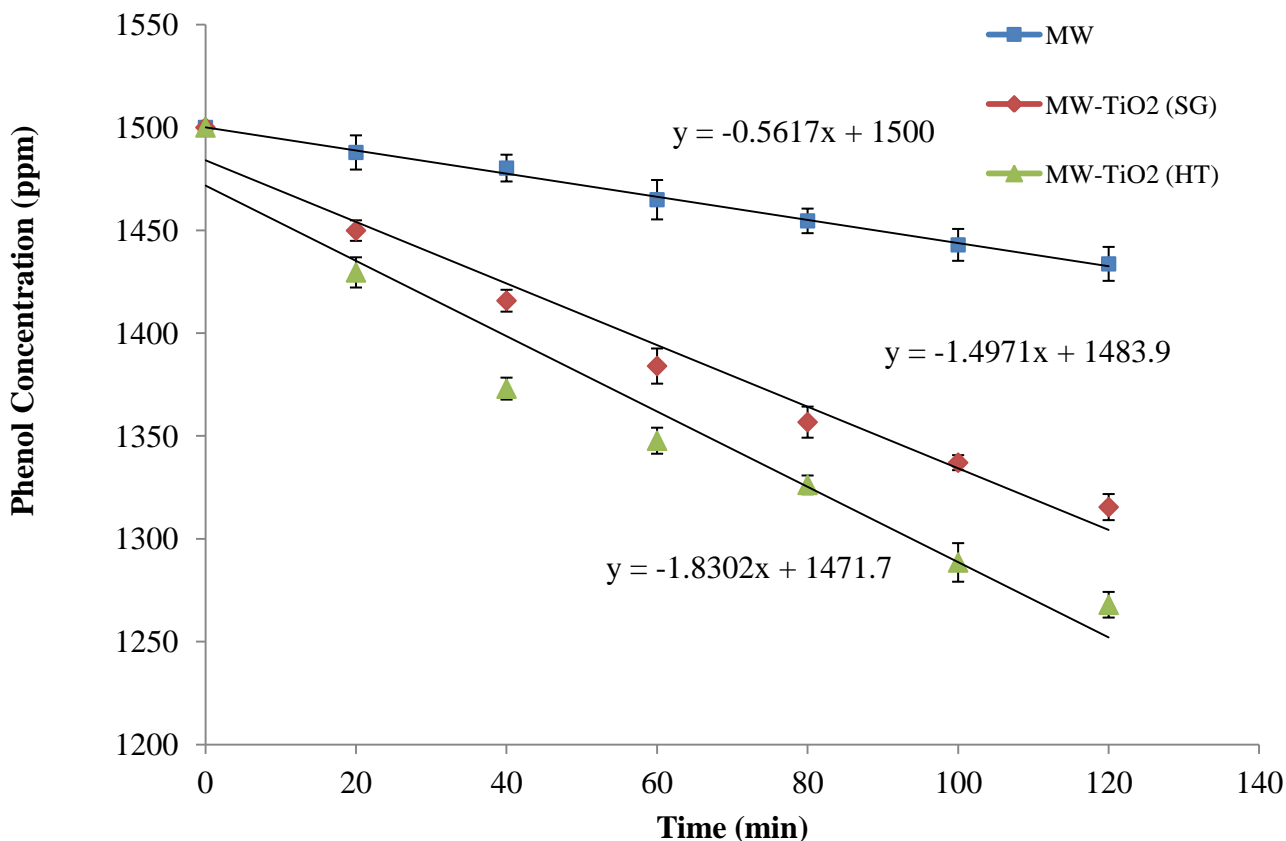


Fig. 4.13: Decrease in phenol initial concentration (1500 ppm) as a function of microwave irradiation at 2.45 GHz with exposure time of 120 min obtained for sol-gel and hydrothermal derived TiO₂ nanoparticles. Error bars represent one standard deviation and may not be visible in some cases due to small values.

4.4.3.3 Effect of the microwave assisted photocatalytic system on degradation of phenol

The effect of microwave radiation combined with UV irradiation on the degradation of phenol was investigated with three processes: (1) MW-UV without catalyst, (2) MW-UV-TiO₂ (HT) and (3) MW-UV-TiO₂ (SG).

The initial phenol concentration was 1500 ppm, the total volume was 300mL with 1 g of catalyst. The energy of MW radiation ($E = 0.4\text{--}40 \text{ kJ mol}^{-1}$ at $\nu = 1\text{--}100 \text{ GHz}$) considerably lower

than that of UV-VIS radiation ($E = 600\text{--}170 \text{ kJ mol}^{-1}$ at $\lambda = 200\text{--}700 \text{ nm}$), so it can not break bonds of common organic molecules (Pavel et al., 2003).

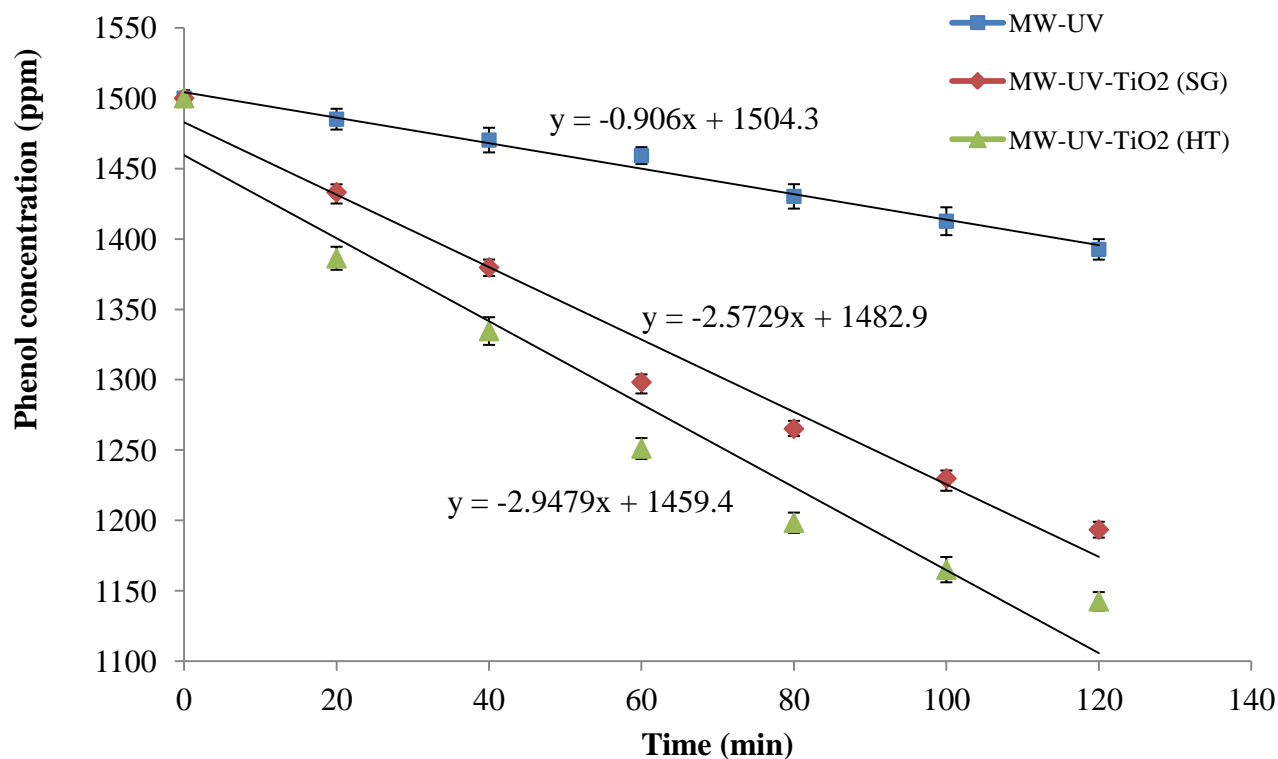


Fig. 4.14: Decrease in initial phenol concentration (1500ppm) as a function of microwave at 2.45 GHz combined UV irradiation exposure time of 120 min obtained for sol-gel and hydrothermal derived TiO₂ nanoparticles. Error bars represent one standard deviation and may not be visible in some cases due to small value.

It was found that the microwave-assisted photolytic process exhibited effective decomposition of phenol, with degradation efficiencies of 20.46% for MW-UV-TiO₂ (SG) and 23.82% for MW-UV-TiO₂ (HT) in 120 min, which indicated that the UV light generated by MWLs could destroy phenol.

The result showed that the catalyst prepared by hydrothermal method had better catalytic activity than the catalyst prepared by the sol-gel method. Addition of TiO₂ to the combined MW-

UV treatment system resulted in a significant decrease in phenol concentration within 120 min whereas the decrease in phenol concentration with MW-UV only was 7.20%.

On the basis of the above results, microwave-assisted photocatalytic degradation was more effective for the degradation of phenol than any other process studied, perhaps because of direct breaking of bond in phenol by UV irradiation produced. UV irradiation can result in h^+ on the surface of TiO_2 particles, which could oxidize phenol. Microwave also creates defective sites on the TiO_2 , and the polarization effect of this defective catalyst in a microwave field increases the transition probability of photon-generated electrons and decreases the recombination of $e^- h^+$ on the semiconductor surface (Ai et al. 2008). Kataoka et al. (2002) mentioned that under irradiation with combined microwave and UV-VIS light surface of TiO_2 becomes more hydrophobic, and increases the hydroxyls on the surface resulting in oxidation to $\cdot OH$. Horihoshi et al. (2004) proved using electron spin resonance that about 20% more $\cdot OH$ were generated by photocatalysis with microwave irradiation than by photocatalysis alone by electron spin resonance. Figure 4.15 shows the decrease in phenol concentration in a microwave combined UV irradiation treatment system with TiO_2 nanoparticles.

4.4.3.4 Effect of initial concentration on phenol degradation in the MW-UV- TiO_2 process

Light intensity, dissolved oxygen and initial concentration of the organic substrate are factors on which the reaction rate depends in photocatalytic oxidation of organic pollutants (Chen et al. 1999, Mehrotra et al. 2003). Previous studies have been done with phenol concentrations above 10 mg/L; in the present study the effect of MW-UV- TiO_2 on phenol degradation was studied using initial concentrations of phenol of 500 ppm, 1000 ppm and 1500 ppm in aqueous solution. The

initial pH was maintained (6.9 ± 0.2) without any modification. The catalyst dose and contact time were 1g and 120 minutes respectively. The results obtained are shown in Figure 4.16.

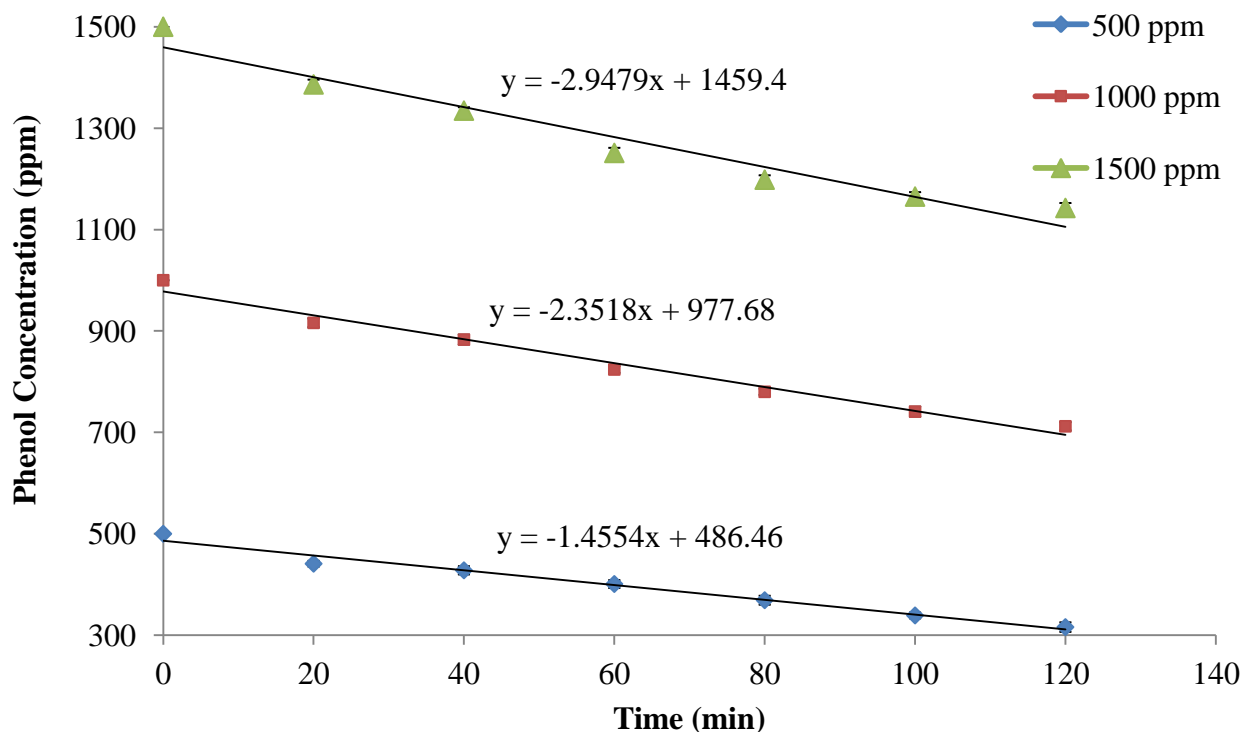


Fig. 4.15: Effect of the initial concentration of phenol on MW-UV-TiO₂ with a microwave at 2.45 GHZ, UV at 8 watts and Tio₂ prepared with sol-gel and hydrothermal methods for Phenol degradation. Error bars represent one standard deviation and may not be visible in some cases due to small values.

The results showed that, the degradation efficiency decreased with an increase in the initial concentration of phenol. The removal percentage of phenol at 120 minutes using the MW-UV-TiO₂ method was 36.8%, 28.8% and 23.8% for 500 ppm, 1000 ppm and 1500 ppm, respectively. Similar photocatalytic studies have been done by Kartal et al (2001) and Alnaizy and Akgerman (2000), and who concluded that with a increase in the initial phenol concentration the rate of photolysis

decreased significantly. Primo et al (2007) reported that the rate of degradation was only 26% using an initial concentration of 1000 ppm under irradiation with a medium pressure lamp of 150 Watt for 600 min.

4.5 Summary

Degradation of phenol in aqueous suspension with TiO_2 was studied under atmospheric pressure. Nanocrystalline TiO_2 catalyst were successfully synthesized via sol-gel and hydrothermal methods, and then structure and morphology were characterized using different techniques. Two laboratory-scale treatment systems, a microwave treatment system and a microwave-assisted UV irradiation system were developed to study the degradation of phenol in water in a dark process. The following are the conclusions.

- Degradation of phenol by microwave-assisted photocatalytic treatment system was more effective than the microwave system alone. Combination method demonstrated the effectiveness and degradation efficiency.
- TiO_2 prepared by the hydrothermal method showed better structural, morphological and catalytic activity than TiO_2 prepared by the sol-gel method which may be attributed to its larger surface area and smaller particle size.
- The removal of phenol from 300 mL of a 1500 ppm phenol-water solution with 1 g of catalyst was found to be 23.82%.
- The effect of initial concentration was studied at three concentrations (500 ppm, 1000 ppm and 1500 ppm) with the microwave-assisted photocatalytic system. It was observed that the degradation efficiency decreased with an increase in the initial concentration of phenol.
- The removal percentage of phenol at 120 minutes by the MW-UV- TiO_2 method was 36.8%, 28.8% and 23.8% for 500 ppm, 1000 ppm and 1500 ppm, respectively.

CHAPTER 5

SUMMARY AND CONCLUSIONS

5.1 Summary

A combined MW-UV reactor was designed by placing a microwave electrode-less UV lamp in a microwave reactor to study the effect of MW-UV on degradation of phenol in aqueous solution in the presence and absence of TiO_2 . The effect of MW, MW- TiO_2 , MW-UV and MW-UV- TiO_2 were studied to see the removal efficiency for phenol.

To develop and evaluate a microwave treatment system using catalyst and a microwave-assisted UV treatment system for phenol remediation, one of the most important design parameters, is the dielectric properties or permittivity of phenol in water, but this had not been reported in the literature. There are critical gaps in knowledge with respect to the permittivity/dielectric properties of phenol in water, and the application and evaluation of microwave and combined microwave UV irradiation treatment systems for the degradation and detoxification of phenol in water. Therefore, the first objective of this study was to measure the dielectric properties of phenol-water mixtures at frequency of 1-5 GHz. With the help of the dielectric properties obtained in chapter 3, penetration depth was calculated and a reactor was designed for the proper interaction of microwaves with the phenol-water mixture.

The overall objective of this research was to develop and evaluate a microwave system and a microwave-assisted UV irradiation treatment system, combined with TiO_2 catalysts prepared by sol-gel and hydrothermal methods, to degrade phenol in water. Appropriate systems utilizing the principles of microwave and microwave-assisted UV irradiation systems, were designed and

developed. These systems were evaluated for degradation of phenol in water to verify the hypothesis that the developed systems would degrade the phenol in water quickly.

Experimental investigations were carried out in order to develop a microwave and integrated MW-UV reactor by incorporating a UV electrode-less lamp in a microwave reactor to study the effect of MW and MW-UV on degradation of phenol in aqueous solution in the presence and absence of TiO_2 . MW, MW-UV, MW- TiO_2 and MW-UV- TiO_2 treatment alternatives were studied. TiO_2 was synthesized by hydrothermal and sol-gel methods, and characterized with FT-IR, XRD, BET, TGA and SEM techniques.

The MW-UV reactor was developed in such a way that the electrodes of the lamp were not directly exposed to microwave radiation. A sample holder with a volume of 300 mL was placed in a microwave oven with output power of 1200 Watts and a frequency of 2450 MHz. A mercury lamp with wavelength of 254 nm and power of 8 Watts was inserted into the sample holder and positioned vertically. A water bath was used to cool the reacting fluid in order to prevent excess heat generation and damage to the reaction during microwave heating.

Two holes were made in the top of the oven for taking the sample and measuring the temperature, and two holes were made in one side of the oven to pass the sample back and forth between the reactor and the water bath. A Teflon cylinder with a capacity of 300 mL and 15 cm height was inserted into the microwave oven. The mercury lamp was inserted into the Teflon reactor and placed centrally with the help of a Teflon plate with holes on it. It has been reported in previous studies (Zhang et al. 2006) that although photocatalytic degradation is effectively accelerated by microwave radiation, a traditional UV lamp could not be placed in a microwave field because the metal electrodes of the lamp will be damaged under microwave irradiation.

Phenol-water solution of known initial concentration was filled into the reactor from the top of the Teflon cylinder. The peristaltic pump was switched on and allowed to circulate the sample throughout the length of the reactor. The cooler was switched on before the reactor and allowed to stabilize the temperature of the solution in the reactor at 40°C. The initial sample was collected immediately after the reactor was switched on. The intermediate samples were collected once in 20 minutes and the total duration of the experiments was 120 minutes. The collected samples were immediately analyzed for the residual concentration of phenol. The values obtained by measuring dielectric properties were helpful in selecting the sample holder to be placed in the microwave reactor that was designed. MW, MW-UV, MW-TiO₂, MW-UV-TiO₂ processes were studied and it was found that the MW-UV-TiO₂ system was the most appropriate system to degrade phenol. The catalyst TiO₂ was prepared with two methods, hydrothermal and sol-gel and it was observed that the catalyst prepared with hydrothermal method showed better and effective catalytic activity than the sol-gel catalyst.

Conclusions from each of the chapters have been presented in Section 5.2 and specific recommendations for future research are listed in section 5.3.

5.2 Conclusions

5.2.1 Dielectric Properties of Phenol in Water

In this study the dielectric properties of phenol in water were determined as there was no information on these properties in the literature.

It is concluded the dielectric properties of phenol-water mixtures were successfully determined over the microwave frequency range of 1-5 GHz.

The effects of process parameters such as temperature, concentration and frequency of microwave on the dielectric properties of phenol in water were determined. The concentration of the sample had little effect on the value of the loss tangent. At lower frequencies the temperature had no effect on loss tangent or power factor, but at frequencies higher than 1 GHz, there was a decrease in the value of the loss tangent and power factor with an increase in temperature at a particular frequency. Concentration did not affect the penetration depth for the sample. Trends were observed for both dielectric constant and loss factor, as a result of change in concentration and frequency.

5.2.2 Microwave and microwave assisted AOPs treatment of phenol in water

The simultaneous effect of MW and UV on degradation of phenol was studied in aqueous solution in the presence and absence of TiO_2 under controlled temperature. It was found that the efficiency of MW and MW-UV processes on the degradation of phenol was less than 10% after 120 minutes of treatment. However, it is concluded the efficiency of MW- TiO_2 (HT) and MW- TiO_2 (SG) was slightly higher at 12 to 15% at 120 minutes, which might be due to adsorption of the phenolic pollutants over the surface of TiO_2 particles.

It was observed that MW-UV- TiO_2 was superior to any other processes studied for the degradation of phenol. At natural pH, the degradation efficiency of MW-UV- TiO_2 (HT) on 1500 ppm of phenol was 23%, and for MW-UV- TiO_2 (SG) was 20%.

Three different concentrations of phenol (500 ppm, 1000 ppm and 1500 ppm) were studied with the MW-UV- TiO_2 treatment system, and it was observed that the rate of degradation decreased as the pollutant concentration increases. The removal percentage of phenol at 120 minutes with the MW-UV- TiO_2 method was 36.8%, 28.8% and 23.8% for 500 ppm, 1000 ppm and 1500 ppm, respectively.

TiO₂ nanoparticles were systematically synthesized by two methods; hydrothermal and sol-gel methods. The synthesized catalysts were then characterized and photocatalytic activity was compared using two developed treatment systems, microwave only and microwave-assisted UV irradiation for the degradation of phenol.

It can be summarized, that oxidation of substrate can happen by reacting with holes or hydroxyl radicals on the photocatalyst (TiO₂) surface, but the result of oxidized intermediates again react with reducing species, giving back the substrate, and finally decrease in the degradation rate of the substrate happens (in this case it is phenol) with increasing initial concentration.

Specifically, it can be concluded that the MW-UV reactor developed indigenously could be successfully used for degradation of pollutants that are especially recalcitrant in nature.

5.3 SCOPE FOR FUTURE STUDY

In this area of study, scope still exists for investigation of the following aspects:

- To study the effect of MW power and thermal effect of MW radiation on biodegradability of recalcitrant compounds.
- To study the effect of MW and MW-UV irradiation using alternate oxidants and using different catalysts.
- To scale-up and optimize the reactor systems and further investigate the degradation efficiencies by testing higher concentration of phenol.

References

- Ai Z.H., P. Yang, X.H. Lu. (2005). Degradation of 4-chlorophenol by microwave irradiation enhanced advanced oxidation processes, *Chemosphere* 60, 824–827.280, 89–103.
- Agarwal S.K. (2009). *Water Pollution*, 2nd edition. A P H publishing corporation.
- Agustina, T.E., Ang, H.M., Vareek, V.K. A. (2005). Review of synergistic effect of photocatalysis and ozonation on wastewater treatment. *Journal of Photochemistry and Photobiology C: Photochemistry Reviews*, 6 (4), pp. 264-273.
- Ahmaruzzaman M. and Sharma D.K. (2005). Adsorption of phenols from wastewater, *J.Collo. Interf. Sci*, 287(1) 14-24.
- Allen N. S., M. Edge , J. Verran , J. Stratton , J. Maltby , C. Bygott. (2008). Photocatalytic titania based surfaces: Environmental benefits. *Polymer Degradation and Stability* 93 (2008) 1632–1646.
- Alnaizy, R. and Akgerman, A. (2000). Advanced oxidation of phenolic compounds. *Advances in Environmental Research*, Vol. 4, pp. 233-244.
- Andreozzi, R., Caprio, V., Insola, A., Marotta. (1999). Advanced oxidation processes (AOP) for water purification and recovery. *Catalysis Today*, 53 (1), pp. 51-59.
- Arana J., E. P. Melia, L. Rodriguez, A. P. Alonso, J. M. Rodriguez, O. G. Diaz, P. J. Perez. (2007). Photocatalytic degradation of phenol and phenolic compounds Part 1. Adsorption and FTIR study. *J. Hazard. Mater.* 146, 520-528.
- Ayranci E., O. Duman. (2005). Adsorption behaviors of some phenolic compounds onto high specific area activated carbon cloth. *J. Hazard. Mater.* B124, 125–132.

Badoga S., S.K. Pattanayek, A. Kumar, and L.-M. Pandey. (2011). Effect of polymer-surfactant structure on its solution viscosity,” Asia-Pacific Journal of Chemical Engineering, vol.6, no.1, pp.78–84.

Badoga Sandeep, K. Chandra Moulia, Kapil K. Soni, A.K. Dalai, J. Adjaye. (2012). Beneficial influence of EDTA on the structure and catalytic properties of sulfided NiMo/SBA-15 catalysts for hydrotreating of light gas oil Applied catalyst B: Environmental 125 (2012) 67-84.

Bahnemann W., Muneer M., Haque, M. (2007). Titanium dioxidedmediated photocatalysed degradation of few selected organic pollutants in aqueous suspensions. *Catal. Today*, 124, 133.

Banat F. A., B. Al-Bashir, S. Al-Asheh, O. Hayajneh. (2000). Adsorption of phenol by bentonite. *Environ. Pollut.* 107, 391-398.

Bayly RC, Barbour G. (1984). The degradation of aromatic compounds by the meta and gentisate pathways: biochemistry and regulation. New York, pp 253–294.

Bond et al., G. Bond, R.B. Moyes and D.A. Whan. (1993). Recent applications of microwave heating in catalysis, *Catalysis Today* 17, pp. 427–437.

Bottcher, C.J.F., O.C.V. Belle, P. Bordewijk and A. Rip. (1973). In: *Theory of electric polarization (2nd Ed): The dielectric constant in the continuum approach to the environment of the molecules. Vol-I, Ch-V:159-204*. Elsevier, Amsterdam.

Boyd, T.J., Carlucci, A.F. (1993). Degradation rates of substituted phenols by natural populations of marine bacteria. *Aquatic Toxicology*, 25 (1-2), pp. 71-82.

Buffler C.R. (1993). *Microwave cooking and processing*. Van Nostrand Reinhold, New York.

Busca G, S. Berardinelli, C. Resini, L. Arrighi. (2008). Technologies for the removal of phenol from fluid streams: A short review of recent developments,” *J. Hazard. Mater.* 160, 265–288.

Busca, (2010). Acid catalysts in industrial hydrocarbon chemistry,” Chem. Rev. 107, 5366–Butanol and Acetone: Measurement and Computational Study. J Solution Chem 39: 701–708

Castle, J.E., and Zhdan, P.A. (1997). *Characterisation of surface topography by SEM and SFM: problems and solutions*. Journal physics. D: applied physics, 30: p. 722-740.

Cha, S.Y., Jeon, J.S., Lim, J.L, Yang, H.Y. and Han, D. H. (1999). “Effect of Microwave on Oxidative Degradation of Phenol in UV/H₂O₂ Oxidation process”, J. Korean Inst. Chem. Engineers, Vol.37, No.2, pp. 284-289, 1999.

Chen X. and S. S. Mao. (2007). Titanium Dioxide Nanomaterials: Synthesis, Properties, Modifications, and Applications. Chem. Rev.,107, 2891-2959

Chen, X.; Mao, S. (2007). Titanium dioxide nanomaterials: Synthesis, properties, modifications, and applications. *Chem. Rev.*, 107, 2891.

Chen D., Ray A.K. (1999). Photocatalytic kinetics of phenol and its derivatives over UV irradiated TiO₂. Applied Catalysis B: Environmental 23 (1999) 143–157

Chen-Chi Wang and Jackie Y. Ying. (1999). Sol-Gel Synthesis and Hydrothermal Processing of Anatase and Rutile Titania Nanocrystals” *Chem. Mater.* 11, 3113-3120.

Chhabra V., V. Pillai, B. K. Mishra, A. Morrone,t and D. O. Shah. (1995). Synthesis, Characterization, and Properties of Microemulsion-Mediated Nanophase TiO₂ Particles” *Langmuir*,11, 3307-3311.

Chiou, C.H., Wu, C.Y. and Juang, R.S. (2008a). “Influence of operating parameters on photocatalytic degradation of phenol in UV/TiO₂ process, “Chemical Engineering Journal, Vol. 139, pp. 322-329.

Crittenden, J. C., Liu, J., Hand, D. W. and Perrram, D. L.: (1997), 'Photocatalytic oxidation of chlorinated hydrocarbons in water', *Wat. Res.* 31, 429–438.

Deichmann WB, Keplinger ML. (1981). Phenols and phenolic compounds. Patty's industrial hygiene and toxicology, vol. 2A. John Wiley & Sons, New York Chichester Brisbane Toronto, pp 2567–2627.

Doll, T. E. and F.H. Frimmel. (2005). Removal of selected persistent organic pollutants by heterogeneous photocatalysis in water. *Catalysis Today* 101:195–202.

Drzazga, W., Paluszynski, J., and Slowko, W. (2006). *Three-dimensional characterization of microstructures in a SEM*. Measurement Science and Technology. 17: p. 28-31.

Ellen L. Kruger, Todd A. Anderson, Joel R. Coats. (1997). Phytoremediation of Soil and Water Contaminants. American Chemical Society. Volume 664.

Erik W. Allen, (2008). Process water treatment in Canada's oil sands industry: 1. Target pollutants and treatment objectives. *Journal of Environmental Science* 7: 123–38.

Esplugas, S., Giménez, J., Contreras, S., Pascual, E., Rodríguez, M. (2002). Comparison of different advanced oxidation processes for phenol degradation *Water Research*, 36 (4), pp. 1034-1042.

Fedorak, P.M., and Hrudey, S.E. (1988). Anaerobic degradation of phenolic compounds with applications to treatment of industrial waters. In Biotreatment systems. Vol. 1. Edited by D.L. Wise. CRC Press, Inc., Boca Raton, FL. pp. 169-225.

Ferrando, 1996 A.C. Ferrando, Coal desulphurisation with hydroiodic acid and microwaves. (1996). *Fuel and Energy Abstracts*, 37 9, p. 333.

Gallawa J. Carlton. (2004). Complete Microwave Oven Service Handbook: Operation, Maintenance, Troubleshooting, and Repair. Pennsylvania State University. Prentice Hall publication.

Gallet, C., and Pellissier, F. (1997). Phenolic compounds in natural solutions of a coniferous forest. *J. Chem. Ecol.* 23:2401–2412.

Gao Z., Yang S., Sun C., Hong J. (2007). Microwave assisted photocatalytic degradation of pentachlorophenol in aqueous TiO₂ nanotubes suspension. *Separation and Purification Technology*, 58 (1), pp. 24-31.

Garcia-Araya J. F., F.J. Beltran, P. Alvarez and F.J. MASA. (2003). Activated Carbon Adsorption of Some Phenolic Compounds Present in Agro industrial Wastewater Adsorption 9,107–115.

Gimeno, O.; Carbajo, M.; L_opez, M. J.; Melero, J. A.; Beltr_an, F.; Rivas, F. J. (2007). Photocatalytic promoted oxidation of phenolic mixtures: An insight into the operating and mechanistic aspects. *Water Res.* 41, 4672–4684.

García-Serrano J., E. Gómez-Hernández, M. Ocampo-Fernández, and U. Pal. (2009). Effect of Ag doping on the crystallization and phase transition of TiO₂ nanoparticles,” *Current Applied Physics*, vol. 9, no. 5, pp. 1097–1105.

Granados, G.O., Carlos, A., Paez, M., Martinez, F .O. and Mozo, E.A. (2005). Photocatalytic degradation of phenol on TiO₂ and TiO₂/Pt sensitized with metallophthalocyanines”, *Catalysis Today*, Vol. 107-108, pp. 589-594, 205.

Gully, J.R. (1992). Study of oil sands sludge reclamation under the tailing sludge abandonment research program. Final Report. Canada Centre for Mineral and energy Technology (CANMET), Energy, Mines and Resources Canada, Edmonton, Alta.

Hafizah Nor and I. Sopyan. (2009). Nanosized TiO₂ Photocatalyst Powder via Sol-Gel Method: Effect of Hydrolysis Degree on Powder Properties. International Journal of Photoenergy Volume, Article ID 962783.

Hardwood, C. S., Rivelli, M., and Ornston, L. N. (1984). Aromatic acids are chemoattractants for *Pseudomonas putida*. J. Bacteriol. 160:622-628.

Harold P. Klug, Leroy E. Alexander. (2009). X-Ray Diffraction Procedures: For Polycrystalline and Amorphous Materials, Wiley Interscience Publication.

Heipieper, H. J., R. Diefenbach, and H. Keweloh. (1992). *Conversion of cis-unsaturated fatty acids to trans, a possible mechanism for the protection of phenol-degrading Pseudomonas putida P8 from substrate toxicity*. Appl. Environ. Microbiol. 58:1847-1852.

Hoffmann M R, Martin S T, Choi W. (1995). Environmental applications of semiconductor photocatalysis. Chem Rev, 95: 69–96.

Horikoshi, S, H. Hidaka and N. Serpone. (2004). Environmental remediation by an integrated microwave/UV illumination technique VI A simple modified domestic microwave oven integrating an electrodeless UV-Vis lamp to photodegrade environmental pollutants in aqueous media. *Journal of Photochemistry and Photobiology A: Chemistry* 161: 221–225.

Hsien, Y. H., K.H. Wang, R.C. Ko and C.Y. Cang. (2000). Photocatalytic degradation of wastewater from manufactured fiber by titanium dioxide suspensions in aqueous solution: a feasibility study. *Water Sci. Tech.* 42:95–99.

Huang J., X. Wanga, Q. Jina, Y. Liua, Y. Wang. (2007). Removal of phenol from aqueous solution by adsorption onto OTMAC-modified attapulgite. J. Environ. Manage. 84, 229–236.

Hunter, J.V., S.D. Faust. (1971). Origin of organics from artificial contamination (Eds.), Organic Compounds in Aquatic Environments Marcel Dekker, New York, pp. 51–94.

Ismail, A.I., Chan, K.W., Moriod, A.A. and Ismail, M. (2010). Phenolic content and antioxidant activity of canta-loupe (*Cucumis melo*) methanolic extracts. *Food Chemistry*. 119, 643-647.

Kape, R., Wex, K., Parniske, M., Gorge, E., Wetzell, A., Werner, D. (1992). Legume root metabolites and VA- mycorrhiza development. *J Plant Physiol*, 141, pp. 54-60.

Mehrotra Kanheya, Gregory S. Yablonsky, and Ajay K. Ray. (2003). Kinetic Studies of Photocatalytic Degradation in a TiO_2 Slurry System: Distinguishing Working Regimes and Determining Rate Dependences. *Ind. Eng. Chem. Res.* 2003, 42, 2273-2281.

Kartal, O.E., Erol, M. and Ogluz, H. (2001). Photocatalytic Destruction of Phenol by TiO_2 Powders”, *Chem. Eng. Technol.* Vol.24 (6), pp. 645-649.

Kataoka, S., Tompkins, D.T., Zeltner, W.A., and Anderson, M.A. (2002). Photocatalytic oxidation in the presence of microwave irradiation: Observations with ethylene and water. *J. Photochem. Photobiol.* A148, 323.

Kavitha M., Dr.C.Gopinathan and P.Pandi. (2013). Synthesis and Characterization of TiO_2 Nanopowders in Hydrothermal and Sol-Gel Method. *International Journal of Advancements in Research & Technology*, Volume 2, Issue4, April-2013. ISSN 2278-7763.

Kirk-Othmer, (1999). *Concise Encyclopedia of Chemical Technology*,” 4th ed., Wiley, New York, 1514.

Klán, P and V. Církva. (2002). “Microwave Photochemistry” in *Microwaves in organic synthesis*; Ed: André Loupy Pub: Weinheim ; [Cambridge] : Wiley-VCH. Ch-14: 463-486.

Kong, L, S. Zhao, Q. Zhang, P. Li and L. Zhuang.(2006). Removing Naphthenic Acids from Diesel Oil by Microwave Irradiation. *Petroleum Science and Technology* 24:2,157 -166.

Ku, Y., Leu, R.-M. Lee, K.-C. (1996). Decomposition of 2-chlorophenol in aqueous solution by UV irradiation with the presence of titanium dioxide” *Water Research* Volume 30, Issue 11, November Pages 2569-2578.

Kumar P. (2010). Remediation of high phenol concentrations using chemical and biological technologies. Ph.D. Dissertation, University of Saskatchewan, Saskatoon.

Lin L., S. Yuan, J. Chen, Z. Xu, X. Lu. (2009). Removal of ammonia nitrogen in wastewater by microwave radiation, *J. Hazard. Mater.* 161, 1063–1068.

Luis De, J. I. Lombrana, A. Menendez, and J. Sanz. (2011). Analysis of the Toxicity of Phenol Solutions Treated with H₂O₂/UV and H₂O₂/Fe Oxidative Systems. *Ind. Eng. Chem. Res.*, 50, 1928–1937.

Luo, Y., Ollis, D.F. (1996). Heterogeneous photocatalytic oxidation of trichloroethylene and toluene mixtures in air: Kinetic promotion and inhibition, time-dependent catalyst activity *Journal of Catalysis*, 163 (1), pp. 1-11.

Mackinnon, M.D., and Retallack, J.T. (1981). Preliminary characterization and detoxification of tailings pond water at the syncrude Canad Ltd Oil sands Plant. In *Land and Water Issues Related to Energy Development*. Ann Arbor Science, Denver, Colo. Pp. 185-210.

MacKinnon, M.D., and Sethi, A. (1993). A comparison of the physical and chemical properties of the tailing ponds at the syncrude and Suncor oil sands plants. In *Proceedings of our Petroleum Future Conference*, Alberta Oil Sands Technology and Research Authority (AOSTRA), Edmonton, Alta.

Madill, R.E., Orzechowski, M.T., Chen, G., Brownlee, B.G., and Bunce, N.J. (2001). Preliminary risk assessment of the wet land scape option for reclamation of oil sands mine tailings: bioassays with mature fine tailings pore water. *Environ. Toxicol.* 16: 197-208. Doi: 10.1002/tox.1025. PMID:11409191.

- Mahamuni, N.N., Pandit, A.B. (2006). "Effect of additives on ultrasonic degradation of phenol". *Ultrasonics Sonochemistry*, Volume 13, Issue 2, February 2006, Pages 165-174.
- Mahvi, A.H., J. Nouri, G.A. Omrani and F. Golami, (2007). Application of *Platanus orientalis* leaves in removal of cadmium from aqueous solution, *World Applied Sciences Journal*, 2(1): 40-44.
- Mantzavinos D., M. Sahibzada, A. G. Livingston, I. S. Metcalfe. (1999). Wastewater treatment: wet air oxidation as a precursor to biological treatment", *Catal. Today* 53, 93–106.
- Martin, A. K., (1982). The origin of urinary aromatic compounds excreted by ruminants 1. The metabolism of quinic, cyclohexanecarboxylic and non-phenolic aromatic acids to benzoic acid. *Br. J. Nutr.* 47:139.
- Menendez, J.A , M Inguanzo, J.J Pis. (2002). Microwave-induced pyrolysis of sewage sludge. *Water Research* Volume 36, Issue 13, Pages 3261–3264.
- Mishra S., (2009). Microwave Assisted Photocatalytic Treatment of Naphthenic Acids in Water. Ph.D. Dissertation, University of Saskatchewan, Saskatoon.
- Mishra, S., V. Meda and A.K. Dalai (2006a). "Dielectric properties measurement of naphthenic acid-water mixture", *Proc. 40th IMPI symposium*, ISSN: 1070- 0129, Boston, USA.
- Mishra, S., V. Meda, A.K. Dalai, J. Headley and D.W. McMartin. (2006b). "Microwave Assisted Photolysis of NAs in Water". *Proc.19th Canadian Symposium on Catalysis*, Canadian Society of Chem Engineers (CSCHE), Canada.
- Mishra, S., V. Meda, A.K. Dalai. (2007). "Permittivity of naphthenic acid-water mixture", *Journal of Microwave Power and Electromagnetic Energy (JMPEE)*, Vol 41(2): 18-29, ISSN: 0832-7823.
- Muneer M. Ba-Abbad¹, Abdul Amir H. Kadhumi¹, Abu Bakar Mohamad¹, Mohd S. Takriff¹, Kamaruzzaman Sopian. (2012). Synthesis and Catalytic Activity of TiO₂ Nanoparticles for

Photochemical Oxidation of Concentrated Chlorophenols under Direct Solar Radiation. *Int. J. Electrochem. Sci.*, 7, 4871 – 4888.

Nair C.I., K Jayachandran, S Shashidhar.(2008). *Biodegradation of Phenol*. African Journal of Biotechnology, Vol 7, No 25.

Neyens, E., Baeyens, J. A. (2003). Review of classic Fenton's peroxidation as an advanced oxidation technique. *Journal of Hazardous Materials*, 98 (1-3), pp. 33-50.

Nia M. Mohsen, H. Amiri-B. Jazi. (2010). Dielectric Constants of Water, Methanol, Ethanol, complex permittivity of dielectric reference liquids at frequencies up to 5 GHz.

NPL (2001) Tables of the *NPL Report* (CETM 33).

Patsoura, A.; Kondarides, D. I.; Verykios, X. E. (2007). Photocatalytic degradation of organic pollutants with simultaneous production of hydrogen. *Catal. Today*, 124, 94.

Pavel M., K. Petr, C. Vladimir. (2003). The electrodeless discharge lamp: a prospective tool for photochemistry. Part 4. Temperature- and envelope material-dependent emission characteristics, *J. Photochem. Photobiol.* 158, 1–5.

Pavia, Donald L., Gary M. Lampman, James A. Vyvyan and George S. Kriz. (2009). *Introduction to Spectroscopy*, fourth edition.

Polaert I., L. Estel,A. Ledoux. (2005). Microwave-assisted remediation of phenolwastewater on activated charcoal. *Chemical Engineering Science* 60, 6354 – 6359.

Porkodi K., S. Daisy Arokiamary. (2007). Synthesis and spectroscopic characterization of nanostructured anatase titania: A photocatalyst. *Materials Characterization* 58 495–503.

Primo Oscar, Mar'ia J. Rivero, Inmaculada Ortiz, Angel Irabien. (2007). Mathematical modelling of phenol photooxidation: Kinetics of the process toxicity. *Chemical Engineering Journal* 134 (2007) 23–28.

Rajeshwar, K. (1995). Photoelectrochemistry and the environment. *Journal of Applied Electrochemistry* Volume 25, Issue 12, December, Pages 1067-1082.

Remya N. Jih-Gaw Lin. (2011). Current status of microwave application in wastewater treatment—A review. *Chemical Engineering journal* 166: 797-813.

Rogers, V.V., M. Wickstrom, K. Liber and M.D. MacKinnon. (2002b). Acute and subchronic mammalian toxicity of naphthenic acids from oil sands tailings. *Toxicological Sciences* 66: 347-355.

Mishra Sabyasachi, Venkatesh Meda and Ajay Dalai . (2007). Permittivity of naphthenic acid-water mixture. *Journal of Microwave Power & Electromagnetic Energy* Vol. 41, No. 2.

Schmidt-Baumler K, Heberer T, Stan HJ (1999). Occurrence and distribution of organic contaminants in the aquatic system in Berlin part II: Substituted phenols in Berlin surface water. *Acta hydrochim. Hydrobiol.* 27(3): 143-149.

Senturk H. B., D. Ozdesa, A. Gundogdua, C. Durana, M. Soylakb. (2009). Removal of phenol from aqueous solutions by adsorption onto organomodified Tirebolu bentonite: Equilibrium, kinetic and thermodynamic study. *J Hazard. Mater.* 172, 353–362.

Sevillano X., J. R. Isasi and F. J. Penas (2008). Feasibility study of degradation of phenol in a fluidized bed bioreactor with a cyclodextrin polymer as biofilm carrier. *Biodegradation* 19, 589-597.

Silverstien, R.M. (2005). Spectrometric Identification of organic compounds (F.X Webster Shun Akari, WILEY 7th Edition.

Skoog D. A., F. J. Holler, S. R. Crouch. (2007). *Principles of Instrumental Analysis*, 6th ed. Belmont, CA. Thomson Higher Education.

Sofía Arellano-Cárdenas, Tzayhrí Gallardo-Velázquez, Guillermo Osorio-Revilla, Ma. del Socorro López-Cortéz and Brenda Gómez-Perea. (2005). Adsorption of Phenol and Dichlorophenols from Aqueous Solutions by Porous Clay Heterostructure (PCH)", *J. Mex. Chem. Soc.*, 49(3), 287-291.

Stroscher, M.T., and Peake, E. (1978). Characterization of organic constituents in waters and wastewaters of Athabasca Oil Sands mining area. Report No. 20. Alberta Oil Sands Environmental Research Program (AOSERP), Alberta Environment, Edmonton, Alta.

Thompson, T. L.; Yates, J. T., Jr. (2006). Surface science studies of the photoactivation of TiO₂ New photochemical processes. *Chem. Rev.* 106, 4428.

Tian, B., Z. Luan and M. Li. (2005). Low-temperature synthesis of allyl dimethylamine by selective heating under microwave irradiation used for water treatment. *Radiation Physics and Chemistry*. 73(6): 328-333.

Topudurti, K. V., Lewis, N.M. and Hirs, S. H.: (1993), 'The applicability of UV/oxidation technologies treat contaminated groundwater', *Environ. Progr.* 12, 54–60.

Venkatesh, M.S. and G.S.V. Raghavan. (2004). "An overview of microwave processing and dielectric properties of agri-food materials". *Biosystems Engineering*. 88(1), 1-18.

Venkatesh, M.S., V. Orsat and G.S.V. Raghavan. (2005). In: H. Schubert and M. Regier (eds). *The microwave processing of foods: Microwave heating and the dielectric properties of foods*, CRC Press LLC, USA.

Villota, N., Mijangost, F., Varona, F., Andrés, J. (2007). Kinetic modelling of toxic compounds generated during phenol elimination in wastewaters *International Journal of Chemical Reactor Engineering*, 5, art. no. A63.

Wei T.-Y. and Wan C.-C. 1999. Heterogeneous photocatalytic oxidation of phenol with titanium dioxide powders. *Ind. Eng. Chem. Res.* 30, 1293–1300.

Wang Wendong , Philippe Serp, Philippe Kalck, Joaquim Luís Faria. (2005). Visible light photodegradation of phenol on MWNT-TiO₂ composite catalysts prepared by a modified sol–gel method. *Journal of Molecular Catalysis A: Chemical*. Volume 235, Issues 1–2, 1 July 2005, Pages 194–199.

Wicks and Schulz, Wicks GG, Schulz RL. (2001). Microwave remediation of Hazardous and Radioactive Wastes. *Journal of the South Carolina Academy of Science*, [2011], 9(1) 25

Yang C. F., C. M. Lee. (2007). Enrichment, isolation, and characterization of phenol-degrading *Pseudomonas resinovorans* strain P-1 and *Brevibacillus* sp. strain P-6, *Int. Biodeter. Biodegr.* 59, 206–210.

Yavuz, Y., Koparal, A., and Ogutveren, U. (2010). "Treatment of petroleum refinery wastewater by electrochemical methods." *Desalination*, 258(1-3), 201-205.

Zazo, J.A., Casas, J.A., Molina, C.B., Quintanilla, A., Rodriguez, J.J. (2007). Evolution of ecotoxicity upon Fenton's oxidation of phenol in water *Environmental Science and Technology*, 41 (20), pp. 7164-7170.

Zhang, X, G. Li, Y. Wang and J. Qu. (2006). "Microwave electrodeless lamp photolytic degradation of acid orange-7". *Journal of Photochemistry and Photobiology A: Chemistry*. 184: 26–33.

Zhang et al., H. Zhang, D.O. Hayward and D.M.P. (2003). Mingos, Effects of microwave dielectric heating on heterogeneous catalysis, *Catalysis Letters* 88 (1–2), pp. 33–38.

Zhang et al., H. Zhang, D.O. Hayward, L. Colleen and D.M.P. Mingos, (2001). Microwave assisted catalytic reduction of sulfur dioxide with methane over MoS₂ catalysts, *Applied Catalysis B: Environmental* 33, pp. 137–148.

Zhihui, A., Y. Peng, and L. Xiaohua. (2005). Degradation of 4-chlorophenol by a microwave assisted photocatalysis method. *J. Hazard. Matter. B.* 124: 147-152.

APPENDIX A1

Dielectric Measurements of Methanol:

Relative Dielectric constant

Frequency	Literature	Experimental	% Error
1	30.5	31.4	3.1
2	24.2	25.3	4.5
3	18.7	19.4	3.4
4	14.9	15.6	4.9
5	12.4	12.5	0.9

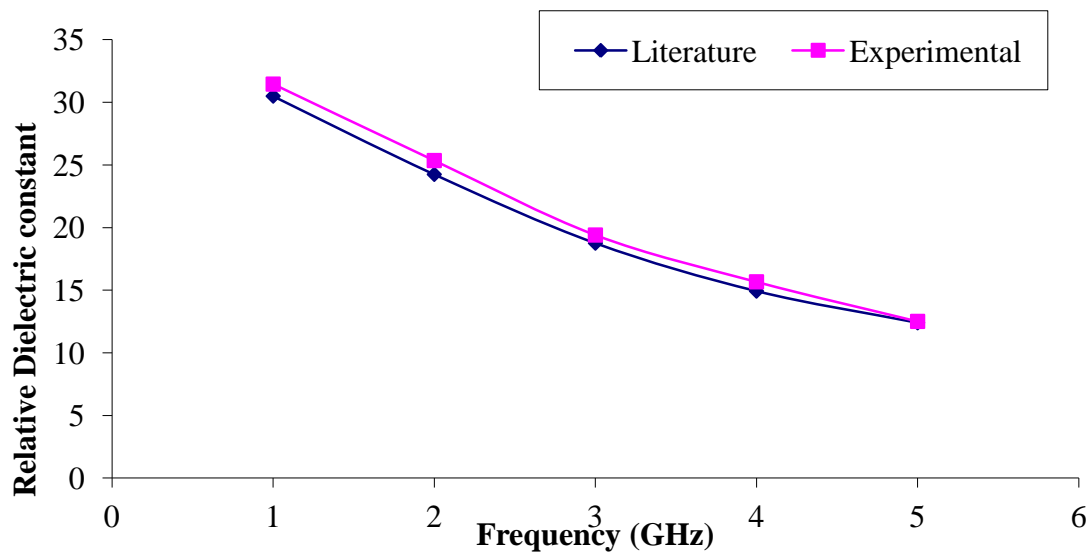


Figure 1: Relative dielectric constant of methanol at 25°C

Relative Loss Factor

Frequency	Literature	Experimental	% Error
1	8.8	8.8	0.2
2	13.2	13.2	0.5
3	13.9	14.6	5.2
4	13.1	14.3	8.6
5	11.9	13.1	10.0

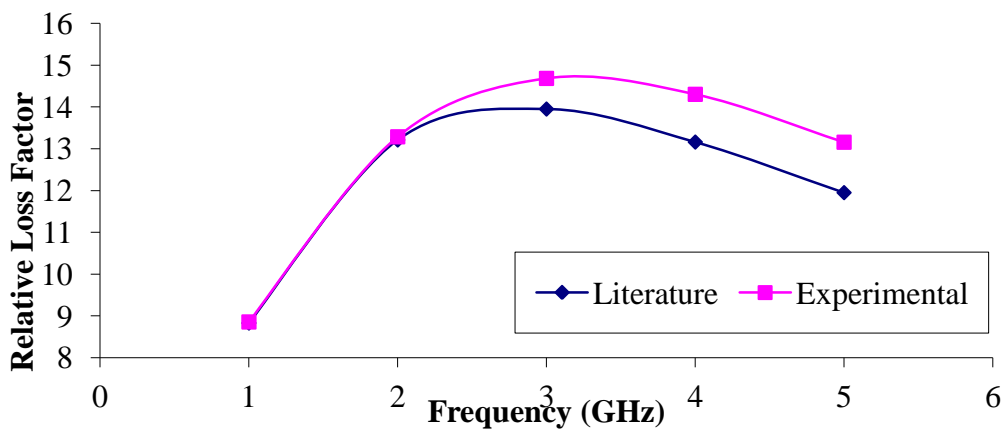


Figure 2: Relative Loss factor of methanol at 25°C

Relative Dielectric constant

Frequency	Literature	Experimental	% Error
1	28.5	30.1	5.3
2	25.4	26.5	4.2
3	21.7	21.1	-2.7
4	18.3	17.5	-4.6
5	15.6	15.9	2.0

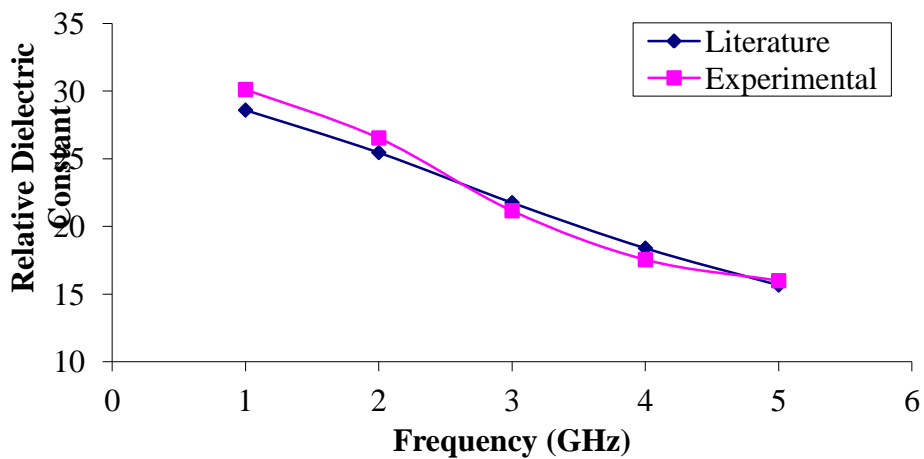


Figure 3: Relative dielectric constant of methanol at 40°C

Relative Loss Factor

Frequency	Literature	Experimental	% Error
1	5.4	6.0	9.9
2	9.4	10.0	6.7
3	11.5	12.3	6.5
4	12.2	13.2	8.1
5	12.1	13.1	8.2

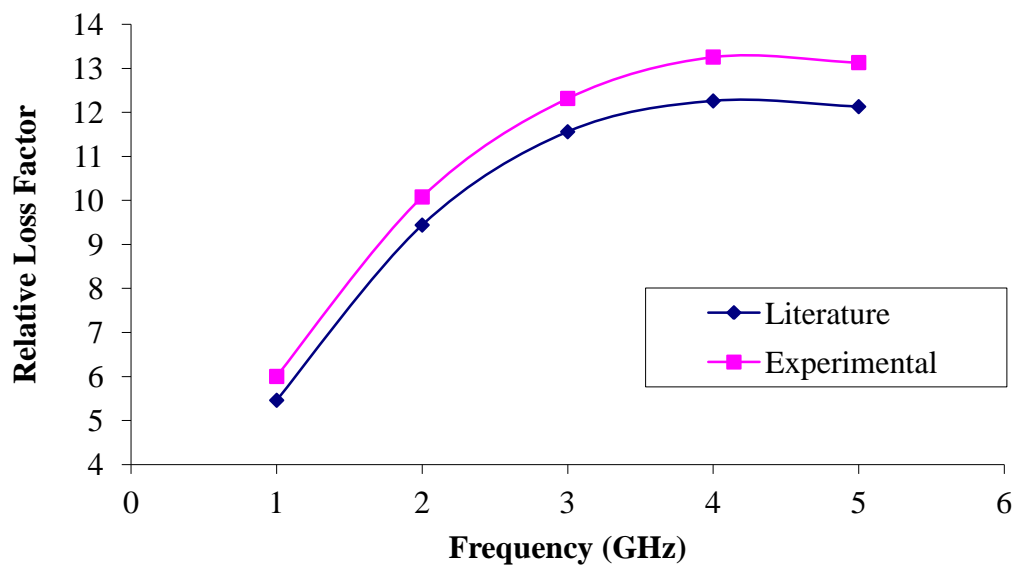


Figure 4: Relative Loss factor of methanol at 40°C

Appendix A2

The quantification of phenol was determined using an HPLC. A calibration curve was prepared for standard solution. Three injections of each sample were injected into the HPLC and average and standard deviations were used to prepare calibration curves shown in the Figures 6.

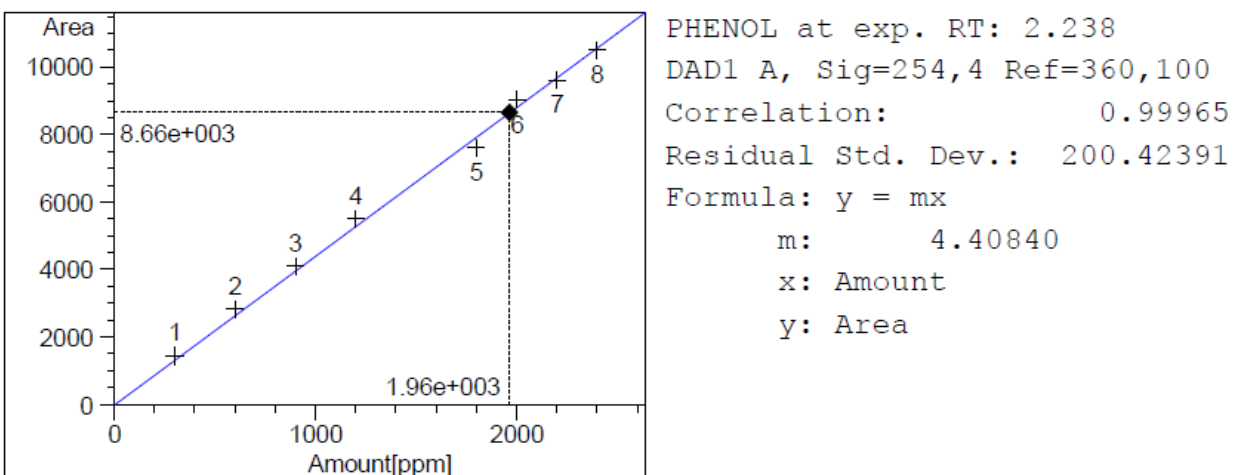


Figure 5: Calibration of phenol